Dissertation zur Erlangung des Doktorgrades (Dr. rer. nat.)
des Fachbereichs Mathematik/Informatik/Physik der Universität Osnabrück

Combinatorial Aspects of Horizontal Visibility Graphs, Symmetric Edge- and Laplacian Polytopes

vorgelegt von:
Daniel Köhne

Betreuer:
Prof. Dr. Martina Juhnke-Kubitzke

Osnabrück, 2023

Contents

Introduction **1**

1 Background on graphs, simplicial complexes and polytopes **9**

1.1 Graphs . . . 9

1.1.1 Basic notion . . . 9

1.1.2 Horizontal visibility graphs . . . 10

1.2 Simplicial complexes and Laplacian matrices . . . 13

1.3 Lattice polytopes . . . 15

1.3.1 Basic notion . . . 15

1.3.2 Ehrhart theory . . . 16

1.3.3 Triangulations and Gröbner bases . . . 17

2 Counting horizontal visibility graphs **21**

2.1 Horizontal visibility graphs from distinct data . . . 22

2.1.1 From horizontal visibility graphs to data sequences . . . 22

2.1.2 Horizontal visibility graphs and degree sequences . . . 23

2.1.3 Counting horizontal visibility graphs in $\mathcal{G}_{N,\neq}$ . . . 26

2.1.4 Horizontal visibility graphs and parentheses . . . 28

2.2 Horizontal visibility graphs from arbitrary data . . . 29

2.2.1 From horizontal visibility graphs to data sequences . . . 30

2.2.2 Counting horizontal visibility graphs – Schröder numbers . . . 30

2.3 Open problems . . . 32

3 A scalable linear time algorithm for horizontal visibility graphs **35**

3.1 Related work . . . 36

3.2 Proposed method . . . 38

3.2.1 Correctness of the algorithm . . . 39

3.2.2 Time complexity . . . 41

3.2.3 Online version . . . 42

3.2.4 Multi-processing . . . 43

3.3 Numerical experiments . . . 45

3.3.1 Synthetic time series . . . 45

3.3.2 Audio and financial time series . . . 46

3.3.3 Acceleration time series . . . 48

3.3.4 Multi-processing . . . 49

4 On the gamma vector of symmetric edge polytopes **51**

4.1 Basic properties of symmetric edge polytopes . . . 52

4.2 Non-negativity of γ_2 . . . 54

4.3 On a conjecture of Lutz and Nevo . . . 65

4.4 Symmetric edge polytopes for Erdős-Rényi random graphs . . . 68

4.4.1 Edges and cycles in Erdős-Rényi graphs . . . 68

4.4.2 The subcritical regime . . . 69

4.4.3 The supercritical regime . . . 70

5 Laplacian polytopes of simplicial complexes **77**

5.1 Laplacian matrices of boundaries of simplices . . . 77

5.2 General properties of Laplacian polytopes . . . 79

5.3 The facet description and the combinatorial type of $P_{\partial(\sigma_{d+1})}$ . . . 82

5.4 Regular unimodular triangulations and h^*-vectors . . . 84

5.4.1 Triangulations through interior polytopes . . . 84

5.4.2 Unimodality and real-rootedness . . . 90

5.5 Open problems . . . 92

5.6 Appendix . . . 93

Bibliography **97**

List of Figures

The figures in this thesis were created using GeoGebra, Canva and Ipe.

1.1 The data sequence $D = (4,3,1,2,5)$ and its associated HVG. 11
1.2 The HVG $G = \mathrm{HVG}((4,1,1,3))$. 12
1.3 Two different triangulations of the hexagon, and a subdivision into simplices which is not a triangulation. 17
1.4 A regular and a non-regular triangulation. 18
1.5 Two regular unimodular triangulations of the unit square associated to Gröbner bases. 20

2.1 The HVG of the sequences $(4,3,1,2,7,5,6)$ and $(7,4,1,2,6,3,5)$. . . . 23
2.2 The graph $\mathrm{HVG}((1,8,4,7,6,5,2,3))$. 24
2.3 The unique HVG with ordered degree sequence $(2,3,2,5,2,2)$. 26
2.4 Two HVGs with the same ordered degree sequence $(2,2,3,2,3,2,2)$. . 26
2.5 The graph $G = \mathrm{HVG}((10,6,2,4,5,8,9,1,3,7))$. 29
2.6 Applying ψ_{10} to G. 29
2.7 The graph $\xi_8(B)$. 32

3.1 Examples of an HVG and a VG. 35
3.2 Example of visible data points in the list decreasing. 39
3.3 Illustration of the LT-Algorithm for an example. 40
3.4 Numbers of non-nested vertices of i.i.d data. 44
3.5 Runtime comparisons for different types of data. 46
3.6 A box plot of the TIMIT audio data set and the intraday prices of S&P 500 stocks for the different algorithms. 47
3.7 The acceleration signals of normal and low tire pressure. 49
3.8 UMAP embedding of HVG features. 49
3.9 Parallizable versions of the DTHVG and LT-algorithm in comparison. 50

4.1 Example of a triangulation of the boundary of $\mathcal{P}_{C_4}$. 52
4.2 The double cone of a graph and the bipartite cone of a 6-cycle. 58
4.3 The construction of the graph H as in the proof of Proposition 4.2.9. 59
4.4 The bad pairs of edges for the graph H in Figure 4.3. 61
4.5 The graphs G_6 and $K_{2,4}$. 63

5.1 $\widetilde{P}_{\partial(\sigma_3)}$ and its interior polytope $Q_{\partial(\sigma_3)}$ translated to the origin. 85
5.2 The triangulation of $3 \cdot \Delta_2$ given by $\mathrm{esd}_3(\Delta_2)$. 87

List of Tables

3.1 HVG computation times in seconds for the TIMIT audio data set and intraday prices of S&P 500 stocks for the different algorithms. 47

5.1 The h^*-vectors of $P_{\partial\sigma_{d+1}}$ for $d = 1, \ldots, 8$. 93

List of Symbols

$[n]$	$\{1,\dots,n\}$, $n \in \mathbb{N}$
$[m,n]$	$\{m, m+1\dots,n\}$, $m,n \in \mathbb{N}$
$\mathcal{B}_N$	the set of balanced parentheses with N pairs of parentheses
$\widetilde{\mathcal{B}}_N$	the set of bracketings of length N
$C(N)$	the N^{th} Catalan number
C_n	the n-cycle graph
$\mathrm{cy}(G)$	the cyclomatic number of a graph G
$\gamma(\Delta)$	the γ-vector of a simplicial sphere Δ
$\gamma(\Delta;t)$	the γ-polynomial of Δ
$d(u,v)$	the distance between vertices u and v in a graph
$\dim(\Delta)$	the dimension of Δ
$\dim(P)$	the dimension of the polytope P
$\delta(v)$	the degree of $v \in V(G)$
$\delta_{\text{nest}}(v)$	the nesting-degree of $v \in V(G)$
Δ	a finite simplicial complex
Δ_d	the d-standard simplex
Δ_G	a regular unimodular triangulation of $\partial\mathcal{P}_G$
$\Delta(G)$	the (ordered) degree sequence of G
Δ/F	the edge contraction of Δ at F
$\Delta \smallsetminus F$	the face deletion of F from Δ
$\Delta \star \Gamma$	the join of simplicial complexes Δ and Γ
∂_i	the i-th boundary map in homology
∂P	the boundary of the polytope P
$\partial\Delta$	the boundary complex of the simplicial complex Δ
$e_{i,j}$	the difference of standard basis vectors $e_i - e_j$
$E(G)$	the edge set of G
$E_P(n)$	the Ehrhart polynomial of a polytope P
$\mathbb{E}(X)$	the expectation of the random variable X
$f(\Delta)$	the f-vector of Δ
$f(\Delta;x)$	the f-polynomial of Δ
$f_k(G)$	the number of k-faces of Δ_G
$F_i(\Delta)$	the set of i-faces of Δ
$\mathcal{F}(P)$	the set of facets of the polytope P
$\langle F_1,\dots,F_m\rangle$	the simplicial complex generated by $F_1,\dots,F_m$
G_n	the graph $K_{2,n-2} \cup \{12\}$ with partition $[n] = [2] \cup \{3,\dots,n\}$
$G \oplus_k H$	the k-clique sum of G and H
$G + H$	the 1-sum of HVGs G and H w.r.t. $N \in V(G)$ and $1 \in V(H)$
$G(n,p)$	an Erdős-Rényi graph on n vertices with probability p
$G(P)$	the facet-ridge graph of the polytope P
$G \cup e$	the graph $(V(G), E(G) \cup \{e\})$
$G \smallsetminus e$	the graph $(V(G), E(G) \smallsetminus \{e\})$
$G \smallsetminus V'$	the graph $G \smallsetminus V' = (V \smallsetminus V', E \smallsetminus \{e \,:\, e \cap V' \neq \varnothing\})$

G_W	the induced subgraph of G on W
$\mathcal{G}_N$	the set of HVGs corresponding to sequences of arbitrary data of length N
$\mathcal{G}_{N,\neq}$	the set of HVGs corresponding to sequences of distinct data of length N
$\mathcal{G}_{N,\neq}^s$	the set of HVGs in $\mathcal{G}_{N,\neq}$ with $m_G(1) = s$
$h(\Delta)$	the h-vector of Δ
$h(\Delta, x)$	the h-polynomial of Δ
$h^*(P)$	the h^*-vector of a polytope P
$h^*(P; x)$	the h^*-polynomial of a polytope P
$H_i(\Delta; \mathbb{Q})$	the i^{th} homology group of Δ
$\text{HVG}(D)$	the horizontal visibility graph corresponding to $D \in \mathbb{R}^N$
K_n	the complete graph on n vertices
$K_{m,n}$	the complete bipartite graph on a partition with m and n vertices
$l(B)$	the length of the bracketing B
$\text{lk}_\Delta(F)$	the link of a face F in Δ
$\mathcal{L}_i(\Delta)$	the i^{th} Laplacian matrix of Δ
$m_G(i)$	the maximal neighbor of the vertex $i \in V(G)$
$\mathcal{M}(P)$	the matrix whose column vectors are the vertices of the polytope P
$n_k(G)$	the number of k-dim. non-faces of Δ_G that do not contain antipodal vertices
$\text{nVol}(P)$	the normalized volume of the polytope P
$N(v)$	the set of neighbors of v
$\mathcal{N}(G)$	the set of all non-nested vertices of G
$\mathcal{P}_G$	the symmetric edge polytope of the graph G
P_n	the path on n vertices
$P \oplus P'$	the free sum of the polytopes P and P'
r_N	the N^{th} Schröder number
s_N	the N^{th} little Schröder number
σ_d	the d-simplex on the vertex set $[d+1]$
$v \to w$	the directed edge from v to w
$V(G)$	the vertex set of the graph G
$V(\Delta)$	the vertex set of the simplicial complex Δ
$\text{VG}(S)$	the visibility graph corresponding to the time series S
$\text{Var}(X)$	the variance of the random variable X
$\mathcal{V}(P)$	the set of vertices of the polytope P
$X_E(G)$	the random variable which is the number of edges for $G \in G(n,p)$
$X_k(G)$	the random variable which is the number of k-cycles for $G \in G(n,p)$
$\blacklozenge_d$	the d-dimensional cross-polytope
$\lozenge_d$	the boundary complex of the $(d+1)$-dimensional cross-polytope
$\cong$	unimodular equivalence

Introduction

A common approach in mathematics is to associate two mathematical objects with one another in order to derive properties and invariants of one via properties and invariants of the other. In discrete mathematics, especially in combinatorics and discrete geometry, a typical choice for one of these objects is a graph [BM86; HHO18; HJM19; LP86; OT22]. In the first part, this thesis focuses on graphs associated to time series; in particular, on horizontal visibility graphs.

Time series analysis plays a significant role in many research areas since physical and economic state variables are often measured at regular time intervals and then studied in their temporal context. New methods constructing graphs from time series have provided a different perspective on time series analysis. They are based, e.g., on recurrence [Don+10; Mar+09; Xia+12], dependency [Che+22; Des+09; Lia+11], visibility [Bal+09; Bal+08] or correlation [YY08]. These methods allow the time series to be analyzed using approaches from the emerging field of complex networks. In particular, horizontal visibility graphs (HVGs), introduced by Ballesteros et al. [Bal+09], have provided strong results in classifying and analyzing time series. For instance, the degree distribution of an HVG is known to be a good measure for distinguishing stochastic from chaotic systems [Bal+09]. Moreover, HVGs have been successfully applied, e.g., in optics [Ara+16], fluid dynamics [MPT15], plasma physics [ATMP21] (in a directed version), neurosciences [Li+14], chemistry [Das+22], EEG analysis of epileptics in physiology [DDK13; LWZ14] and sleep-stage classification via EEG signals [LWZ12], fault diagnosis of rolling bearings [GWY20] and finance [Hu+22; RS18]. For example, by transforming EEG signals of potentially alcoholic patients into a graph using the horizontal visibility algorithm and comparing graph properties of these graphs, alcoholism could be reliably detected [Li+14]. Network-based algorithms have recently also been applied to time series forecasting. These use visibility algorithms as preprocessing for their forecasting models [Cao+20; HX22a; HX22b]. In many of the various aforementioned applications, the time series tend to be very large. Thus, having efficient algorithms transforming the given series into its horizontal visibility graph are crucial. Desirable are algorithms that work efficiently on streamed data, that can be parallelized, and whose runtime is independent of the type of time series. Several approaches have already been investigated with complexities ranging from quadratic to linear time [Bal+09; Che+15; Lac+12; LWZ12; Ste21; Yel+20].

In the second part of this thesis, to a graph and later, more generally, to a simplicial complex, we associate a lattice polytope: more precisely, we consider the symmetric edge polytope of a graph and Laplacian polytopes of simplicial complexes. Lattice polytopes appear and play a role in various fields of mathematics including algebraic geometry and commutative algebra [BH98; Sta80; Stu96], optimization [Sch86; Sch03] and combinatorics [BR15; Sta80; Zie95].

An example for a family of lattice polytopes associated to graphs is the family of symmetric edge polytopes [Hib+10]. There has been a surge of interest in this topic in recent years for their intrinsic combinatorial and geometric properties [CDK23; HKM17; Mat+11; OT21a; OT21b] as well as their relations to metric space theory

[DH20; GP17; Ver15], optimal transport [Çel+21] and physics, where they appear in the context of the Kuramoto synchronization model [Che19; CDM18; DDM22]. There are several pleasant properties that are shared by all symmetric edge polytope. Since a symmetric edge polytope is reflexive [Hig15] and admits a pulling regular unimodular triangulation [HO14; HJM19], the restriction yields a unimodular triangulation of its boundary complex as well. In addition, due to reflexivity, the h^*-vector of a symmetric edge polytope is symmetric [Hib92] and coincides with the h-vector of the triangulation of the boundary [Sta80, Corollary 2.5], which, in particular, is a simplicial sphere. Therefore, questions concerning simplicial spheres can be investigated in this case. This provides a link between the study of the γ-vector of symmetric edge polytopes and the rich world of conjectures on the γ-non-negativity of simplicial spheres. The non-negativity is of special interest since it implies unimodality of the underlying symmetric h-vector [Pet15, Observation 4.1]. For a non-negative h-vector, unimodality is also implied by the stronger property of real-rootedness of the h-polynomial [Brä15, Lemma 1.1], though this is not the case for h-polynomials of the triangulations of boundaries of symmetric edge polytopes in general; the 5-cycle is a counterexample. One of the most prominent objects studied in topological combinatorics is the h-vector of a simplicial sphere. For flag spheres, Gal's conjecture [Gal05] states that the γ-vectors are non-negative. Several related conjectures exist, including the Charney–Davis conjecture [CD95], claiming non-negativity only for the last entry of the γ-vector, and the Nevo–Petersen conjecture [NP11] which even postulates that the γ-vector of a flag sphere is the f-vector of a balanced simplicial complex. Those conjectures have been a very active area of research in the last few years. However, even though proofs have been provided in special cases [Ais14; AV20; Ath12; DO01; Gal05; LN17; NP11; NPT11] and new approaches have been developed towards their solution [CN20; CN22], they remain wide open in general. Note that symmetric edge polytopes are not flag in general; nevertheless, the lack of flagness, in all the cases known so far, the γ-vector of any symmetric edge polytope is non-negative. This led Ohsugi and Tsuchiya to formulate their non-negativity conjecture for γ-vectors of symmetric edge polytopes [OT21b, Conjecture 5.11]. This conjecture has been verified for special classes of graphs, mostly by direct computation. As shown in [OT21b, Section 5.3], these classes encompass cycles, suspensions of graphs (which includes both complete graphs and wheels), outerplanar bipartite graphs and complete bipartite graphs. The latter was originally proved in [HJM19] but was generalized in [OT21b] to a larger class of bipartite graphs.

Another way of associating a lattice polytope to a given simple graph was introduced by Braun and Meyer in 2017 [BM17]. They defined Laplacian simplices as the convex hull of the columns of the Laplacian matrix of a graph. These polytopes were further studied from a coding theory perspective [MT18]. Furthermore, the definition of Laplacian simplices was later extended from simple to directed graphs [Bal+18]. Since each simple graph can be seen as a 1-dimensional simplicial complex, and since to each simplicial complex, we can associate Laplacian matrices defined via their boundary maps in simplicial homology, it is natural to extend the definition of Laplacian simplices to arbitrary simplicial complexes and their Laplacian matrices. This yields a new family of lattice polytopes, the study of which is initiated in this thesis.

The original contributions of this thesis are contained in Chapters 2, 3, 4 and 5, whose content can be found in the preprints [JKK23; JKKS21] and the publications [D'A+23; KS23].

Summary of the thesis

Chapter 1 provides relevant background and notions. We start with graphs in general and then focus on the main objects of Chapter 2 and Chapter 3, horizontal visibility graphs, and prove some basic properties of these. Next, we introduce background on simplicial complexes, a generalization of graphs. Lastly, we turn to lattice polytopes. Here, the main focus lies on the theory of lattice point enumeration, known as Ehrhart theory, and triangulations with their connection to Gröbner bases.

In Chapter 2, we study horizontal visibility graphs. We first focus on HVGs corresponding to data sequences with pairwise distinct entries. After providing a specific data sequence that realizes a given HVG (see Theorem 2.1.1), we prove that HVGs from data sequences without equal entries are uniquely determined by their ordered vertex degree sequence (see Theorem 2.0.1). This improves the results from [LL17] and [O'P19] by weakening the assumptions on the HVG and requiring less information to guarantee uniqueness, respectively. Moreover, we provide an explicit algorithm to reconstruct an HVG from its ordered vertex degree sequence (see Remark 2.1.7). We then take a similar viewpoint as in [GMS11], where HVGs are studied from a purely combinatorial perspective and connections with several combinatorial statistics are established. More precisely, we are interested in the number of HVGs on a fixed number of vertices corresponding to data sequences with and without equal entries, where we consider two HVGs equal if they are equal as labeled graphs. Surprisingly, Catalan numbers and large Schröder numbers determine those cardinalities. More precisely, we show that the number of HVGs on N vertices corresponding to data sequences without equal entries equals the $(N-1)^{\text{st}}$ Catalan number (see Theorem 2.0.2 (i)), and the cardinality of an HVG on N vertices corresponding to arbitrary data sequences is given by the $(N-2)^{\text{nd}}$ Schröder number (see Theorem 2.0.2 (ii)). For the result on Catalan numbers, we provide two different proofs: one purely algebraic and one via a bijection to the set of balanced parentheses of length $N-1$. To determine the number of HVGs corresponding to arbitrary data sequences, we first provide a specific data sequence that realizes a given HVG (see Theorem 2.2.1), analogous to the case of HVGs corresponding to distinct data. The main step to show Theorem 2.0.2 (ii) is to construct a bijection between HVGs on N vertices not containing the edge $1N$ and bracketings of a string of $N-1$ identical letters, which are known to be counted by the $(N-2)^{\text{nd}}$ little Schröder number (see Theorem 2.2.4).

Chapter 3 focuses on algorithmic aspects of HVGs. We are interested in the computability of HVGs given an arbitrary data sequence of length N. We start with a short survey about known approaches and algorithms, whose complexities range from $O(N^2)$ to $O(N \log N)$ in the average case [Che+15; Yel+20] to a linear runtime $O(N)$ in best [Bal+09; Lac+12] or even worst case [LWZ12; Ste21] scenarios. Some of these algorithms show heavy dependence on the structure of the given data sequence. Although, the approach in [Ste21] already has a desirable complexity, its drawback is that it uses a complex data structure to achieve this. Our algorithm builds on the algorithm in [LWZ12]. The latter algorithm has runtime $O(N)$, but a proof of its correctness is missing. Moreover, the proof of complexity of the algorithm in [LWZ12] relies on it being correct. Another drawback of this algorithm is that it does not work on streamed data. Our algorithm constructs an HVG for every possible time series and works in linear time with only minor fluctuations in runtime for different types of time series while in contrast to [Ste21] not requiring a complex data structure (see Section 3.2). Furthermore, the HVG of every intermediate time series is generated implicitly if the algorithm is stopped prematurely. We further prove its correctness (see Theorem 3.2.1) and provide a proof that it is worst-case in $O(N)$ (see Theorem 3.2.2). Thus its runtime is independent of the structure of the sequence. Moreover, the algorithm has online functionality (see Subsection 3.2.3), i.e., it works on streamed data, and can be used for multi-processing (see Subsection 3.2.4). This allows for the computation of HVGs with millions of vertices within a few minutes or even seconds, opening up new application areas of HVGs for time series generated batch-wise or resulting from measurements with a high sampling rate. We verify and compare our observations to the given algorithms on some numerical experiments on synthetic and real world data (see Section 3.3).

In Chapter 4, the central objects of interest are symmetric edge polytopes. We start by providing some basic properties of symmetric edge polytopes and characterizing their edges (see Theorem 4.1.3). Moreover, we classify all graphs having a simple symmetric edge polytope (see Proposition 4.1.5). We then shift our focus to γ-vectors associated to the h^*-vectors of symmetric edge polytopes. The main goal of this chapter is to provide supporting evidence for the γ-non-negativity conjecture of Oshugi and Tsuchiya [OT21b, Conjecture 5.11], which, in contrast to previously known results in this direction, is independent of the associated graph.

We take two different approaches: a deterministic and a probabilistic one. In the deterministic part, we focus on the coefficient γ_2 of a symmetric edge polytope $\mathcal{P}_G$ of a graph G. Through some delicate combinatorial analysis, we are able to prove that γ_2 is always non-negative (see Theorem 4.2.2). Moreover, we provide a characterization of those graphs for which $\gamma_2(\mathcal{P}_G) = 0$ (see Theorem 4.2.12 and Corollary 4.2.13). We want to point out that the symmetric edge polytopes of the graphs from the characterization in the case of equality indeed admit a flag triangulation. This justifies that, as an application, we confirm a conjecture by Lutz and Nevo [LN16, Conjecture 6.1] characterizing flag piecewise linear spheres with $\gamma_2 = 0$, in the restricted context of some natural Gröbner-induced triangulations of boundaries of symmetric edge polytopes (see Theorem 4.3.4). Using a simple but elegant argument, we also show non-negativity of γ_1 (see Corollary 4.2.4), a result that was later confirmed by [KT22, Theorem 4.1.] in a more complex way using Jaeger trees.

Finally, the last section brings random graphs into the picture. The Erdős-Rényi model $G(n, p(n))$ is one of the most popular and well-studied ways to generate a random graph on the vertex set $[n]$. We consider the case where $p(n) = n^{-\beta}$ for a real number $\beta > 0$. We address the following question: for an Erdős-Rényi graph $G \in G(n, p(n))$, what is the probability that all of the entries of the γ-vector of $\mathcal{P}_G$ are non-negative? As an extension, we pose the question of how *big* those entries are most likely to be. With our main result, we are able to answer both questions in two regimes: subcritical ($\beta > 1$) and supercritical ($0 < \beta < 1$) (see Theorem A). More precisely, in the subcritical regime, we show that asymptotically almost surely $\gamma_\ell = 0$ for all $\ell \geq 1$ (see Theorem 4.4.5). Furthermore, in the supercritical regime, $0 < \beta < 1$, we prove that asymptotically almost surely $\gamma_\ell \in \Theta(n^{(2-\beta)\ell})$ for every $0 < \ell \leq k$ and any fixed integer k (see Theorem 4.4.12). In particular, this shows that $\gamma_\ell \geq 0$ for $1 \leq \ell \leq k$ with high probability, thereby proving that (up to a fixed entry of the γ-vector) Gal's conjecture [Gal05] holds with high probability. For the proof, we derive concentration inequalities for the number of non-faces and faces of the triangulation of $\mathcal{P}_G$ studied in [HJM19, Proposition 3.8]. We do not address the critical regime $\beta = 1$.

Extending the approach of [BM17] in Chapter 5, we define Laplacian polytopes of simplicial complexes (see Definition 5.2.1). We initiate this study by establishing some general combinatorial and geometric properties of these polytopes and then focus on the particular case in which the underlying simplicial complex is the boundary of a simplex. In the general case, we determine the number of vertices (see Proposition 5.2.4) and provide a criterion for the Laplacian polytope to be a simplex based on simplicial homology (see Proposition 5.2.5). We then consider the situation in which the underlying simplicial complex is the boundary of the $(d+1)$-simplex restricting exclusively to its highest Laplacian. We determine the dimension of these particular Laplacian polytopes (see Proposition 5.2.6) and prove simpliciality (see Theorem 5.2.8). Though Laplacian polytopes are never full-dimensional, we provide a full-dimensional unimodular equivalent polytope in this special setting (see Lemma 5.2.10). Through a slight abuse of notation, we will also call this polytope the Laplacian polytope. This is justified since we are only investigating combinatorial properties that are preserved under unimodular equivalence. If d is even, it can easily be seen that the Laplacian polytope is a $(d+1)$-simplex (see Corollary 5.2.7), as for graphs. If d is odd, the situation is more complicated. By deriving a complete facet description (see Theorem 5.3.3) in this case, we are able to show that the Laplacian polytope is combinatorially equivalent to a d-dimensional cyclic polytope on $d+2$ vertices (see Theorem 5.3.4). The first main theorem guarantees the existence of a regular unimodular triangulation for every integer d (see Theorem B). As a byproduct of the proof of Theorem B, we can also compute the normalized volume of the Laplacian polytope (see Corollary 5.4.7). Moreover, Theorem B is one of the key ingredients for our second main theorem, which states that the h^*-polynomial of the Laplacian polytope has only real roots for every odd integer d, and that its h^*-vector is unimodal for all integers d (see Theorem C).

Acknowledgements

The first person I have to thank is my advisor Martina Juhnke-Kubitzke. Without her excellent guidance already during my masters thesis and her encouragement, I would not even have started my PhD. I am especially grateful to her for her invaluable help, for always having an open door whenever I had questions and taking the time to listen and talk, for all the time and work she spent on my projects and giving me new ideas, for pointing out workshops and also providing the opportunities to visit them, and for a really pleasant time at the university, both personally and work-wise.

I also very much want to thank Lorenzo Venturello and Alessio D'Alì. They both always had an open ear for my numerous (and probably often trivial) questions and took their time to help me understand. Thanks to both for the nice meetings while collaborating. A special thanks to Lorenzo for the enjoyable time at the combinatorial coworkspace in Kleinwalsertal, on and off the slope.

With Jonas Schmidt I spend many hours working on horizontal visibility graphs where most of these had to take place virtually due to the corona virus. Nonetheless, it was always a pleasure talking to him about work and also everything and anything.

A big thank you goes to Mathias Hockmann who accompanied me throughout my bachelor, master and my PhD at the University of Osnabrück. We first met in the mathematical preliminary course during our first semester as freshmen. During our studies at the University of Osnabrück, we took several courses together and almost always collaborated on our exercises. I owe him a lot since, at least during the bachelor, he was usually the one who made sure that we earned enough points on the exercises – and because he often took oral exams before me, I was able to benefit from his advice.

I am really grateful that I met Justus Bruckamp and Tarek Emmrich. They both became PhD students of Martina's group during my last one-and-a-half years, and it was a pleasure working and laughing together and of course spending time together during lunch, at the office during numerous breaks and at the workshop in Bielefeld. Of course, I also want to thank the other PhD students and postdocs for the nice times at lunch, playing cards, going out for dinner and for attending the pub quiz at The Red Shamrock: Christian Ahring, Paul Catala, Lianne de Jonge, Xiaowen Dong, Sarah Eggleston, Bernhard Hafer, Kumar Harsha, Fynn Pörtner and Anna Strotmann. Also, thanks to all professors in the department. I have always felt very welcome to come and ask questions without hesitation. Thanks to Marianne Gausmann, and all of the secretaries at the institute, who helped with every bureaucracy involved in completing a PhD. I wish to thank Jan-Marten Brunink and Alexander Nover for their help during my first days in the office. I am thankful that I had the chance to meet you all and for the pleasant atmosphere in the department that made me really enjoy my time working at the institute.

I would also like to thank all the people who made the workshop at the American Institute of Mathematics in San José as enjoyable as it was. I especially want to thank Derek Hanely, Giulia Codenotti, Esme Bajo and Marie Meyer for the nice conversations, many games of pickleball and rounds of board games in the evening, and the organizers of the workshop for having invited me.

A special and big thanks goes again to Derek Hanely and Sarah Eggleston for proof-reading parts of this thesis.

Last but not least, I have to thank my family and friends. Above all, thanks to my parents Jutta and Markus: thank you for your constant unconditional support, your advice in every situation, your care and love and for always having my back, no matter what. This would not have been possible without you. Thanks to both of my grandmothers Anneliese and Wilma for being proud of what I do without really understanding much of it. And thanks to my sister Theresa, my brother Tobias, and Axel, Susanne, Michael, Conny, Mechthild and all of my friends for being there, especially at times when having a distraction was exactly what I needed.

Chapter 1

Background on graphs, simplicial complexes and polytopes

In this chapter, we provide the relevant definitions and notations concerning graph theory, in particular horizontal visibility graphs, simplicial complexes and polytope theory. For more background, we refer to [Bal+09; Die17; GMS11] and [Aig06, Chapter 6 and Chapter 7] for graphs, to [BH98, Section 5.1], [Gol02] and [Sta96, Chapter 2] for simplicial complexes and to [Zie95], [BG09, Part 1], [BH98, Section 5.2] and [Stu96, Chapter 8] for polytopes and triangulations.

1.1 Graphs

1.1.1 Basic notion

An (undirected) *simple graph* is a pair $G = (V(G), E(G))$ where $V(G)$ is a set and $E(G) \subseteq \binom{V}{2}$ is a set of two-element subsets of V. We often write V and E instead of $V(G)$ and $E(G)$, respectively, if it is clear from context which graph we are referring to. The elements of V are called *vertices* and the ones of E *edges*. We set $[n] := \{1, \dots, n\}$ and $[m, n] := \{m, m+1, \dots, n\}$ for $m, n \in \mathbb{N}$. Most of the time, we will set $V = [n]$. For an edge $\{v, w\} \in E$, we use the shorthand notation vw. If $vw \in E$, v and w are called *neighbors* and the set of all neighbors of v is denoted by $N(v)$. The *degree* of a vertex $v \in V$ is the number $\delta_G(v) = |N(v)|$. Often, we will omit the subscript if G is clear from context. For $V = \{v_1, \dots, v_n\}$, the sequence $\Delta(G) = (\delta(v_1), \dots, \delta(v_n))$ is called the *(ordered) degree sequence* of G. By abuse of notation, we will also use $\Delta(G) = (\delta_{v_1}, \dots, \delta_{v_n})$. The *adjacency matrix* $A = (a_{ij})_{1 \le i,j \le n}$ of G is the $(n \times n)$-matrix indexed by the vertices $v_1, \dots, v_n \in V$, where $a_{ij} = 1$ if $v_i v_j \in E$ and $a_{ij} = 0$, otherwise. The graph $P_n = ([n], \{12, 23, \dots, (n-1)n\})$ on n distinct vertices is called a *path* of length $n-1$, or n-*path*. A *cycle* of length n, or n-*cycle*, denoted by C_n, is the graph $C_n = (\{v_1, \dots, v_n\}, \{v_1 v_2, \dots, v_{n-1} v_n, v_n v_1\})$ on n distinct vertices. A connected graph which has no cycles is a *tree*. If all components are trees, we call the graph a *forest*. We further use K_n and $K_{n,m}$ to denote the complete graph on n vertices and the complete bipartite graph on n and m vertices, respectively. A graph G on vertex set $[n]$ is called *non-crossing* if there are no vertices $i < j < k < \ell$ with $\{(i,k), (j,\ell)\} \subseteq E(G)$. Intuitively, this means that one can draw the vertices $1, \dots, n$ on a horizontal line such that all edges are on or above this line and there is no pair of edges that cross. Similarly, a vertex $i \in [n]$ is called *nested* if there exist $1 \le j < i < k \le n$ such that $jk \in E(G)$. Otherwise, i is called *non-nested*. We use $\mathcal{N}(G)$ to denote the set of all non-nested vertices of G. And for $i \in [n-1]$ we denote by $m_G(i)$ the *maximal* neighbor of the vertex i in G, i.e.,

$$m_G(i) = \max\{1 \le \ell \le n \ : \ i\ell \in E\}.$$

If two graphs G and H both contain a subgraph isomorphic to a k-clique K_k, the graph $G \oplus_k H$ obtained by gluing G and H together along K_k is called the *k-clique sum* of G and H. The *distance* $d(u,v)$ between vertices u and v is given as the length of a shortest path from u to v. We denote by $G \cup e$ and $G \smallsetminus e$ the graph obtained from G by *adding* and *removing* an edge $e \in E(G)$, respectively. We define *deleting* a vertex set $V' \subseteq V$ as $G \smallsetminus V' = (V \smallsetminus V', E \smallsetminus \{e \ : \ e \cap V' \neq \emptyset\})$. Given $W \subseteq V$, the subgraph *induced* by W is the graph $G_W = (W, \{uv \in E \ : \ u, v \in W\})$. The *cyclomatic number* of a graph G with c connected components is defined as $\mathrm{cy}(G) = |E| - |V| + c$. Note, $\mathrm{cy}(G) \ge 0$ for all G. It is well-known that G is 2-connected if and only if it has an *open ear decomposition*, meaning that G is either a cycle (the closed ear) or can be obtained from a cycle by successively attaching paths (the open ears) whose internal vertices are disjoint from the previous ears and whose distinct two end vertices belong to the already constructed graph. It is easy to see that the number of ears in any such decomposition equals the cyclomatic number of G. Moreover, every graph decomposes uniquely into its 2-*connected components*, i.e., inclusion-maximal 2-connected subgraphs, and single edges.

1.1.2 Horizontal visibility graphs

In Chapter 2 and Chapter 3, we will focus on horizontal visibility graphs. They were introduced in [Bal+09], where it was shown that the degree distribution of these graphs can be used as a simple tool to discriminate randomness in time series. Moreover, HVGs have found applications in many different areas. Besides physics, where they are employed in optics [Ara+16], plasma physics [ATMP21] (in a directed version), fluid dynamics [MPT15] or the fault diagnosis of rolling bearings [GWY20], their usage ranges from finance [RS18] to the EEG analysis of epileptics in physiology [DDK13], to the identification of alcoholic patients in neuroscience [Li+14]. In many of those applications, simple metrics such as the vertex degree sequence, the graph entropy and moments have shown to be particularly helpful indicators for the classification of the considered data sequences.

Definition 1.1.1. *Given $D = (d_1, \dots, d_N) \in \mathbb{R}^N$, the* horizontal visibility graph *(or* HVG *for short) of D is the graph* $\mathrm{HVG}(D) = ([N], E)$, *where*

$$E = \{ij \ : \ d_i > d_k < d_j \textit{ for all } 1 \le i < k < j \le N\}.$$

See Figure 1.1 for an example of a data sequence and its corresponding HVG. Since an HVG is clearly invariant under translation of the underlying sequence D by any vector with equal entries, it does not cause any restriction to consider only non-negative data sequences. This also makes sense from the point of view of applications since D is usually a data sequence or time series with non-negative entries. Further, applications motivate the convention that HVGs have to be considered as graphs with fixed vertex labels $1, \dots, N$. Consequently, two HVGs are considered to be the same if and only if their edge sets are the same and not just if they are isomorphic as unlabeled graphs, i.e., with this labeling all HVGs are different. We set $\mathcal{G}_N = \{\mathrm{HVG}(D) \ : \ D \in \mathbb{R}^N_{\ge 0}\}$ and $\mathcal{G}_{N,\neq} = \{\mathrm{HVG}(D) \ : \ D = (d_1, \dots, d_N) \in \mathbb{R}^N_{\ge 0},\ d_i \neq d_j \text{ for all } 1 \le i < j \le N\}$. We note that those two sets are different for $N \ge 4$ (see Example 1.1.4) and that P_N is the (inclusion)-minimal HVG in both $\mathcal{G}_N$ and $\mathcal{G}_{N,\neq}$.

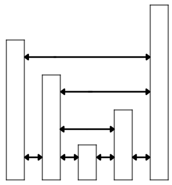

(A) Arrows between entries of D indicate edges in the corresponding HVG.

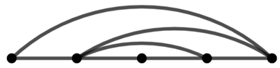

(B) The HVG associated to $D = (4, 3, 1, 2, 5)$.

FIGURE 1.1: The data sequence $D = (4, 3, 1, 2, 5)$ and its associated HVG.

Remark 1.1.2. *Let $D = (d_1, \dots, d_N) \in \mathbb{R}^N$. We define $\Phi_N : \mathbb{R}^N \to [N]^N$ by*

$$\Phi_N(D)_i = |\{j \ : \ d_j \le d_i\}| \quad \text{for } 1 \le i \le N.$$

i.e., $\Phi(D)$ reflects the order of the entries of D, and, clearly, $\mathrm{HVG}(D) = \mathrm{HVG}(\Phi(D))$. Hence, any HVG is the HVG of a vector of non-negative integers (of size at most N). Moreover, if all entries of D are distinct, then $\Phi(D)$ is a permutation of $[N]$.

We summarize some easy but useful properties of HVGs in the following lemma. First, we introduce a simple graph operation. Given $G \in \mathcal{G}_N$ and $H \in \mathcal{G}_M$, we use $G + H$ to denote the 1-sum of G and H with respect to the vertices $N \in V(G)$ and $1 \in V(H)$, i.e., $G + H$ is obtained by taking the union of G and H and identifying the vertices $N \in V(G)$ and $1 \in V(H)$. Abusing notation, we do not use $G \oplus_1 H$ here, since we want to stress that the 1-sum is with respect to the vertices 1 and N. To simplify notation, vertices of $V(H) \setminus \{1\}$ will be numbered with $N+1, \dots, N+M-1$ in $G + H$, and the identified vertex will be numbered with N.

Lemma 1.1.3. *Let $N \in \mathbb{N}$ and $G \in \mathcal{G}_N$. Let $\mathcal{N}(G) = \{i_1 < \dots < i_k\}$ and let $\ell \in \mathcal{N}(G)$. Then*

(i) G *is non-crossing.*

(ii) 1*,* N *and* $m_G(\ell)$ *are non-nested.*

(iii) *Let $1 \le i < j \le N$, then (after relabelling the vertices) $G_{[i,j]} \in \mathcal{G}_{j-i+1}$. Moreover, if $G \in \mathcal{G}_{N,\neq}$, then $G_{[i,j]} \in \mathcal{G}_{j-i+1,\neq}$.*

(iv) $i_j i_m \in E(G)$ *if and only if* $m = j+1$ *or* $m = j-1$*.*

(v) *There exists $D = (d_1, \dots, d_N) \in \mathbb{N}^N$ such that $\mathrm{HVG}(D) = G$ and $d_1 = N$. Moreover, D can be chosen as a permutation if $G \in \mathcal{G}_{N,\neq}$.*

(vi) $G = G_{[i_1,i_2]} + \dots + G_{[i_{k-1},i_k]}$.

Proof. (i) was shown in [GMS11, Corollary 5].

For (ii) note that 1 and N are non-nested by definition. Now assume by contradiction that $m_G(\ell) \notin \mathcal{N}(G)$. Together with (i), it follows that there exist $i < \ell < m_G(\ell) < m$ with $im \in E(G)$. But then ℓ is nested, a contradiction.

For (iii) it suffices to note that after relabelling the vertices of $G_{[i,j]}$ by $1, \dots, j-i+1$ increasingly, $G_{[i,j]} = \mathrm{HVG}((d_i, d_{i+1}, \dots, d_j))$, where $G = \mathrm{HVG}((d_1, \dots, d_N))$. The second statement readily follows.

For (iv), let $i_m \in \mathcal{N}(G) \setminus \{N\}$. (ii) implies that $m_G(i_m) = i_j$ for some j. Moreover, we must have $j = m+1$ since otherwise $i_{m+1} \notin \mathcal{N}(G)$. This shows $i_m i_{m+1} \in E(G)$. The same argument also shows that $i_m i_j \notin E(G)$ if $j \ge m+2$. The claim follows.

(v) This is an easy consequence of Theorem 2.1.1 and Theorem 2.2.1.
(vi) follows from (iii) and (iv). □

We provide an example to illustrate the difference between $\mathcal{G}_N \setminus \mathcal{G}_{N,\neq}$.

Example 1.1.4. *The graph* $G = \mathrm{HVG}((3,1,1,4))$*, shown in Figure 1.2, is the (inclusion-wise) smallest HVG that cannot be realized by a sequence with pairwise distinct entries, i.e.,* $G \in \mathcal{G}_4 \setminus \mathcal{G}_{4,\neq}$*. The sequence* $(4,1,1,3)$ *yields the same HVG and satisfies the first assumption from (v) of the previous lemma.*

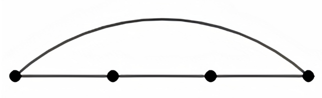

FIGURE 1.2: The HVG $G = \mathrm{HVG}((4,1,1,3))$.

Motivated by Lemma 1.1.3 (iii), it is natural to ask if the set of all HVGs (without fixing the vertex set) is closed under certain graph operations.

Lemma 1.1.5. *Let* $M, N \in \mathbb{N}$*,* $G \in \mathcal{G}_N$*,* $H \in \mathcal{G}_M$ *and* $e \in E(G) \setminus \{i(i+1) : 1 \leq i \leq N-1\}$*. Then:*

(i) $G \setminus e \in \mathcal{G}_N$*.*

(ii) If $j, \ell \in \mathcal{N}(G)$ *with* $f = j\ell \notin E(G)$*, then* $G \cup f \in \mathcal{G}_N$*.*

(iii) $G + H \in \mathcal{G}_{N+M-1}$*. Moreover, if* $G \in \mathcal{G}_{N,\neq}$ *and* $H \in \mathcal{G}_{N,\neq}$*, then* $G + H \in \mathcal{G}_{N+M-1,\neq}$*.*

Before providing the proof of this lemma, we remark that (i) and (ii) are not true if one restricts to $\mathcal{G}_{N,\neq}$. For instance, the graph G in Figure 1.2 is obtained from $G \cup \{13\} \in \mathcal{G}_{4,\neq}$ and $P_4 \in \mathcal{G}_{4,\neq}$ by removing and adding the edge 13 and 14, respectively.

Proof. Let $D = (d_1, \ldots, d_N) \in \mathbb{N}^N$ such that $\mathrm{HVG}(D) = G$. For (i) assume that $e = k\ell$ with $k < \ell$. Let $m = \max\{d_i : k < i < \ell\}$ and let $M = \{k < i < \ell : d_i = m\}$. Define $\widetilde{D} = (\widetilde{d}_1, \ldots, \widetilde{d}_N)$ by

$$\widetilde{d}_i = \begin{cases} d_i, & \text{if } i \notin M \\ \min(d_k, d_\ell), & \text{if } i \in M. \end{cases}$$

It is straightforward to show that $\mathrm{HVG}(\widetilde{D}) = G \setminus e$, which proves the claim.

For (ii) let $m = \max\{d_i : i \in \mathcal{N}(G), j \leq i \leq \ell\}$ and set

$$\widetilde{d}_i = \begin{cases} m+1, & \text{if } i \in \{j, \ell\} \\ m, & \text{if } i \in \mathcal{N}(G) \text{ and } j < i < \ell \\ d_i, & \text{otherwise.} \end{cases}$$

It is easy to see that $\mathrm{HVG}(\widetilde{D}) \supset G \cup f$. If there exists $e \in E(\mathrm{HVG}(\widetilde{D})) \setminus E(G \cup f)$, then we can apply (i) and delete those edges.

For (iii) we can assume by Lemma 1.1.3 (v) that $d_1 = N$. Further, let $F = (f_1, \ldots, f_M) \in \mathbb{N}^M$ with $\mathrm{HVG}(F) = H$ and $f_1 = M$. Define $K = (k_1, \ldots, k_{M+N-1}) \in \mathbb{N}^{M+N-1}$ by

$$k_i = \begin{cases} d_i + M & \text{if } 1 \leq i \leq N \\ f_{i-N+1} & \text{if } N < i \leq M+N-1 \end{cases}$$

and set $J = \mathrm{HVG}(K)$. We obviously have $J_{[N]} = G$, and since $k_N = d_N + M > M = f_1 \geq f_{i-N+1}$ for all $N < i \leq M+N-1$ it also holds that $J_{[N,N+M-1]} = H$. The same argument shows that $ij \notin E(J)$ for any $1 \le i < N$ and $N < j \le M + N - 1$, which, together with the previous discussion, implies $J = G + H$. Hence $G + H \in \mathcal{G}_{N+M-1}$. Moreover, if D and F have only distinct entries, so does K, which shows the second claim. □

Remark 1.1.6. *Combining Lemma 1.1.3 (iii) and (vi) with Lemma 1.1.5 (i) and (ii), it is easy to see that if $G \in \mathcal{G}_N$ and $1 \le j < \ell \le N$ such that $G \cup j\ell$ is non-crossing, then $G \cup j\ell \in \mathcal{G}_N$.*

1.2 Simplicial complexes and Laplacian matrices

A *simplicial complex* Δ on a vertex set $V(\Delta)$ is any collection of subsets of $V(\Delta)$ closed under inclusion. We also use V instead of $V(\Delta)$ if Δ is clear from context. A simplicial complex Δ is *finite* if V is. In this thesis, we always assume our simplicial complexes to be finite. The elements of Δ are called *faces*, and a face that is maximal with respect to inclusion is called a *facet*. A subset of $V(\Delta)$ that is not in Δ is a *non-face*. A non-face is called *minimal* if it is minimal with respect to inclusion. A simplicial complex is called a *flag* complex if the minimal non-faces have cardinality 2. We will sometimes write $\langle F_1, ..., F_m\rangle$ to denote the simplicial complex with facets $F_1, ..., F_m$. The *dimension* of a face F is defined as $\dim(F) := |F| - 1$, and the dimension of Δ is $\dim(\Delta) = \max(\dim(F) \ : \ F \in \Delta)$. We use $F_i(\Delta)$ to denote the set of i-dimensional faces of Δ. 0-dimensional and 1-dimensional faces of Δ are called *vertices* and *edges*, respectively. If all facets of Δ have the same dimension, Δ is said to be *pure*. The 1-skeleton of Δ is the simplicial complex consisting of all edges and vertices of Δ, and thus can be understood as a graph. We also refer to the 1-skeleton as the *graph* of Δ. We let $\sigma_d = \{F \ : \ F \subseteq [d+1]\}$ be the *d-simplex* and we use $\partial(\sigma_d)$ to denote its boundary, i.e., $\partial(\sigma_d) = \sigma_d \smallsetminus \{[d+1]\}$. A d-dimensional simplicial complex Δ homeomorphic to a sphere is also called a *(simplicial) sphere* or d-sphere for short. Given a $(d-1)$-dimensional simplicial complex Δ, its f-vector $f(\Delta) = (f_{-1}(\Delta), f_0(\Delta), \dots, f_{d-1}(\Delta))$ is defined by $f_i(\Delta) = |\{f \in \Delta \ : \ \dim(F) = i\}|$ for $-1 \le i \le d-1$ and its *h-vector* $h(\Delta) = (h_0(\Delta), h_1(\Delta), \dots, h_d(\Delta))$ by the polynomial equality

$$\sum_{k=0}^{d} h_k(\Delta) \cdot t^{d-k} = \sum_{k=0}^{d} f_{k-1}(\Delta) \cdot (t-1)^{d-k},$$

which yields

$$h_j(\Delta) = \sum_{i=0}^{j} (-1)^{j-i} \binom{d-i}{d-j} f_{i-1}(\Delta). \tag{1.1}$$

The polynomial $h(\Delta; x) = \sum_{i=0}^{d} h_i(\Delta) x^i$ is called the *h-polynomial* of Δ. If $h(\Delta)$ is *symmetric*, i.e., $h_i(\Delta) = h_{d-i}(\Delta)$ for every choice of i, the γ-vector $\gamma(\Delta) = (\gamma_0(\Delta), \gamma_1(\Delta), \dots, \gamma_{\lfloor \frac{d}{2} \rfloor}(\Delta))$ of Δ is defined via the following change of basis:

$$h(\Delta; x) = \sum_{i=0}^{\lfloor \frac{d}{2} \rfloor} \gamma_i(\Delta) x^i (1+x)^{d-2i}. \tag{1.2}$$

Thus, $\gamma(\Delta)$ stores the same information as $h(\Delta)$ in a more compact form.

We call the polynomial $\gamma(\Delta; x)$ the *γ-polynomial* of Δ. More generally, in the same way, one can associate a γ-vector $\gamma(v)$ and γ-polynomial $\gamma(p; x)$ with any symmetric vector v and symmetric polynomial p. The following lemma can easily be seen by induction.

Lemma 1.2.1. *Let $p(x), p_1(x), \dots, p_k(x)$ be symmetric polynomials. Then $p(x) = \prod_{i=1}^k p_i(x)$ if and only if $\gamma(p;x) = \prod_{i=1}^k \gamma(p_i;x)$.*

The γ-vector of simplicial spheres has been studied extensively as described on page 2 of the Introduction with several open conjectures existing. One of the most recent once in the context of symmetric edge polytopes was formulated by Ohsugi and Tsuchiya [OT21b, Conjecture 5.11] stating the non-negativity of the γ-vector of any symmetric edge polytopes and will be the the starting point of Chapter 4.

One way to study a simplicial complex Δ locally is to look at the *link* of a face F, i.e., the subcomplex of Δ defined as $\mathrm{lk}_\Delta(F) = \{H \in \Delta \ : \ H \cap F = \emptyset, \ F \cup H \in \Delta\}$. For an edge $F = \{v, w\} \in \Delta$, the *edge contraction* Δ/F of Δ at F is the simplicial complex obtained from Δ by identifying v with w in all faces of Δ, i.e., $\Delta/F = \{H \in \Delta \ : \ v \notin H\} \cup \{H \setminus \{v\} \cup \{w\} \ : \ v \in H\}$. The *face deletion* $\Delta \setminus F$ of a face $F \in \Delta$ from Δ is defined as $\Delta \setminus F = \{H \in \Delta \ : \ F \notin H\}$. Given simplicial complexes Δ and Γ, the simplicial complex $\Delta \star \Gamma = \{F \cup H \ : \ F \in \Delta, \ H \in \Gamma\}$ is called the *join* of Δ and Γ.

In order to introduce general Laplacian matrices of a simplicial complex Δ, we need to recall some basic notions from simplicial homology. For this purpose, let Δ be a $(d-1)$-dimensional simplicial complex on vertex set V, and assume that the vertices are ordered. Without loss of generality, assume $V = [n] = \{1, \dots, n\}$ endowed with the natural ordering induced by $\mathbb{N}$. We denote by $C_i(\Delta)$ the $\mathbb{Q}$-vector space with basis $\{e_\sigma \ : \ \sigma \in F_i(\Delta)\}$ and set $C_i(\Delta) = \{0\}$ for $i \leq -1$ and $i > n-1$. The i^{th} *boundary map* is the linear map $\partial_i : C_i(\Delta) \to C_{i-1}(\Delta)$ defined by

$$\partial_i(e_\sigma) \coloneqq \sum_{k=1}^{i+1} (-1)^{k-1} e_{\sigma \setminus \{j_k\}}, \tag{1.3}$$

where $\sigma = \{j_1 < \ldots < j_{i+1}\} \in F_i(\Delta)$. By abuse of notation, we will use ∂_i to denote both the map and its corresponding matrix. The i^{th} *Laplacian matrix of* Δ is defined as $\mathcal{L}_i(\Delta) = \partial_{i+1}\partial_{i+1}^\top + \partial_i^\top \partial_i$. Note that $\mathcal{L}_i(\Delta)$ provides a linear map from $C_i(\Delta)$ to itself which depends on the chosen ordering of the vertices. We recall that $H_i(\Delta;\mathbb{Q}) = \ker(\partial_i)/\mathrm{Im}(\partial_{i+1})$ is the i^{th} *(simplicial) homology group* of Δ. To provide an explicit description of $\mathcal{L}_i(\Delta)$, we need some further notation. Faces $F, G \in F_i(\Delta)$ are called *lower adjacent* if $F \cap G \in F_{i-1}(\Delta)$. If, additionally, $e_{F \cap G}$ appears with the same sign in $\partial_i(e_F)$ and $\partial_i(e_G)$, we call $F \cap G$ the *similar common lower simplex* of F and G. Otherwise, $F \cap G$ is referred to as the *dissimilar common lower simplex* of F and G. The *upper degree* of $F \in F_i(\Delta)$, denoted $\deg_U(\sigma)$, is the number of $(i+1)$-faces of Δ containing F. We will use the following description of $\mathcal{L}_i(\Delta)$ from [Gol02, Theorem 3.3.4].

Theorem 1.2.2. *Let Δ be a simplicial complex on vertex set $[n]$, ordered $1 < \cdots < n$, and let $i \in \mathbb{N}$ with $0 \leq i \leq \dim(\Delta)$. For $F, G \in F_i(\Delta)$, let $\ell_{F,G}$ denote the entry of $\mathcal{L}_i(\Delta)$ in row and column corresponding to F and G. Then $\mathcal{L}_i(\Delta)$ is symmetric. Moreover:*

(i) If $i = 0$, then $\ell_{F,G} = \deg_U(F)$ if $F = G$, $\ell_{F,G} = -1$ if $F \cup G \in F_{i+1}(\Delta)$, and $\ell_{F,G} = 0$, otherwise.

(ii) If $i > 0$, then

$$\ell_{F,G} = \begin{cases} \deg_U(F) + i + 1, & \textit{if } F = G, \\ 1, & \textit{if } F \neq G, \ F \cup G \notin F_{i+1}(\Delta), \ F \cap G \in F_{i-1}(\Delta) \textit{ similar} \\ -1, & \textit{if } F \neq G, \ F \cup G \notin F_{i+1}(\Delta), \ F \cap G \in F_{i-1}(\Delta) \textit{ dissimilar} \\ 0, & \textit{otherwise.} \end{cases}$$

Note that $\mathcal{L}_0(\Delta)$ is the Laplacian matrix of the graph of Δ, i.e., $\mathcal{L}_i(\Delta)$ is the degree matrix minus the adjacency matrix of Δ. In this case, the upper degree of a vertex in Δ coincides with the usual definition of the degree of a vertex in a graph.

1.3 Lattice polytopes

1.3.1 Basic notion

A *polytope* P is the convex hull of finitely many points in $\mathbb{R}^d$. Equivalently, P is the bounded intersection of finitely many closed half-spaces in $\mathbb{R}^d$. The *dimension* of P is the dimension of its affine hull. If $\dim P = k$, we call P a *k-polytope* and if $\dim P = d$, P is said to be *full-dimensional*. A linear inequality $a^\top x \le b$ for $a \in \mathbb{R}^d$ and $b \in \mathbb{R}$ is called a *valid inequality* for P if $a^\top y \le b$ for all $y \in P$. A (proper) *face* of P is a (non-empty) set of the form $P \cap \{x \in \mathbb{R}^d \ : \ a^\top x = b\}$ for some valid inequality $a^\top x \le b$ with $a \ne 0$. Each face is itself a polytope and we call the faces of dimension 0, 1, $\dim P - 2$ and $\dim P - 1$ *vertices*, *edges*, *ridges* and *facets*, respectively. We use $\mathcal{V}(P)$ and $\mathcal{F}(P)$ to denote the set of vertices and facets of P, respectively. A valid inequality $a^\top x \le b$ is *facet-defining* if $F = P \cap \{x \in \mathbb{R}^d \ : \ a^\top x = b\}$ for some $F \in \mathcal{F}(P)$. A description of P in terms of half-spaces is given, e.g., by taking the system of all facet-defining inequalities. If $\mathcal{V}(P) \subseteq \mathbb{Z}^d$, P is called a *lattice polytope*. For a matrix M, we define $\operatorname{conv} M$ to be the polytope given by the convex hull of the columns of M. Moreover, we set $\mathcal{M}(P)$ to be the matrix whose columns are the vertices of P. Then by [Grü03, p.4],

$$\dim P = \operatorname{rank} \begin{pmatrix} \mathcal{M}(P) \\ 1 \cdots 1 \end{pmatrix} - 1.$$

The *facet-ridge graph* $G(P)$ of P is the graph on vertex set $\mathcal{F}(P)$ where $\{F, G\}$ is an edge if and only if F and G intersect in a ridge. For simplicity, we refer to the adjacency matrix of $G(P)$ as the adjacency matrix of P. Two polytopes P, $Q \subseteq \mathbb{R}^d$ are *unimodularly equivalent*, denoted as $P \cong Q$, if there exist a unimodular matrix $U \in \mathbb{Z}^{d \times d}$ and a vector $b \in \mathbb{Z}^d$ such that $U \cdot P + b = Q$. A *simplex* of dimension k, k-simplex for short, is the convex hull of $k+1$ many affinely independent points. We denote by $\mathbb{1}_d$ and $\mathbf{0}_d$ the all-ones and all-zero vector of dimension d, respectively. If the dimension is clear from context, we omit the subscript. We use Δ_d to denote the *standard d-simplex*, i.e., $\Delta_d = \operatorname{conv}\{\{\mathbf{0}\} \cup \{\mathbf{e}_i \in \mathbb{R}^d \ : \ i \in [d]\}\}$, where $\mathbf{e}_i$ is the i^{th} standard basis vector. A polytope P is *simplicial* if all of its facets are simplices. A d-polytope P is *simple* if all of its vertices are adjacent to exactly d edges. The *normalized volume* of a d-dimensional lattice polytope $P \subseteq \mathbb{R}^d$ is given by $\operatorname{nVol}(P) = d! \cdot \operatorname{Vol}(P)$, where $\operatorname{Vol}(P)$ denotes the usual Euclidean volume. A lattice d-simplex Δ with normalized volume 1 is called *unimodular*. In this case, $\Delta \cong \Delta_d$. A lattice polytope P is *reflexive* if $P = \{x \in \mathbb{R}^d \ : \ Ax \le \mathbb{1}\}$ for an integral matrix A. In this case, $\mathbf{0}$ is the unique interior lattice point of P. There exist only a finite number of equivalence classes of reflexiv polytopes in any given dimension [LZ91]. Reflexive polytopes of dimension d were classified for $d \le 4$ by Kreuzer and Skarke [KS98; KS00]. Additionally, the simplicial reflexive polytopes of dimension d with $3d-1$ vertices are classified [AJP13; Øbr08]. For a positive integer n the polytope $nP = \{nx \in \mathbb{R}^d : x \in P\}$ is the n^{th} dilation or the n^{th} dilate of P. For two polytopes P and P' of dimension d and d', respectively, we denote the *free sum*, i.e., $\operatorname{conv}((P \times \mathbf{0}_{d'}) \cup (\mathbf{0}_d \times P'))$ by $P \oplus P'$. We denote the boundary of the polytope P by ∂P.

1.3.2 Ehrhart theory

One question concerning polytopes that frequently arises is the following: Given a lattice polytope, how many lattice points does it contain? A basic motivating example where this question naturally emerges can be found in [BR15, p.ix – p.x] and focuses on the more general study of discrete and continuous volume of a given geometric body $P \in \mathbb{R}^d$. In fact, counting lattice points can be seen as a discrete analogue of the continuous volume.

If P is a lattice d-polytope, Eugène Ehrhart [Ehr62] proved that the number of lattice points in the n^{th} dilation of P, i.e., $|nP \cap \mathbb{Z}^d|$, is given by a polynomial $E_P(n)$ of degree d in n for all integers $n \geq 0$, the so called *Ehrhart polynomial*. The *Ehrhart series* of P is the generating series

$$\sum_{n\geq 0} E_P(n)t^n = \frac{h^*(P;t)}{(1-t)^{d+1}} = \frac{h_0^*(P) + h_1^*(P)t + \cdots + h_s^*(P)t^s}{(1-t)^{d+1}},$$

where $h^*(P;t) \in \mathbb{Z}[t]$ is a polynomial of degree at most d, called h^**-polynomial* of P. The vector $h^*(P) = (h_0^*(P), \ldots, h_s^*(P))$ is called h^**-vector* of P. We will often omit P from the notation and just write $h^* = (h_0^*, \ldots, h_s^*)$ if P is clear from context. The h^*-polynomial can be obtained by applying a particular change of basis to $E_P(n)$, where $\binom{a}{b} = \frac{a(a-1)\cdots(a-b+1)}{b!}$; namely,

$$E_P(n) = h_0^*(P)\binom{n+d}{d} + h_1^*(P)\binom{n+d-1}{d} + \cdots + h_d^*(P)\binom{n}{d}. \tag{1.4}$$

Some coefficients of $E_P(n)$ are known in general. For example, the constant term is always 1 and the leading coefficient equals $\mathrm{Vol}(P)$ [Bec+04; Sta74]. Moreover, the second highest coefficient of $E_P(n)$ equals half the surface area of P [BR15, Theorem 5.6]. Another natural question to ask is whether the vectors appearing as coefficient vectors of Ehrhart polynomials can be characterized. This was done for 2-polytopes in [Bec+04, p.4–5] but remains wide open in higher dimensions. Concerning the entries of the h^*-vector of a lattice polytope, Stanley provided his well-known and famous non-negativity theorem.

Theorem 1.3.1. [Sta80, Theorem 2.1] *For every lattice polytope P, the h^*-vector of P has only non-negative entries.*

Since all entries of h^* are non-negative, it is natural to ask whether they might count something. A few entries have known combinatorial interpretations. For example, $h_0^* = 1$ and $h_1^* = E_P(1) - d - 1$, which directly follows from Equation (1.4) with $n = 0$ and $n = 1$. Additionally, the Ehrhart-Mcdonald reciprocity [Mcd71, Theorem 4.6] (i.e., $E_P(-n) = (-1)^d E_{P\smallsetminus\partial P}(n)$) implies that $E_P(-1) = h_d^*\binom{-1}{d} = (-1)^d h_d^*$ and thus $h_d^* = \left|(P \smallsetminus \partial P) \cap \mathbb{Z}^d\right|$. There are several known inequalities that are satisfied by the entries of the h^*-vector [Hib90; Hib94; Hib95; Hib+19; Sta91; Sta09], but a general combinatorial interpretation for every entry remains wide open. Other interesting properties of the h^*-vector and the h^*-polynomial, which are heavily studied and an active field of research, are unimodality, log-concavity and real-rootedness (see, e.g., [BJ21; Joc18; OT20]). We call a sequence $a = (a_0, \ldots, a_n)$ *unimodal* if there exists an index $0 \leq i \leq n$ such that $a_0 \leq a_1 \leq \cdots \leq a_i \geq \cdots \geq a_n$. A sequence is *log-concave* if $a_{k-1}a_{k+1} \leq a_k^2$ for all $1 < k < n$. A polynomial is *real-rooted* if it is constant or if all of its roots are real. If a polynomial $p(x) = a_n x^n + \cdots + a_1 x + a_0$ is real-rooted and has only non-negative coefficients, then a is log-concave. The log-concavity and non-negativity together imply unimodality as shown in [Brä15, Lemma 1.1]. In the realm of symmetric sequences, unimodality of a follows if $\gamma(a)$ is non-negative [Pet15, Observation 4.1]. Moreover, if $p(x)$ has a symmetric coefficient vector, then $p(x)$ is real-rooted if and only if $\gamma(p;x)$ is real-rooted [Pet15, Observation 4.2]. Additionally, if the coefficients of $p(x)$ are also non-negative, then the coefficients of $\gamma(p;x)$ are non-negative [Pet15, Observation 4.2]. A connection between unimodality of the h^*-vector of a reflexive polytope P and P having the integer decomposition property (IDP for short) was long conjectured. A lattice polytope $P \subseteq \mathbb{R}^d$ has the *IDP* if, for every integer k and for all $\alpha \in P \cap \mathbb{Z}^d$, there exist $\alpha_1, \dots, \alpha_k \in kP \cap \mathbb{Z}^d$ such that $\alpha = \alpha_1 + \dots + \alpha_k$. Note that it is well-known that if a lattice polytope P admits a unimodular triangulation, then P has the IDP [Haa+14, Section 1.2.5]. Thus, until October 2022, a result of Bruns and Römer from 2007 was the state of the art where they proved that if P is reflexive and admits a regular unimodular triangulation, then P has a unimodal h^*-vector [BR07, Theorem 1]. In a recent breakthrough, Adiprasito et al. were able to confirm that every reflexive lattice polytope having the IDP has a unimodal h^*-vector [Adi+22, Corollary 2.2].

By work of Hibi, if P is reflexive then $h^*(P;t)$ is *symmetric*, i.e., $h^*(P,x) = x^d h^*\left(P, \frac{1}{x}\right)$. Moreover, this property together with the existence of an interior lattice point characterizes reflexive polytopes, as given in the following theorem.

Theorem 1.3.2. [Hib92] *A lattice polytope $P \subseteq \mathbb{R}^d$ is reflexive (up to unimodular equivalence) if and only if P is d-dimensional, P contains an interior lattice point, and $h^*(P)$ satisfies $h_i^*(P) = h_{d-i}^*(P)$.*

1.3.3 Triangulations and Gröbner bases

Definition 1.3.3. *A* triangulation *of a lattice d-polytope P is a finite collection $\mathcal{T}$ of lattice d-simplices such that*

(i) $P = \bigcup_{\Delta \in \mathcal{T}} \Delta$

(ii) For all $\Delta_1, \Delta_2 \in \mathcal{T}$ the intersection $\Delta_1 \cap \Delta_2$ is a face of both Δ_1 and Δ_2.

Note, triangulations can be defined more generally for arbitrary polytopes, but since we only study lattice polytopes here, we restrict the definition to this case. The set $\mathcal{V}(\mathcal{T}) = \{v \,:\, v \in \mathcal{V}(\Delta) \text{ for } \Delta \in \mathcal{T}\}$ is the set of vertices of $\mathcal{T}$. For every polytope there exists a triangulation without using new vertices, i.e., vertices which are not vertices of P [BR15, Theorem 3.1].

Example 1.3.4. *The illustration in Figure 1.3 on the left is a triangulation of the hexagon without using new vertices. The one in the middle is a triangulation of the hexagon using one new vertex. The rightmost illustration is not a triangulation since Definition 1.3.3 (ii) is violated.*

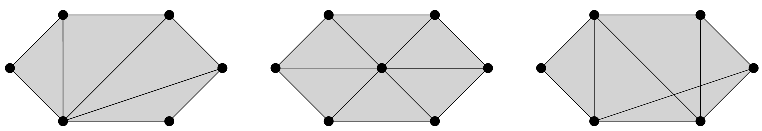

FIGURE 1.3: Two different triangulations of the hexagon (left and middle), and a subdivision into simplices which is not a triangulation (right).

Instead of focusing on triangulations of the whole polytope, it can be useful to focus on triangulations of ∂P. A triangulation of the boundary is a collection of triangulations of each facet which are consistent in terms of Definition 1.3.3 (ii). We note that every triangulation is, in particular, a simplicial complex. In fact, a triangulation of the boundary of a polytope is a simplicial sphere. Thus, questions about its γ-vector and corresponding conjectures can be investigated. Given a reflexive polytope P, we can extend a triangulation Δ of ∂P to a triangulation $\mathcal{T}$ of P by coning over the unique interior lattice point. Then $h(\Delta;x) = h(\Delta * 0;x) = h(\mathcal{T};x)$. $\mathcal{T}$ is called *unimodular*, if all simplices in $\mathcal{T}$ are. Unimodular triangulations are in fact rare and do not always exist for $d \geq 3$. A famous example of a polytope not having a unimodular triangulation is Reeve's tetrahedron [Ree57].

Example 1.3.5. *Given a number $q \in \mathbb{Z}$ with $q > 1$, Reeve's tetrahedron is defined as*

$$R_q = \operatorname{conv}\left((0,0,0),\ (1,0,0),\ (0,1,0),\ (1,1,q)\right) \subseteq \mathbb{R}^3.$$

Since there are no lattice points in R_q other than its vertices, the unique triangulation of R_q is the simplicial complex with R_q as its only facet. Since

$$\operatorname{nVol}(R_q) = \det\begin{pmatrix} 1 & 0 & 1 \\ 0 & 1 & 1 \\ 0 & 0 & q \end{pmatrix} = q,$$

the volume of R_q can be arbitrarily large. Therefore, R_q is not a unimodular simplex.

In the event that P admits a unimodular triangulation $\mathcal{T}$, the normalized volume of P is given by the number of d simplices in $\mathcal{T}$, i.e., $\operatorname{nVol}(P) = |\mathcal{T}|$. More importantly, in this case, the h^*-vector of P coincides with the h-vector of $\mathcal{T}$.

Theorem 1.3.6. [Sta80, Corollary 2.5] *If P is lattice polytope and $\mathcal{T}$ is any unimodular triangulation of P, then $h^*(P) = h(\mathcal{T})$.*

$\mathcal{T}$ is called *regular* if there exists a lifting function $\omega : \mathcal{V}(\mathcal{T}) \to \mathbb{R}$ such that $\mathcal{T}$ is the projection of the lower envelope of $\operatorname{conv}\left(\{(v,\omega(v)\ :\ v \in \mathcal{V}(\mathcal{T})\}\right) \subseteq \mathbb{R}^{d+1}$ to the first d coordinates. To emphasize that ω is the lifting function of a certain polytope P, we will also write ω_P.

Example 1.3.7. *A regular triangulation is shown in Figure 1.4 on the left. Here the lifting function is given by $\omega(1) = 3$, $\omega(2) = 1$, $\omega(3) = 2$ and $\omega(4) = \omega(5) = \omega(6) = 0$. The most common example of a non-regular triangulation is illustrated in Figure 1.4 on the right. A detailed discussion of the example can be found in [Stu96, Example 8.2]. To show it is indeed non-regular, assume $\omega(4) = \omega(5) = \omega(6) = 0$. Then we must have $\omega(3) > \omega(2)$ to get the edge 26. Also, $\omega(1) > \omega(3)$ to get the edge 34 and $\omega(2) > \omega(1)$ to get the edge 15. All in all, the contradiction $\omega(1) > \omega(3) > \omega(2) > \omega(1)$ follows.*

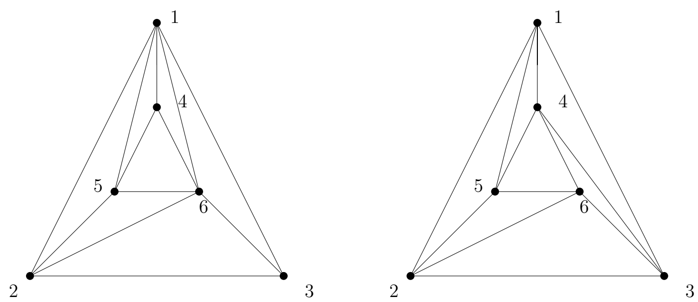

FIGURE 1.4: A regular (left) and a non-regular (right) triangulation.

If a lattice polytope P admits a regular unimodular triangulation, Athanasiadis proved that the second half of its h^*-vector is decreasing.

Theorem 1.3.8. [Ath04, Theorem 1.3] *Let P be a d-dimensional lattice polytope with h^*-vector $(h_0^*, h_1^*, ..., h_d^*)$. If P has a regular unimodular triangulation, then $h_i^* \geq h_{d-i+1}^*$ for $1 \leq i \leq \lfloor (d+1)/2 \rfloor$,*

$$h^*_{\lfloor (d+1)/2 \rfloor} \geq \cdots \geq h^*_{d-1} \geq h^*_d$$

and $h_i^* \leq \binom{h_1^*+i-1}{i}$ for $0 \leq i \leq d$. In particular, if $h^*(P)$ is symmetric and P has a regular unimodular triangulation, then $h^*(P)$ is unimodal.

From the previous theorem, we can directly deduce that a reflexive polytope admitting a regular unimodular triangulation has a unimodal h^*-vector.

A famous and important tool to calculate triangulations are Gröbner bases. Let $\mathbb{K}$ be a field and $\mathbb{K}[u_1^{\pm}, \ldots, u_d^{\pm}, t]$ denote a *subring of the ring of Laurent polynomials* in $d+1$ variables. Let $P \subseteq \mathbb{R}^d$ be a lattice polytope. For every lattice point $\alpha = (\alpha_1, \ldots, \alpha_d) \in P \cap \mathbb{Z}^d$, let u^α be the Laurent monomial given by $u_1^{\alpha_1} \cdots u_d^{\alpha_d}$. The *toric ring* of P is given as $\mathbb{K}[P] = \mathbb{K}[u^\alpha t \ : \ \alpha \in P \cap \mathbb{Z}^d] \subseteq \mathbb{K}[u_1^{\pm}, \ldots, u_d^{\pm}, t]$. Moreover, let $S = \mathbb{K}[x_\alpha \ : \ \alpha \in P \cap \mathbb{Z}^d]$ be a polynomial ring with $|P \cap \mathbb{Z}^d|$ variables and $\deg(x_\alpha) = 1$ for all $\alpha \in P \cap \mathbb{Z}^d$. Then the map $\pi : S \to \mathbb{K}[P]$, $x_\alpha \mapsto u^\alpha \cdot t$, is a surjective ring homomorphism and we call $I_P := \ker(\pi)$ the *toric ideal* of P. Note that $\mathbb{K}[P]$ is isomorphic to S/I_P. A total order $<$ on the monomials of a polynomial ring is called a *monomial order* if for all monomials x^α, x^β, x^γ one has $x^\alpha \cdot x^\gamma < x^\beta \cdot x^\gamma$ whenever $x^\alpha < x^\beta$ and $1 < x^\alpha$ for all non-constant monomials. Common monomial orders are, for example, the degree lexicographic order (deglex for short) or the degree reverse lexicographic order $<_{degrevlex}$ (degrevlex for short). Given the total order $x_1 < x_2 < x_3 < \ldots < x_n$ and two monomials x^α and x^β, then $x^\alpha <_{degrevlex} x^\beta$ if and only if $\sum_{i=1}^n \alpha_i < \sum_{i=1}^n \beta_i$ or $\sum_{i=1}^n \alpha_i = \sum_{i=1}^n \beta_i$ and $\alpha_\ell > \beta_\ell$ for $\ell = \min(j \ : \ \alpha_j \neq \beta_j)$. If we fix a monomial order $<$, then the *initial term* $\text{in}_<(f)$ of a polynomial f is the largest monomial appearing in f. Given an ideal $I \subseteq \mathbb{K}[x_1, \ldots, x_n]$, we denote by $\text{in}_<(I)$ the ideal generated by all the initial terms of all polynomials in I and call it the *initial ideal* of I. A system of generators $\{g_1, \ldots, g_k\}$ of I is called a *Gröbner basis* if the initial terms of $g_1, \ldots, g_k$ already generate $\text{in}_<(I)$, i.e., if $\text{in}_<(I) = \langle \text{in}_<(g_1), \ldots, \text{in}_<(g_k) \rangle$. Let $\sqrt{I} = \{f \ : \ f^m \in I \text{ for some } m \in \mathbb{N}_{>0}\}$ be the *radical* of I. We set

$$\Delta_{\text{in}_<}(I_P) = \left\{ A \subseteq P \cap \mathbb{Z}^d \ : \ \prod_{\alpha \in A} x_\alpha \notin \sqrt{\text{in}_<(I_P)} \right\}.$$

By definition, $\Delta_{\text{in}_<}(I_P)$ is the simplicial complex whose Stanley-Reisner ideal is $\sqrt{\text{in}_<(I_P)}$. We call a monomial x^α *squarefree* if every coordinate of α is 0 or 1. The following famous result was shown on [Stu96, Theorem 8.3, Corollary 8.4, Corollary 8.9].

Theorem 1.3.9. *Let $P \subseteq \mathbb{R}^d$ be a lattice polytope and $<$ a monomial order on $\mathbb{K}[x_\alpha \ : \ \alpha \in P \cap \mathbb{Z}^d]$. Then*

$$\mathcal{T}_{\text{in}_<(I_P)} = \{\text{conv}(A) \ : \ A \in \Delta_{\text{in}_<}(I_P)\}$$

is a triangulation of P. Moreover, $\mathcal{T}_{\text{in}_<(I_P)}$ is unimodular if and only if $\text{in}_<(I_P)$ is squarefree.

Thus, a triangulation $\mathcal{T}_P$ of P can be calculated by finding a Gröbner basis $\mathcal{B}$ of I_P. Then the minimal non-faces of $\mathcal{T}_P$ are in 1-to-1-correspondence to the initial terms in $\mathcal{B}$. Moreover, regular triangulations are in 1-to-1-correspondence to triangulations coming from a Gröbner basis. Any monomial order $\prec$ can be represented by a vector ω such that $x^\alpha \prec x^\beta$ if and only if $\langle\alpha,\omega\rangle < \langle\beta,\omega\rangle$. It can be shown that the ω representing the monomial order in Theorem 1.3.9 is a lifting function of the regular triangulation $\mathcal{T}_{\mathrm{in}_<(I_P)}$. Thus, we could rephrase Theorem 1.3.9 as follows: P has a regular (unimodular) triangulation if and only if I_P has a (squarefree) Gröbner basis, where a Gröbner basis $\{g_1,\dots,g_k\}$ is said to be squarefree if all its initial terms $\mathrm{in}_<(g_1),\dots,\mathrm{in}_<(g_k)$ are squarefree.

Example 1.3.10. *Let* $P = \mathrm{conv}((0,0),(1,0),(0,1),(1,1))$. *The toric ring is given by* $\mathbb{K}[P] = \mathbb{K}[t,u_1t,u_2t,u_1u_2t]$ *and* $S = \mathbb{K}[x_{(0,0)},x_{(1,0)},x_{(0,1)},x_{(1,1)}]$. *Then* $\ker(\pi) = \langle x_{(0,0)}x_{(1,1)} - x_{(1,0)}x_{(0,1)}\rangle$. *If we choose the degrevlex monomial order with respect to* $x_{(1,0)} < x_{(0,1)} < x_{(1,1)} < x_{(0,0)}$, *then* $\mathrm{in}_<(I_P) = \langle x_{(0,0)}x_{(1,1)}\rangle$ *and the triangulation of* P *is shown on the left-hand side of Figure 1.5. On the other hand, if we choose the degrevlex order with respect to* $x_{(0,0)} < x_{(1,1)} < x_{(1,0)} < x_{(0,1)}$, *then* $\mathrm{in}_<(I_P) = \langle x_{(1,0)}x_{(0,1)}\rangle$ *and the triangulation of* P *is shown on the right-hand side of Figure 1.5. Since both triangulations come from a squarefree Gröbner basis, both triangulations are unimodular.*

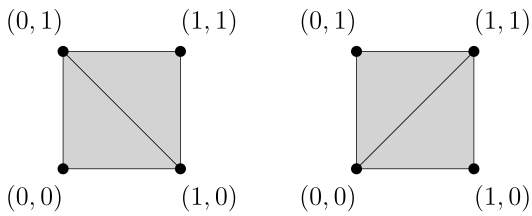

FIGURE 1.5: Two regular unimodular triangulations of the unit square associated to Gröbner bases.

Chapter 2

Counting horizontal visibility graphs

In many applications using horizontal visibility graphs, simple metrics such as the vertex degree sequence, the graph entropy and moments have shown to be particularly helpful indicators for the classification of the considered data sequences [ATMP21; Ara+16; Bal+09; DDK13; Li+14; MPT15; RS18]. It is therefore natural to ask whether such properties already determine an HVG. In the case of vertex degree sequences, this question is known to have partial answers. Luque and Lacasa [LL17] provided an affirmative answer for the class of canonical HVGs by providing an explicit bijection to the set of possible ordered degree sequences. Here, an HVG is called *canonical* if the underlying time series has pairwise distinct entries, and the first and last value are the largest ones. Whereas the first condition is met by most (even discrete) real-world time series with a sufficiently high resolution, the second condition is a huge restriction as it is very unlikely to be satisfied in applications. Another positive result in this direction was given by O'Pella [O'P19] showing that any HVG (without additional requirements) can be recovered from its directed vertex degree sequence through an explicit algorithm. It is essential that the degree sequence is directed since for arbitrary degree sequences, it is easy to construct examples where the statement does not hold (see Figure 2.4). However, in all those examples, it turns out that the underlying data sequences have some equal entries. Indeed, we prove the following statement:

Theorem 2.0.1. *Let $N \in \mathbb{N}$. If G and H are different HVGs on N vertices corresponding to data sequences with pairwise distinct entries, then their ordered vertex degree sequences $\Delta(G)$ and $\Delta(H)$ are different. In particular, HVGs from data sequences without equal entries are uniquely determined by their ordered vertex degree sequence.*

In the second part of this chapter, we take a similar viewpoint as in [GMS11] where HVGs are studied from a purely combinatorial perspective and connections with several combinatorial statistics are established. More precisely, we are interested in the number of HVGs on a fixed number of vertices corresponding to data sequences with and without equal entries, where we consider two HVGs equal if they are equal as labeled graphs. Miraculously, Catalan numbers and large Schröder numbers determine those cardinalities. More precisely, we show the following:

Theorem 2.0.2. *Let $N \in \mathbb{N}$ and let $\mathcal{G}_{N,\neq}$ and $\mathcal{G}_N$ be the set of HVGs on N vertices corresponding to data sequences without and with equal entries, respectively. Then:*

(i) $|\mathcal{G}_{N,\neq}| = C(N-1)$, *where* $C(N-1) = \frac{1}{N}\binom{2N-2}{N-1}$ *denotes the* $(N-1)^{\text{st}}$ Catalan number.

(ii) For $N \geq 2$, one has $|\mathcal{G}_N| = r_{N-2}$, where r_N denotes the N^{th} large Schröder number*.*

2.1 Horizontal visibility graphs from distinct data

In this section, we focus on HVGs in $\mathcal{G}_{N,\neq}$, i.e., HVGs corresponding to data sequences with pairwise distinct entries. We have seen in Remark 1.1.2 that such an HVG is the HVG of some permutation of $[N]$. Our first goal is to construct such a permutation, solely from knowledge of the graph, without knowing a realizing data sequence. In the second part of this section, we prove Theorem 2.0.1, i.e., we show that HVGs in $\mathcal{G}_{N,\neq}$ are uniquely determined by their *ordered* degree sequence. Our proof also yields an algorithm for constructing such a data sequence. This extends corresponding results for *directed* ordered degree sequences (see [O'P19, Proposition 5]) as well as for HVGs in canonical form, i.e., HVGs such that the first and last entry of the corresponding data sequence are the maximal ones [LL17, Theorem 1]. In the last two subsections, we consider the enumerative question of how many HVGs in $\mathcal{G}_{N,\neq}$ exist. In particular, we provide two proofs of Theorem 2.0.2 (i), a purely algebraic one and a bijective one.

2.1.1 From horizontal visibility graphs to data sequences

In the following, we let $N \in \mathbb{N}$, $G = ([N], E) \in \mathcal{G}_{N,\neq}$ and we are seeking $D \in \mathbb{N}^N$ such that $\mathrm{HVG}(D) = G$. To this end, we first need some further notation. A vertex $v \in [N]$ is called *m-nested* if

$$\delta_{\text{nest}}(v) := |\{ij \ : i < v < j, ij \in E\}| = m.$$

The value $\delta_{\text{nest}}(v)$ is also called the *nesting degree* of v and an edge $ij \in E$ with $i < v < j$ is referred to as *nesting edge* of v.

Theorem 2.1.1. *Let $N \in \mathbb{N}$ and $G \in \mathcal{G}_{N,\neq}$. Let $\sigma : [N] \to [N]$ be the unique permutation of the vertices of G such that:*

(i) $\delta_{\text{nest}}(\sigma^{-1}(1)) \geq \delta_{\text{nest}}(\sigma^{-1}(2)) \geq \cdots \geq \delta_{\text{nest}}(\sigma^{-1}(N-1)) \geq \delta_{\text{nest}}(\sigma^{-1}(N))$, and,

(ii) if $\delta_{\text{nest}}(\sigma^{-1}(i)) = \delta_{\text{nest}}(\sigma^{-1}(j))$, then $i < j$ iff $\sigma^{-1}(i) > \sigma^{-1}(j)$.

Let $d_i = \sigma(i)$ and $D = (d_1, \ldots, d_N)$. Then D realizes G, i.e., $HVG(D) = G$. In particular, $d_1 = N$.

Intuitively, the permutation σ corresponds to the ordering $\sigma^{-1}(1), \ldots, \sigma^{-1}(N)$ of the vertices of G, that first orders the vertices by decreasing nesting degree and then from right to left among vertices with the same nesting degree. In particular, the vertex 1 is always the vertex at the last position, i.e., $d_1 = \sigma(1) = N$. In the following, we refer to the sequence D in Theorem 2.1.1 as the *standard sequence* of a given HVG.

Proof. Let $\widetilde{D} = (\widetilde{d}_1, \ldots, \widetilde{d}_N) \in \mathbb{N}^N$ with $\mathrm{HVG}(\widetilde{D}) = G$ and let $H = \mathrm{HVG}(D)$. We need to show that $H = G$. For this aim let $ij \in E(G)$ with $2 \leq i + 1 < j \leq N$. Since we must have $\widetilde{d}_i > \widetilde{d}_k < \widetilde{d}_j$ for $i < k < j$, there is no edge in $E(G)$ of the form uv with $u < i < v < j$ or $i < u < j < v$. In particular, if uv is a nesting edge of i, then $u < i < j \leq v$ and thus uv is a nesting edge for any $i < k < j$. As ij is also a nesting edge for any $i < k < j$, we conclude that $\delta_{\text{nest}}(k) > \delta_{\text{nest}}(i)$, i.e., $d_k = \sigma(k) < \sigma(i) = d_i$ for any $i < k < j$. The analogous reasoning shows $d_k < d_j$ for $i < k < j$. This implies $ij \in E(H)$.

Let now $ij \in E(H)$ with $2 \le i+1 < j \le N$. In order to show that $ij \in E(G)$, we need to prove that $\widetilde{d}_i > \widetilde{d}_k < \widetilde{d}_j$ for all $i < k < j$. Assume by the contrary that there exists $i < k < j$ with $\widetilde{d}_k > \min(\widetilde{d}_i, \widetilde{d}_j)$. We distinguish two cases.
Case 1: There exists $i < k < j$ with $\widetilde{d}_k > \widetilde{d}_j$. Let k be the maximal vertex with this property. We then have $\widetilde{d}_\ell < \widetilde{d}_j$ for all $k < \ell < j$. If uv is a nesting edge of k (in G), it follows that $u < k < j < v$ and hence $\delta_{\text{nest}}(j) \ge \delta_{\text{nest}}(k)$ (in G). Using that $k < j$ we infer that $d_j = \sigma(j) < \sigma(k) = d_k$, which contradicts the assumption that $ij \in E(H)$. Thus, $ij \in E(G)$.
Case 2: There exists $i < k < j$ with $\widetilde{d}_k > \widetilde{d}_i$ and $\widetilde{d}_\ell < \widetilde{d}_j$ for all $i < \ell < j$. Let k be minimal with this property. Similar arguments as in Case 1 show that $\delta_{\text{nest}}(k) \ge \delta_{\text{nest}}(j)$. If $\delta_{\text{nest}}(k) = \delta_{\text{nest}}(j)$, we conclude that $d_k = \sigma(k) > \sigma(j) = d_j$ (as $k < j$) which is a contradiction to $ij \in E(H)$. If $\delta_{\text{nest}}(k) > \delta_{\text{nest}}(j)$, there has to exist an edge $uv \in E(G)$ with $u < k < v < j$. Since $\widetilde{d}_k > \widetilde{d}_i$ and $\widetilde{d}_\ell < \widetilde{d}_i$ for all $i < \ell < k$, we must have $u < i$. It follows from the first part of this proof that we also have $uv \in E(H)$. But then the edges uv and ij are crossing in H, contradicting the fact that H is an HVG (see Lemma 1.1.3 (i)). Hence, $ij \in E(G)$.

Since $i(i+1)$ for $1 \le i \le N-1$ lies in any HVG, we conclude $G = H$. □

Next, we provide an example for the standard sequence.

Example 2.1.2. *The sequences* $(4,3,1,2,7,5,6)$ *and* $(7,4,1,2,6,3,5)$ *both realize the HVG shown in Figure 2.1. The second sequence meets the condition in Lemma 1.1.3 (v) and is constructed using Theorem 2.1.1.*

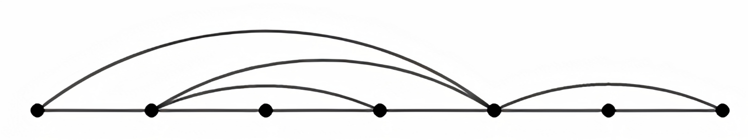

FIGURE 2.1: The HVG of the sequences $(4,3,1,2,7,5,6)$ and $(7,4,1,2,6,3,5)$.

2.1.2 Horizontal visibility graphs and degree sequences

We start with some simple lemmas that will be crucial to prove that an HVG in $\mathcal{G}_{N,\neq}$ is uniquely determined by its ordered degree sequence.

Lemma 2.1.3. *Let* $N \in \mathbb{N}$, $N \ge 3$ *and* $G \in \mathcal{G}_{N,\neq} \setminus \{P_N\}$. *Then there exists* $2 \le i \le N-1$ *such that* $\delta_i = 2$ *and* $(i-1)(i+1) \in E(G)$.

Proof. Let $D \in [N]^N$ be the standard sequence of G (see Theorem 2.1.1). We then have $d_1 = N$ and $d_N = N - |\mathcal{N}(G)| + 1$. Since $G \neq P_N$, we have $|\mathcal{N}(G)| < N$ and hence $d_N \neq 1$. In particular, there exists $1 < i < N$ with $d_i = 1$. As D is the standard sequence, we have $d_j > 1$ for all $j \neq i$ which implies that $\delta_i = 2$ and $(i-1)(i+1) \in E(G)$. □

The drawback of the previous lemma is that we cannot yet tell from a given degree sequence which inner 2s fulfill the assumption of the corresponding neighboring vertices being adjacent. The next lemma solves this difficulty.

Lemma 2.1.4. *Let* $N \in \mathbb{N}$, $N \ge 3$, $G \in \mathcal{G}_{N,\neq} \setminus \{P_N\}$ *and* $\Delta = (\delta_1, \ldots, \delta_N)$ *be the ordered degree sequence of* G. *Then:*

(i) If $\delta_2 = 2$ *and* $\delta_1 \neq 1$, *then* $13 \in E(G)$.

(ii) If $\delta_2 \neq 2$ or $\delta_1 = 1$ and $3 \leq i \leq N-1$ is minimal with $\delta_i = 2$ and $\delta_{i-1} \geq 3$, then $(i-1)(i+1) \in E(G)$.

Proof. We first note for $N = 3$, $(2,2,2)$ is the only degree sequence meeting the conditions in (i). Since the corresponding HVG is $([3], \{12, 13, 23\})$, the claim follows in this case.

Let $N \geq 4$ and let $D = (d_1, \ldots, d_N) \in \mathbb{N}^N$ be the standard sequence of G. First assume that we are in situation (i). As D is the standard sequence of G, we have $d_1 = N > d_2$. If, by contradiction, $13 \notin E(G)$, it follows that $d_1 > d_2 > d_3$. Let $3 < m \leq N$ be minimal with $d_m > d_2$. Note that such m exists since $\delta_1 \geq 2$ implies the existence of $3 < \ell \leq N$ with $1\ell \in E(G)$ and hence $d_\ell > d_2$. It follows that $2m \in E(G)$, a contradiction to $\delta_2 = 2$.

Now, assume the assumptions of (ii) are satisfied. We first show, there exists $i+1 \leq \ell \leq N$ with $(i-1)\ell \in E(G)$. This is clear if $i = 3$ since $\delta_2 \geq 3$. So let $i > 3$. If there is no such edge, there has to exist an edge $j(i-1)$ with $1 \leq j \leq i-3$. Lemma 1.1.3 (iii) implies that $G_{[j,i-1]} \in \mathcal{G}_{i-j,\neq} \setminus \{P_{i-j}\}$. As $i-j \geq 3$, we conclude with Lemma 2.1.3 that there exists an inner vertex k of $G_{[i-j]}$ of degree 2. In the following, we choose k minimal. Lemma 1.1.3 (i) together with the fact that $j(i-1) \in E(G)$ implies that $\delta_k = 2$ also in G. By assumption, we further have $k \neq 2$ and the minimality of k implies $\delta_{k-1} \geq 3$. Since i was the minimal vertex of degree 2 in G, we have hence reached a contradiction. Hence there exists $i+1 \leq \ell \leq N$ with $(i-1)\ell \in E(G)$. If $i = N-1$, we must have $\ell = i+1$ and the claim follows. If $i \neq N-1$, we must have that $d_{i-1} > d_i$. If, by contradiction, $(i-1)(i+1) \notin E(G)$, we conclude that $d_{i-1} > d_i > d_{i+1}$. The claim now follows by the same argument as in (i). □

We want to point out that Lemma 2.1.3 guarantees that the degree sequence of any HVG in $\mathcal{G}_{N,\neq}$ either satisfies property (i) or (ii) of the previous lemma or is the one of the trivial HVG. As a consequence, it follows that for any $G \in \mathcal{G}_{N,\neq} \setminus \{P_N\}$ there exists $2 \leq i \leq N$ with $\delta_i = 2$ and $(i-1)(i+1) \in E(G)$. Moreover, the following example shows it is important to choose i minimally in (ii) since otherwise the statement is not necessarily true.

Example 2.1.5. *The* HVG $G = \mathrm{HVG}(D)$ *with* $D = (1,8,4,7,6,5,2,3)$ *(see Figure 2.2) has the ordered degree sequence* $\Delta = (1,3,2,3,2,3,2,2)$. *Vertex* 5 *fulfills the assumptions of (ii) except for being minimal and* $46 \notin E(G)$. *However, the minimal inner* 2 *is at position* 3 *and* $24 \in E(G)$.

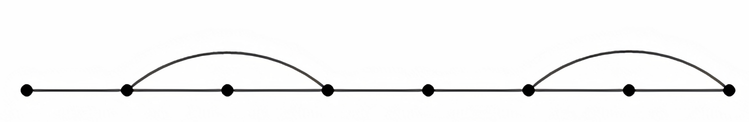

FIGURE 2.2: The graph $\mathrm{HVG}((1,8,4,7,6,5,2,3))$.

The next lemma shows the behavior of the set of degree sequences of HVGs in $\mathcal{G}_{N,\neq}$ with respect to the removal of certain inner 2s.

Lemma 2.1.6. *Let* $N \in \mathbb{N}$, $N \geq 3$, $G \in \mathcal{G}_{N,\neq} \setminus \{P_N\}$ *and* $D \in \mathbb{N}^N$ *with* $\mathrm{HVG}(D) = G$. *Let* $2 \leq i \leq N-1$ *with* $\delta_i = 2$ *and* $(i-1)(i+1) \in E(G)$ *and let* $D[i] \in \mathbb{N}^{N-1}$ *denote the sequence obtained from* D *by removing the* i^{th} *entry. Then* $\mathrm{HVG}(D[i]) = G \setminus \{i\}$ *(after relabelling the vertices* $i+1, \ldots, N$ *of* G *by* $i, \ldots, N-1$*). In particular,* $G \setminus \{i\} \in \mathcal{G}_{N-1,\neq}$.

Proof. As $G \in \mathcal{G}_{N,\neq}$, we may assume that all entries of D are distinct. Since $(i-1)(i+1) \in E(G)$, we must have $d_{i-1} > d_i < d_{i+1}$. Let $D[i] \in \mathbb{N}^{N-1}$ be the sequence obtained from D by removing d_i and let $H = \mathrm{HVG}(D[i])$. We claim that H equals $G \setminus \{i\}$ (up to relabelling the vertices of $G \setminus \{i\}$ with $1, \dots, N-1$). Clearly, $H_{[i-1]} = (G \setminus \{i\})_{[i-1]}$ and $H_{[i,N-1]} = (G \setminus \{i\})_{[i+1,N]}$. Moreover, as $(i-1)(i+1) \in E(G)$, we also have $H_{[i-1,i]} = (G \setminus \{i\})_{\{i-1,i+1\}}$. Now assume that $1 \le j \le i-1 < \ell \le N-1$ with $\{j, \ell\} \ne \{i-1, i+1\}$. Then $j\ell \in E(G \setminus \{i\})$ if and only if $d_j > d_k < d_\ell$ for all $j < k < \ell$. As $d_{i-1} > d_i < d_{i+1}$, this is equivalent to $d_j > d_k < d_\ell$ for all $j < k < \ell$ with $k \ne i$, i.e., $j\ (\ell - 1) \in E(H)$. This completes the proof. □

We now prove the main result of this subsection, showing that HVGs in $\mathcal{G}_{N,\ne}$ are uniquely determined by their ordered degree sequence.

Proof of Theorem 2.0.1 We show the claim by induction on N. If $N \in \{1,2\}$, then $\mathcal{G}_{N,\ne} = \{P_N\}$ and the statement is trivially true. Let $N \ge 3$, $\Delta = (\delta_1, \dots, \delta_N) \in \mathbb{N}^N$. If $\Delta = (1,2,\dots,2,1)$, we clearly have $\Delta(P_N) = \Delta$ and as $P_N \subsetneq G$ for any $G \in \mathcal{G}_{N,\ne}$, the claim follows in this case. Let $\Delta \ne (1,2,\dots,2,1)$. Assume there exists $G, H \in \mathcal{G}_{N,\ne}$ with $\Delta(G) = \delta = \Delta(H)$. Let $2 \le i \le N-1$ be minimal such that $\delta_i = 2$ and $(i-1)(i+1) \in E(G) \cap E(H)$. Note that such i exists due to Lemma 2.1.4. Lemma 2.1.6 implies that $G \setminus \{i\}, H \setminus \{i\} \in \mathcal{G}_{N,\ne}$ and, as those graphs have the same degree sequence $\widetilde{\delta} = (\delta_1, \dots, \delta_{i-2}, \delta_{i-1}-1, \delta_{i+1}-1, \delta_{i+2}, \dots, \delta_N)$, the induction hypothesis yields $G \setminus \{i\} = H \setminus \{i\}$. As $i-1$ and $i+1$ are the only neighbors of i in both G and H, we conclude that $G = H$. □

Remark 2.1.7. *The proof of Theorem 2.0.1 can easily be turned into an algorithm to construct the unique HVG $G \in \mathcal{G}_{N,\ne}$ with a given ordered degree sequence Δ. More precisely, one successively removes the minimal inner 2 satisfying (i) or (ii) of Lemma 2.1.4 from Δ and decreases the two neighboring entries by 1. We note that for each removal the length of the sequence decreases by 1. If the i^{th} entry is removed, one protocols the two edges corresponding to the removal (see Lemma 2.1.6). In this way, one finally reaches a sequence of the form $(1,2,\dots,2,1)$, where also no inner 2 is possible. If the 2s have been obtained from the original entries at positions $j_1, \dots, j_k$, one needs to add the edges $1j_1, j_1j_2, \dots, j_{k-1}j_k, j_kN$ to the list of edges. We illustrate this procedure in an example.*

Example 2.1.8. *We consider the ordered degree sequence $\Delta = (2,3,2,5,2,2)$ and construct the corresponding HVG G as follows. We use E_i and Δ_i to denote the edge set and the changed degree sequence after the removal of i inner 2s.*

- *We first remove the 2 at position 3, which yields $\Delta_1 = (2,2,4,2,2)$ and $E_1 = \{23, 34\}$.*
- *We remove the 2 at position 2 and get $\Delta_2 = (1,3,2,2)$ and the new edges 12 and 24 since what is now vertex 3 was the original vertex 4.*
- *We remove the 2 at position 3 (which was the original position 5 which yields $\Delta_3 = (1,2,1)$ and $E_3 = \{23, 34, 12, 24, 45, 56\}$.*
- *In the last step, we add the edges 14 and 46 since the inner 2 in Δ_3 was obtained from the original vertex 4.*

The obtained graph is shown in Figure 2.3.

Having Theorem 2.0.1 in mind it is natural to ask if this result can be generalized to arbitrary HVGs without restricting to data sequences with pairwise distinct entries. It can be verified computationally that this is possible for $N \le 6$, i.e., any HVG in

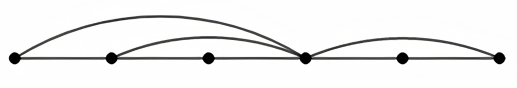

FIGURE 2.3: The unique HVG with ordered degree sequence $(2,3,2,5,2,2)$.

$\mathcal{G}_N$ is uniquely determined by its ordered degree sequence. However, already for $N = 7$ this breaks down, since there exist 394 HVGs compared to 391 ordered degree sequences. An instance of two HVGs with the same ordered degree sequence is shown in Figure 2.4.

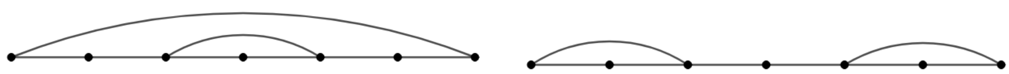

(A) HVG($(3,2,2,1,2,2,3)$) (B) HVG($(2,1,2,2,2,1,2)$)

FIGURE 2.4: Two HVGs with the same ordered degree sequence $(2,2,3,2,3,2,2)$.

We also want to point out that Theorem 2.0.1 cannot be generalized to unordered degree sequences since it is easy to construct examples of different HVGs with the same unordered degree sequence. For instance, the sequences $(4,1,2,3)$ and $(4,2,1,3)$ yield different HVGs having the same (unordered) degree sequence $(2,2,3,3)$ (see also [GMS11]).

2.1.3 Counting horizontal visibility graphs in $\mathcal{G}_{N,\neq}$

The aim of this subsection is to prove Theorem 2.0.2 (i). Namely, to show that HVGs in $\mathcal{G}_{N,\neq}$ are counted by the $(N-1)^{\text{st}}$ Catalan number $C(N-1)$ (see [Sta15] for the numerous interpretations of these). We first introduce some notation. For $N, s \in \mathbb{N}$ with $2 \le s \le N$, let

$$\mathcal{G}^s_{N,\neq} = \{G \in \mathcal{G}_{N,\neq} \ : \ m_G(1) = s\} .$$

Obviously, we have $|\mathcal{G}_{N,\neq}| = \sum_{s=2}^{N} |\mathcal{G}^s_{N,\neq}|$. We start by providing a relation between $|\mathcal{G}^s_{N,\neq}|$, $|\mathcal{G}^s_{s,\neq}|$ and $|\mathcal{G}_{N-s+1,\neq}|$.

Lemma 2.1.9. *Let $N, s \in \mathbb{N}$ with $2 \le s \le N$. Then*

$$|\mathcal{G}^s_{N,\neq}| = |\mathcal{G}^s_{s,\neq}| \cdot |\mathcal{G}_{N-s+1,\neq}|$$

Proof. Let $G \in \mathcal{G}^s_{N,\neq}$. It follows from Lemma 1.1.3 (iii) and the fact that $1s \in E(G)$ that $G_{[s]} \in \mathcal{G}^s_{s,\neq}$ and $G_{[s,N]} \in \mathcal{G}_{N-s+1,\neq}$. Since Lemma 1.1.3 (i), combined with $1s \in E(G)$, implies that G does not have edges between vertices in $[s-1]$ and vertices in $[s+1,N]$, it holds that $G = G_{[s]} + G_{[s,N]}$, i.e., G is uniquely determined by $G_{[s]}$ and $G_{[s,N]}$ and hence, $|\mathcal{G}^s_{N,\neq}| \le |\mathcal{G}^s_{s,\neq}| \cdot |\mathcal{G}_{N-s+1,\neq}|$.

Conversely, let $G \in \mathcal{G}^s_{s,\neq}$, $H \in \mathcal{G}_{N-s+1,\neq}$. Lemma 1.1.5 (iii), together with $1s \in E(G)$ implies that $G + H \in \mathcal{G}^s_{N,\neq}$. Since $G = (G+H)_{[s]}$ and $H = (G+H)_{[s,N]}$, G and H are uniquely determined by $G + H$ and it follows that $|\mathcal{G}^s_{N,\neq}| \ge |\mathcal{G}^s_{s,\neq}| \cdot |\mathcal{G}_{N-s+1,\neq}|$. This finishes the proof. $\square$

The next lemma will be crucial to count the graphs in $\mathcal{G}^s_{s,\neq}$.

Lemma 2.1.10. *Let $G \in \mathcal{G}^s_{s,\neq}$. Then $N(s) = \mathcal{N}(G_{[s-1]})$.*

Proof. Let $D \in \mathbb{N}^s$ with $\mathrm{HVG}(D) = G$ and pairwise distinct entries. We first show that $N(s) \subseteq \mathcal{N}(G_{[s-1]})$. To this end, let $\ell \in N(s)$, i.e., $\ell s \in E(G)$. Since in this case we must have $d_\ell > d_i < d_s$ for all $\ell < i < s$, there is no $uv \in E(G)$ with $1 \leq u < \ell < v \leq s-1$. Hence, $\ell \in \mathcal{N}(G_{[s-1]})$. For the reverse containment, consider $\ell \in \mathcal{N}(G_{[s-1]})$. The statement is trivially true for $\ell = 1$ and $\ell = s-1$. For $\ell \in \mathcal{N}(G_{[s-1]}) \setminus \{1, s-1\}$ assume by contradiction that $\ell s \notin E(G)$. Then there exists $\ell < j < s$ with $d_j > d_\ell$ or $d_j > d_s$. As $1s \in E(G)$, the latter case never occurs and therefore we must have $d_j > d_\ell$. In the following, we assume that j is minimal with this property. Similarly, let $1 \leq k < \ell$ maximal such that $d_k > d_\ell$. Note that such k exists since $d_1 > d_\ell$. It then follows that $kj \in E(G)$ and hence $kj \in E(G_{[s-1]})$ which implies $\ell \notin \mathcal{N}(G_{[s-1]})$, a contradiction. □

We want to remark, the same proof as above shows that Lemma 2.1.10 holds more generally for $G \in \mathcal{G}^s_{N,\neq}$. However, we do not need the statement in such generality. On the other hand, Lemma 2.1.10 does not generalize to arbitrary HVGs (see Example 1.1.4 for an example).

The next lemma is the last ingredient we need for the proof of Theorem 2.0.2 (i).

Lemma 2.1.11. *Let $N \in \mathbb{N}$, $N \geq 2$. Then*

$$|\mathcal{G}^N_{N,\neq}| = |\mathcal{G}_{N-1,\neq}|.$$

Proof. We show the claim by proving that

$$\Phi : \mathcal{G}^N_{N,\neq} \to \mathcal{G}_{N-1,\neq} : G \mapsto G_{[N-1]}$$

is a bijection. By Lemma 1.1.3 (iii) the map Φ is well-defined and it directly follows from Lemma 2.1.10 that Φ is injective. To show surjectivity, let $H \in \mathcal{G}_{N-1,\neq}$ and let $D = (d_1, \ldots, d_{N-1}) \in \mathbb{N}^{N-1}$ be the standard sequence of H. Since all entries of D are distinct, at most $N-1$ and $d_1 = N-1$ it follows that $G = \mathrm{HVG}((d_1, \ldots, d_{N-1}, N)) \in \mathcal{G}^N_{N,\neq}$. Since clearly $\Phi(G) = H$, we conclude that Φ is surjective. □

Finally, we can provide the proof of Theorem 2.0.2 (i).

Proof of Theorem 2.0.2 (i) We show the claim via induction. For $N \in \{1, 2\}$ there exists exactly one graph in $\mathcal{G}_{N,\neq}$ and since $C(0) = C(1) = 1$, the claim is trivially true in this case. Let $N \geq 2$. We then have

$$\begin{aligned}
|\mathcal{G}_{N,\neq}| &= \sum_{s=2}^{N} |\mathcal{G}^s_{N,\neq}| = \sum_{s=2}^{N} |\mathcal{G}^s_{s,\neq}| \cdot |\mathcal{G}_{N-s+1,\neq}| \\
&= \sum_{s=2}^{N} |\mathcal{G}_{s-1,\neq}| \cdot |\mathcal{G}_{N-s+1,\neq}| \\
&= \sum_{s=2}^{N} C(s-2) \cdot C(N-s) = \sum_{s=0}^{N-2} C(s) \cdot C(N-2-s) = C(N-1),
\end{aligned}$$

where the second, third, fourth and sixth equality follow from Lemma 2.1.9, Lemma 2.1.11, the induction hypothesis and Segner's recurrence formula for the Catalan numbers [Seg58], respectively. □

We end this subsection with an identity for the Catalan numbers, which we stumbled over in our study of HVGs but which we were unable to find in the literature.

Proposition 2.1.12. *Let $N \in \mathbb{N}$. Then*

$$C(N) = 1 + \sum_{k=3}^{N+1} \frac{3}{2k-3}\binom{2k-3}{k}.$$

Proof. We prove the statement via induction. Since $C(0) = C(1) = 1$, the statement is trivially true for $N \in \{0,1\}$. Now let $N \geq 2$. In this case, we have

$$\begin{aligned} 1 + \sum_{k=3}^{N+1} \frac{3}{2k-3}\binom{2k-3}{k} &= 1 + \sum_{k=3}^{N} \frac{3}{2k-3}\binom{2k-3}{k} + \frac{3}{2N-1}\binom{2N-1}{N+1} \\ &= C(N-1) + \frac{3}{2N-1}\binom{2N-1}{N+1} \\ &= \frac{(2N-2)!}{N(N-1)!(N-1)!} + \frac{3(2N-2)!}{(N+1)!(N-2)!} \\ &= \frac{1}{N+1}\binom{2N}{N} = C(N) \end{aligned}$$

where the second equality follows from the induction hypothesis, the fourth from an easy computation and the last by definition of the Catalan numbers (see, e.g., [Sta15]). □

2.1.4 Horizontal visibility graphs and parentheses

Since we have seen in Theorem 2.0.2 (i) that HVGs in $\mathcal{G}_{N,\neq}$ are counted by the Catalan number $C(N-1)$, it is natural to ask for a bijective proof of this statement. This is the goal of this subsection. More precisely, we provide an explicit bijection between $\mathcal{G}_{N,\neq}$ and the set $\mathcal{B}_{N-1}$ of balanced parantheses of length N, which are known to be counted by $C(N-1)$ [Kos09, p.134 f.]. We use the definition for balanced parentheses from [LLM10, p. 155].

Definition 2.1.13. *Let ϵ be the empty string. The set $\mathcal{B}$ of* balanced parentheses *is recursively defined via*

(i) $\epsilon \in \mathcal{B}$.

(ii) If $B_1, B_2 \in \mathcal{B}$, then $[B_1]B_2 \in \mathcal{B}$.

The set of balanced parentheses with N pairs of parentheses is denoted by $\mathcal{B}_N$.

It is easily seen from the definition that any balanced parentheses $B \in \mathcal{B}_N$ can be uniquely written in the form $B = [B_1]\ldots[B_k]$ with $B_j \in \mathcal{B}_{i_j}$ for $i_j \in \mathbb{N}$ and $\sum_{j=1}^{k} i_j = N - k$. We will refer to this representation as *normal* representation of B with blocks $B_1, \ldots, B_k$ and to $i_1, \ldots, i_k$ as the *lengths* of the blocks.

We now state the main result of this section.

Theorem 2.1.14. *Let $N \in \mathbb{N}$, $N \geq 1$. Let $\psi_N : \mathcal{G}_{N,\neq} \to \mathcal{B}_{N-1}$ be recursively defined by $\psi_1(P_1) = \epsilon$ and*

$$\psi_N(G) = [\psi_{i_2-i_1}(G_{[i_1+1,i_2]})][\psi_{i_3-i_2}(G_{[i_2+1,i_3]})]\cdots[\psi_{i_k-i_{k-1}}(G_{[i_{k-1}+1,i_k]})]$$

if $N > 1$ and $G \in \mathcal{G}_{N,\neq}$ with $\mathcal{N}(G) = \{i_1 < \cdots < i_k\}$. Then ψ_N is a bijection.

Proof. Since $\sum_{j=2}^{k}(i_j - i_{j-1}) = i_k - i_1 = N - 1$, it is easily seen by induction on N that the map ψ_N is well-defined. Moreover, $\psi_N(G)$ is given in normal representation.

As it follows from Theorem 2.0.2 (i) and [Kos09, p.134 f.] that $|\mathcal{G}_{N,\neq}| = |\mathcal{B}_{N-1}| = C_{N-1}$, it suffices to show that ψ_N is injective for every $N \geq 1$. For $N = 1$, this is trivially true since $\mathcal{G}_{1,\neq} = \{P_1\}$. Let $N \geq 2$ and let $G, H \in \mathcal{G}_N$ such that $G \neq H$. If $\mathcal{N}(G) \neq \mathcal{N}(H)$, then $\psi_N(G)$ and $\psi_N(H)$ must have blocks of different lengths, which already implies $\psi_N(G) \neq \psi_N(H)$. Assume that $\mathcal{N}(G) = \mathcal{N}(H) = \{i_1 < \cdots < i_k\}$. As $G \neq H$, there exists $2 \leq j \leq k$ with $G_{[i_{j-1}+1, i_j]} \neq H_{[i_{j-1}, i_j]}$. The induction hypothesis implies that $\psi_{i_j - i_{j-1}}(G_{[i_{j-1}+1, i_j]}) \neq \psi_{i_j - i_{j-1}}(H_{[i_{j-1}+1, i_j]})$ and hence $\psi_N(G) \neq \psi_N(H)$. □

The next example illustrates the bijection ψ_N.

Example 2.1.15. *For the graph G in Figure 2.5, we get*

$$\psi_{10}(G) = [[[\ ]\ [\ ]\ [\ ]]\ [\ ]]\ [[\ ]\ [\ ]] \in \mathcal{B}_9.$$

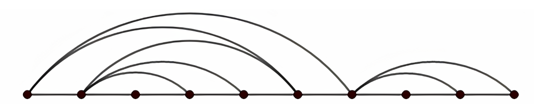

Figure 2.5: The graph $G = \mathrm{HVG}((10, 6, 2, 4, 5, 8, 9, 1, 3, 7))$.

The process of how ψ works is visualized in Figure 2.6.

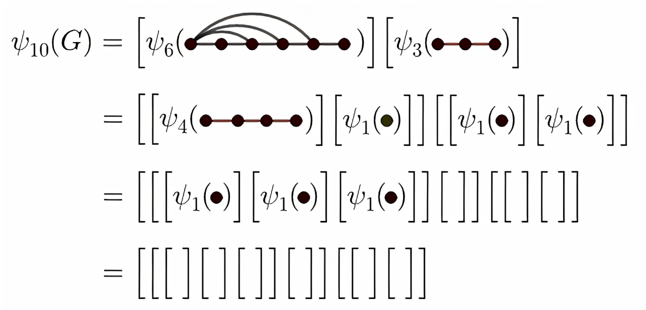

Figure 2.6: Applying ψ_{10} to G.

Remark 2.1.16. *It is easily seen that the inverse map $\psi_N^{-1} : \mathcal{B}_{N-1} \to \mathcal{G}_{N,\neq}$ of ψ_N is given by $\psi_1^{-1}(\epsilon) = P_1$ and*

$$\psi_N^{-1}(B) = \overline{\psi_{i_1}^{-1}(B_1)} + \cdots + \overline{\psi_{i_k}^{-1}(B_k)},$$

if $N > 1$ and $B = [B_1] \cdots [B_k] \in \mathcal{B}_{N-1}$ with $B_j \in \mathcal{B}_{i_j - 1}$ and $\sum_{j=1}^{k} i_j = N - 1$. Here, for an HVG G, we denote by $\overline{G}$ the HVG

$$((\{1,2\}, \{12\}) + G) \cup \{1(i+1) \ : \ i \in \mathcal{N}(G)\},$$

i.e., $\overline{G}$ is obtained from G by adding a "new" vertex 1 that is connected to all non-nested vertices of G.

2.2 Horizontal visibility graphs from arbitrary data

While in the previous section we were focusing on HVGs corresponding to data sequences without equal entries, we will now omit this restriction and allow arbitrary data sequences. As before, it follows from Remark 1.1.2 that we only need to consider integral data sequences.

Our first goal is to describe an explicit method to construct a data sequence D that realizes a given $G \in \mathcal{G}_N$ as its HVG. This is very similar to Theorem 2.1.1. In the second part of this section, we turn to a more combinatorial problem: Namely, counting HVGs in $\mathcal{G}_N$. In particular, we prove Theorem 2.0.2 (ii).

2.2.1 From horizontal visibility graphs to data sequences

In the following, we are asking the analogous question to the one posed in Subsection 2.1.1. Namely, given $N \in \mathbb{N}$, $G = ([N], E) \in \mathcal{G}_N$, we are searching a data sequence $D \in \mathbb{N}^N$ realizing G. An answer is provided by the next theorem, which uses the same notations as in Subsection 2.1.1.

Theorem 2.2.1. *Let $N \in \mathbb{N}$ and $G \in \mathcal{G}_N$. For $1 \le i \le N$, let*

$$d_i = N - \delta_{\text{nest}}(i).$$

Then $D = (d_1, \dots, d_N)$ realizes G, i.e., $\mathrm{HVG}(D) = G$.

Proof. Let $\widetilde{D} = (\widetilde{d}_1, \dots, \widetilde{d}_N) \in \mathbb{N}^N$ with $\mathrm{HVG}(\widetilde{D}) = G$ and let $H = \mathrm{HVG}(D)$. Verbatim the same arguments as in the proof of Theorem 2.1.1 show that $E(G) \subseteq E(H)$.

For the reverse containment, let $ij \in E(H)$ with $i + 1 < j$ and assume that there exists $i < k < j$ with $\widetilde{d}_k \ge \min(\widetilde{d}_i, \widetilde{d}_j)$. Since, in contrast to the proof of Theorem 2.1.1, everything is symmetric with respect to i and j, one can assume that $\min(\widetilde{d}_i, \widetilde{d}_j) = \widetilde{d}_i$. As in Case 1 of the proof of Theorem 2.1.1, it follows that $\delta_{\text{nest}}(i) \ge \delta_{\text{nest}}(k)$ which directly implies $d_i \le d_k$, yielding a contradiction. Since $i(i+1)$ for $1 \le i \le N-1$ lies in any HVG, we conclude $G = H$. □

The graph in Figure 1.2 can be represented with Theorem 2.2.1 via $D = (4, 3, 3, 4)$.

2.2.2 Counting horizontal visibility graphs – Schröder numbers

The aim of this section is to prove Theorem 2.0.2 (ii). Namely, to show that the number of HVGs of length N is given by the $(N-2)^{\text{nd}}$ large Schröder number r_{N-2}. Those are known to count several combinatorial objects including certain types of lattice paths (see [SS00]). We start by providing relevant definitions.

Definition 2.2.2. *A* bracketing *B of a string of identical letters x is*

- *either a single letter x, or*
- *$B = (B_1, \dots, B_k)$, where $k \ge 2$, and $B_1, \dots, B_k$ are bracketings and brackets around a single letter as well as the outer surrounding brackets are omitted.*

The bracketing $x \cdots x$ without any brackets will be referred to as a trivial bracketing. *The* length *$\ell(B)$ of a bracketing B is defined to be the number of enclosed letters, and we use $\widetilde{\mathcal{B}}_N$ to denote the set of bracketings of length N.*

It is easy to see from the definition that every bracketing $B \in \widetilde{\mathcal{B}}_N$ has a unique representation of the form $B = B_1 \cdots B_k$, where for $1 \le i \le k$, B_i is either a trivial bracketing, or, $B_i = (\tilde{B}_i)$ for a bracketing $\tilde{B}_i$ and no two trivial bracketings are adjacent. The last condition means that adjacent trivial bracketings are grouped together into a trivial bracketing of maximal length. We call this representation the *normal form* of a bracketing. $s_N = |\widetilde{\mathcal{B}}_{N+1}|$ is called the N^{th} *little Schröder number*

[Sch70]. It is well-known that $r_N = 2s_N$. Similar to Subsection 2.1.3, we write $\mathcal{G}_N^s$ for the set of HVGs G in $\mathcal{G}_N$ with $m_G(1) = s$. The next lemma allows us to reduce the proof of Theorem 2.0.2 (ii) to counting HVGs without $1N$.

Lemma 2.2.3. *For $N \geq 3$, we have*

$$|\mathcal{G}_N^N| = |\mathcal{G}_N \smallsetminus \mathcal{G}_N^N|, \qquad i.e., \qquad |\mathcal{G}_N| = 2|\mathcal{G}_N^N|.$$

Proof. It is easy to see that the map

$$\varphi : \mathcal{G}_N^N \to \mathcal{G}_N \smallsetminus \mathcal{G}_N^N : G \mapsto G \smallsetminus \{1N\}$$

is a bijection. Indeed, it follows from Lemma 1.1.5 (i) and (ii) that φ is well-defined and surjective, respectively. Since the injectivity is obvious, the claim follows. □

As $r_N = 2s_N$, the next statement completes the proof of Theorem 2.0.2 (ii).

Theorem 2.2.4. *Let $N \in \mathbb{N}$, $N \geq 2$. Then*

$$|\mathcal{G}_N^N| = s_{N-2}.$$

Proof. We clearly have $|\mathcal{G}_2^2| = 1 = s_0$ and hence the claim holds in this case.

For ease of notation, we set $\mathcal{G}_N^* = \mathcal{G}_N \smallsetminus \mathcal{G}_N^N$. To show the claim, we provide a bijection between $\widetilde{\mathcal{B}}_N$ and $\mathcal{G}_{N+1}^*$ for $N \geq 2$. We consider the map $\xi_N : \widetilde{\mathcal{B}}_N \to \mathcal{G}_{N+1}^*$ which is defined by $\xi_2(xx) = P_3$, $\xi_N(x\cdots x) = P_{N+1}$ for any $N \geq 2$. If $N \geq 3$ and $B = B_1 \cdots B_k \in \widetilde{\mathcal{B}}_N$ is in normal form with non-trivial blocks $B_{i_1}, \ldots, B_{i_r}$, where $i_1 < i_2 < \cdots < i_r$, we recursively define

$$\xi_N(B) = \xi_{\ell(B_1)}(\widetilde{B}_1) + \cdots + \xi_{\ell(B_k)}(\widetilde{B}_k) \cup \{(\sum_{j=1}^{i_m - 1} \ell(B_j) + 1)(\sum_{j=1}^{i_m} \ell(B_j) + 1) \ : \ 1 \leq m \leq r\},$$

where $B_j = \widetilde{B}_j \in B_{\ell(B_j)}$ if B_j is trivial and $B_j = (\widetilde{B}_j)$, otherwise. We also set $\xi_1(x) = P_2$. As $\sum_{i=1}^k (\ell(B_i) + 1) - (k-1) = \sum_{i=1}^k \ell(B_i) + 1 = N + 1$ and $\widetilde{B}_j \in \widetilde{\mathcal{B}}_{\ell(B_j)}$, it follows by induction on N and Lemma 1.1.5 (iii) that ξ_N is well-defined. The map ξ_N is obviously injective for $N = 2$, and for $N \geq 3$, using induction, we get injectivity directly from the definition of ξ_N. It remains to show that ξ_N is surjective. For $N = 2$, this is clear. Assume $N \geq 3$ and let $G \in \mathcal{G}_{N+1}^* \smallsetminus \{P_{N+1}\}$. Since $1(N+1) \notin E(G)$, there exists a non-nested vertex s of G with $1 < s < N+1$. Choosing s maximal, it follows that $s(N+1) \in E(G)$. By Lemma 1.1.3 (iii) and Lemma 1.1.5 (i) it holds that $G_{[s,N+1]} \smallsetminus \{s(N+1)\} \in \mathcal{G}_{N+2-s}^*$. We now distinguish two cases. If $1s \notin E(G)$, then again by Lemma 1.1.3 (iii), we have $G_{[1,s]} \in \mathcal{G}_s^*$. By induction, there exist $B_1 \in \widetilde{\mathcal{B}}_{s-1}$ and $B_2 \in \widetilde{\mathcal{B}}_{N-s+1}$ such that $\xi_{s-1}(B_1) = G_{[1,s]}$ and $\xi_{N-s+1}(B_2) = G_{[s,N+1]} \smallsetminus \{s(N+1)\}$. As $B_1(B_2) \in \widetilde{\mathcal{B}}_N$, we further conclude that

$$\begin{aligned}\xi_N(B_1(B_2)) = & \quad \xi_{s-1}(B_1) + \xi_{N-s+1}(B_2) \cup \{s(N+1)\} \\ = & \quad G_{[1,s]} + G_{[s,N+1]} \smallsetminus \{s(N+1)\} \cup \{s(N+1)\} = G.\end{aligned}$$

If $1s \in E(G)$, then $G_{[1,s]} \smallsetminus \{1s\} \in \mathcal{G}_s^*$ and there exists $B_1 \in \widetilde{\mathcal{B}}_{s-1}$ with $\xi_{s-1}(B_1) = G_{[1,s]} \smallsetminus \{1s\}$. A similar computation as in the previous case shows that $\xi_N((B_1)(B_2)) = G$. Hence, the map ξ_N is surjective. Lemma 2.2.3 finishes the proof. □

We provide an example to illustrate the bijection ξ_N.

Example 2.2.5. *Applying ξ_8 to*

$$B = (xx)\big((xxx)x(xx)\big)$$

results in

$$\begin{aligned}\xi_8(B) &= \xi_2(xx) + \xi_6((xxx)x(xx)) \cup \{13,39\}\\ &= \xi_2(xx) + \big(\xi_3(xxx) + \xi_1(x) + \xi_2(xx) \cup \{14,57\}\big) \cup \{13,39\}\\ &= \xi_2(xx) + \xi_3(xxx) + \xi_1(x) + \xi_2(xx) \cup \{36,79\} \cup \{13,39\},\end{aligned}$$

and the graph obtained is shown in Figure 2.7.

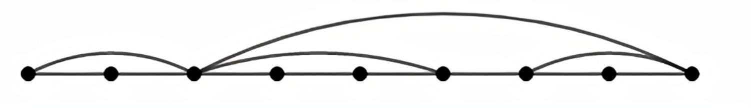

FIGURE 2.7: The graph $\xi_8(B)$.

The little Schröder number s_{N-2} is known to count a variety of combinatorial objects, including *dissections* of a convex polygon Π_N on N vertices, labeled $1,\dots,N$. Here, a dissection of Π_N is defined as a subdivision of Π_N into polygonal regions via non-crossing diagonals between vertices of Π_N (see [FN99, Section 3]). In other words, a dissection is a non-crossing graph containing the cycle $1,\dots,N,1$. In particular, any HVG in $\mathcal{G}_N$ with $1N \in E(G)$ can naturally be viewed as a dissection. Theorem 2.2.4 even implies that every dissection can be obtained this way.

Corollary 2.2.6. *For $N \geq 3$, the sets $\mathcal{G}_N^N$ and Π_N are in natural bijective correspondence, where the map is given by the identity.*

2.3 Open problems

The main goals of this chapter lay on the reconstruction of HVGs in $\mathcal{G}_N$ from a given ordered degree sequence and in counting HVGs in $\mathcal{G}_N$ and $\mathcal{G}_{N,\neq}$ which led us to objects that are counted by the large Schröder and Catalan numbers, respectively. From our results several open questions arose that we now briefly discuss.

As an extension of HVGs, it is natural to consider the more general class of *visibility graphs* (VGs for short) [Bal+08], defined as follows. Given a data sequence $(t_1,d_1),\dots,(t_N,d_N)$, where the t_i are time points, the visibility graph of this sequence is the graph on vertex set $[N]$, where ij is an edge if and only if $d_k < d_j + (d_i - d_j)\frac{t_j - t_k}{t_j - t_i}$ for all t_k with $t_i < t_k < t_j$. It is immediately seen that this graph always contains the HVG of the data sequence $(d_1,\dots,d_N)$ as a subgraph. In line with Theorem 2.0.2, it is natural to ask for the cardinality of VGs on a fixed number of vertices. To this end, in a first step, we successively constructed VGs from random data-sequences of length up to 7 until no new VGs were found. Though there is no guarantee to have exhausted the whole set of VGs on up to 7 nodes in this way, we suspect that the number of those VGs are the ones displayed in the next table:

N	number of VGs on N nodes
1	1
2	1
3	2
4	6
5	25
6	138
7	972
8	8477

.

This sequence seems to be sequence A007815 in OEIS [The], which counts so-called persistent graphs on N nodes. On the one hand, every VG is a persistent graph. On the other hand, there exist persistent graphs which are not VGs [Ame+20]. In particular, sequence A007815 is just an upper bound for the cardinality in question. So, we do not even have a conjectured answer to the following question.

Question 2.3.1. *What is the number of VGs on N nodes?*

Since the set of HVGs on N nodes is contained in the set of VGs on N nodes, one possible way to answer Question 2.3.1 is by means of the following question:

Question 2.3.2. *Can one characterize (graph-theoretically) the VGs that are not HVGs?*

Moreover, one could asked under what constrains on a given data-sequence the associated VG is actually an HVG. More precisely, it would be interesting to consider the following problem:

Question 2.3.3. *Can one characterize data sequences such that the corresponding VG is an HVG? If so, is it possible to construct a data sequence having the considered VG as its HVG? Does the same data sequence work?*

Motivated by what is happening for HVGs, our last question arises.

Question 2.3.4. *Is there a difference between VG associated to sequences with pairwise distinct entries (when restricting to the second coordinate) in contrast to VGs associated to arbitrary sequences where equal entries in the second coordinate are allowed?*

Chapter 3

A scalable linear time algorithm for horizontal visibility graphs

An HVG is formed from a time series by associating each data point with a vertex in the HVG. Two vertices share an edge if the corresponding data points can *see* each other, i.e., if the data points can be connected with a horizontal line, whereby all data points in between must lie below it. This criterion, also called *horizontal visibility*, only allows a straight line with a zero gradient [Bal+08]. The *(natural) visibility*, on the other hand, allows straight lines with arbitrary gradients [Bal+09]. The difference can be seen in Figure 3.1.

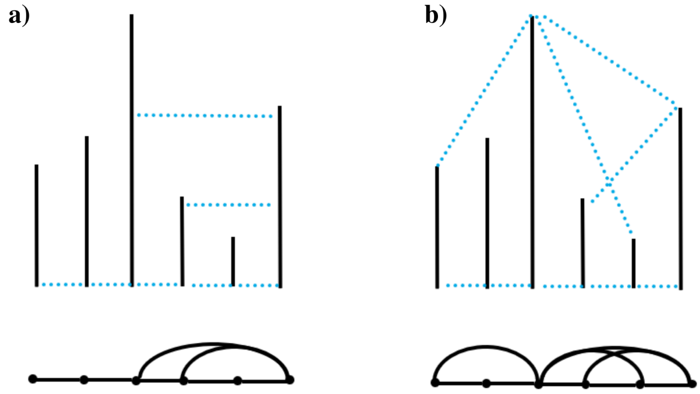

FIGURE 3.1: (a) and (b) show the edges of an HVG and a VG for an identical time series, respectively. Note that an HVG is always a subgraph of the VG given the same time series.

In more formal notation, consider a time series S of length N with

$$S = \big((t_1, s_1), \dots, (t_N, s_N)\big).$$

Two points (t_i, s_i) and (t_j, s_j), $1 \leq i < j \leq N$, are called *horizontally visible* if for every intermediate point (t_k, s_k) with $i < k < j$, it holds that

$$s_k < \min(s_i, s_j).$$

We set $\mathrm{HVG}(S) = \mathrm{HVG}((s_1, \dots, s_N))$ and $\mathrm{VG}(S) = (V, F)$ and call it the horizontal visibility graph and *visibility graph* (VG for short) of S, respectively. For $\mathrm{VG}(S)$, the set of nodes V is the same as in the HVG-case and $ij \in F$ if and only if (t_i, s_i) and

(t_j, s_j), $1 \le i < j \le N$, are *(naturally) visible*, i.e.,

$$s_k < s_i + (s_j - s_i)\frac{t_k - t_i}{t_j - t_i}$$

for every data point (t_k, s_k) with $i < k < j$. The HVG is always a subgraph of the VG since two vertices seeing each other horizontally can also see each other naturally. Like HVGs, every VG contains P_N as a subgraph. Furthermore, they are also invariant to (strictly positive) horizontal and vertical scaling and horizontal and vertical translations. A big advantage of the horizontal visibility is that it is computationally less complex than the natural visibility [Nic+20]. In the following, we will only consider HVGs; note that since these just depend on the order of their data points, we will no longer explicitly refer to the time index t_i.

There exist several approaches to compute the HVG of a given series. A naive implementation is in the complexity class $O(N^2)$ which has led to several publications with optimized algorithms [Bal+09; Che+15; Lac+12; LWZ12; Ste21; Yel+20]. For stochastic time series, Lacasa has developed an algorithm that, in the average case, claims to work in linear time [Bal+09; Lac+12]. Since this approach is an offline algorithm, the whole time series data must be available at the calculation time. If new data is added, the graph has to be recalculated entirely, which is particularly problematic with streamed data. Using an approach based on binary search trees, Fano Yela et al. have implemented an algorithm calculating HVGs and VGs in the average case in $O(N \log N)$, which also works efficiently on batch-wise incoming data [Yel+20]. When applied to real-life time series, however, it becomes apparent that this algorithm increases its runtime significantly towards $O(N^2)$. A recently published algorithm by Stephen that computes HVGs using a dual tree representation of the time series is worst-case in $O(N)$ [Ste21]. Additionally, the runtime of this approach is not affected by the type of time series, it works efficiently on streamed data, and it is scalable; thus, it is suitable for multi-processing. The drawback of this algorithm is that it uses a complex data structure. Our algorithm builds on the approach in [LWZ12], which we extend such that it also works efficiently on streamed data and becomes scalable. Moreover, we do not use a complex tree-like data structure and still achieve a state-of-the-art runtime. We introduce an algorithm that constructs an HVG for every possible time series in linear time with only minor fluctuations in runtime for different types of time series and that works on streamed data without additional computational costs. Furthermore, the HVG of every intermediate time series is generated implicitly if the algorithm is stopped prematurely.

3.1 Related work

The simplest method to implement an HVG algorithm is based on the idea of checking for each of the N data points of the time series whether it can see the remaining $N-1$ data points. Since the visibility property is symmetric, the number of checks could be halved. But with $N(N-1)/2$ checks, it still remains in $O(N^2)$. A better complexity class can be achieved using a "divide and conquer" approach, as described by Lan et al. [Che+15]. Suppose the maximum value M of the time series is known. In that case, it is also clear that no data point to the left of M can see a data point to the right of M. This approach is then applied recursively to the left and right halves and new maxima are determined for which it is known that they have an edge with the previous maximum. Overall, it can be proven that this algorithm lies on average in

$O(N \log N)$. This approach can also be applied to natural visibility graphs and lies within the same complexity class there.

An algorithm developed by Lacasa enables an even faster calculation [Bal+09; Lac+12]. The approach works as follows: Given a time series $S = (s_1, \ldots, s_N)$ of length N, for each of these N data points it is determined which set of data points it can see that lie to its right, i.e., have a larger time index. Then an edge between the current index and each index of data points in the set of visible ones is added. Note, with such a procedure all edges in an HVG are found. Let us assume that the current index is $1 \leq idx \leq N - 1$. All data points s_i with index $idx < i \leq N$ are ascendingly checked for visibility between them and s_{idx} until one data point s_j is larger than or equal to s_{idx}. From this specific data point s_j on, s_{idx} cannot see any data point s_k with $k > j$. Therefore, the check for visibility is stopped here. This procedure is performed for all data points s_{idx} with $1 \leq idx \leq N - 1$. For noisy (stochastic and chaotic) time series, it is shown empirically that this algorithm has a time complexity of $O(N)$. While the approach can be very fast for some types of time series, it has two significant drawbacks. First, as it traverses the data points, the algorithm does not remember which data points are larger than others. Pictorially, this can be seen as if a person would run to the right and stop at a certain point, then would run back and forget what it already saw and therefore did not use shortcuts. Second, the algorithm does not work efficiently on streamed data in its implemented form. Meaning, if the HVG has already been determined for a time series and new data comes in, the algorithm must run again over the entire data of the extended time series. But, the latter issue can be fixed via a minor extension of the implementation.

Fano Yela's approach is based on *binary search trees* (BST), and achieves an average runtime in $O(N \log N)$ for both HVGs and VGs. At the same time, efficient calculation on streamed data is possible [Yel+20]. Additionally, the algorithm is parallelizable where the merging of the computed parts is in $O(\log N)$. Clearly, this is an improvement compared to Lan et al., since Fano Yela's algorithm is in the identical complexity class but also has the so-called *online* functionality, which the divide and conquer approach does not have. The algorithm consists of an encoding and a decoding part. In the encoding part, the time series' values are sorted in descending order and entered in a maximum BST based on their index. Since the BST encodes the size relationships of the data points, each edge can be reconstructed from the HVG through cleverly chosen lookup operations in the search tree. For a special class of BSTs, so called balanced BSTs, a lookup operation can be executed in time $O(\log N)$ and because this has to be done for all N data points of the time series, the average runtime is $O(N \log N)$. When new data in batch form comes in, a BST is also created for this new data. With the help of a merge operation, both BSTs are then combined, and an average runtime of $O(N \log N)$ can be achieved even for streamed data. A disadvantage of the approach is that the lookup operations in the search tree become computationally more costly if the search tree is not balanced. A solution to this problem is provided by Stephen's *dual tree horizontal visibility graph* (DTHVG) *algorithm*, which relates HVGs to time series merge trees [Ste21]. A time series merge tree contains the HVG in its dual. Using this new data structure, merging two HVGs in $O(N)$ is possible. The main reason for this is that only leading and trailing branches of two merge trees are needed to merge the corresponding HVGs, which makes the methodology particularly efficient. Overall, this approach allows the computation of HVGs in worst-case $O(N)$, has online functionality, and efficient scalability. However, we show that our proposed method also satisfies these properties while not requiring a complex data structure and achieve state-of-the-art runtime. For this purpose, we build on the fast horizontal visibility algorithm (FHVG) algorithm of Zhu et al. to work efficient with streamed data and develop a version for multiprocessing and distributed computing [LWZ12]. Moreover, we provide a proof that our algorithm is correct, which is missing for both algorithms in [Ste21] and [LWZ12] although crucial for their observations.

3.2 Proposed method

We call our proposed algorithm the *Linear Time algorithm*, and it is described in the following pseudo-code (LT-algorithm).

LT-algorithm: Returns the set of edges E of HVG(s).

```
Input  : series = (s_1, ..., s_n), edges, decreasing
Output: edges
if edges and decreasing are None then
    edges = list();
    decreasing = list((1, series[1]));
else
    s*_1 = last element decreasing;
    series = (s*_1, s*_2, ..., s*_{n+1}) where s*_{i+1} = s_i for 1 ≤ i ≤ n;
for idx = 2 to len(series) do
    counter = 0;
    if series[idx − 1] > series[idx] then
        edges.append(edge from idx − 1 to idx));
    else
        for element ∈ reversed(decreasing) do
            edges.append(
                edge from element[0] to idx
            );
            if series[idx] > element[1] then
                counter = counter + 1;
            if series[idx] == element[1] then
                counter = counter + 1;
                break;
            else
                break;
    delete last counter elements of decreasing;
    decreasing.append((idx, series[idx]));
return edges
```

The algorithm loops through the time series once, chronologically, and determines for each data point which previous data points it can see. Since the visibility to previous data points can already be blocked by others, the main idea of the algorithm is to use a reduced list containing only all potentially visible data points for the current one. This list is then traversed backwards and checked against which data points of the list are visible for the current data point until the visibility gets blocked for the first time or the list ends (see Figure 3.2). The algorithm's procedure is shown visu-

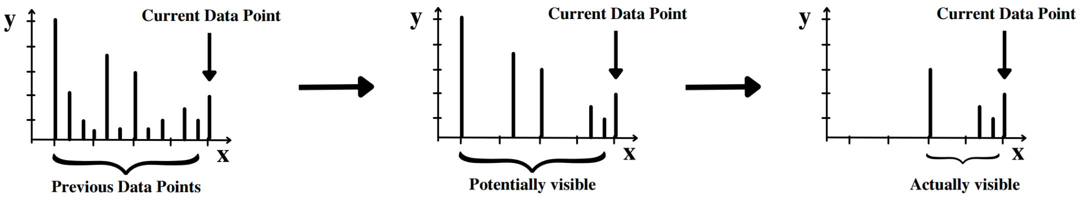

FIGURE 3.2: From the list of potentially visible data points, the list of actual ones is determined by traversing the list backward until a data point is at least as large as the current one.

ally in Figure 3.3 for a whole time series. The intermediate results of the algorithm are presented step by step.

In the following, we describe the LT-algorithm in detail:

Consider the time series $S = (s_1, \dots, s_N)$, which will be the input of the LT-algorithm, and the vertices of HVG(S) named $1, \dots, N$. The steps are:

First, if *edges* and *decreasing* have not been passed as input, a list *edges* is initialized for storing the edges of the HVG. The list *decreasing*, which will be central to the algorithm's efficiency and in which the potentially visible previous points will be stored, is created and s_1, the first value of the time series, is added to it. In the other case, if *edges* and *decreasing* of a previously calculated HVG is passed as input, we are dealing with streamed data explained in Subsection 3.2.3. Thus, in the following, we deal with the case that $edges = decreasing = \varnothing$.

Chronologically, the algorithm loops through S starting at $idx = 2$. First, the last added entry of *decreasing*, equal to $series[idx - 1]$, is compared with the current element $series[idx]$. Suppose $series[idx - 1] > series[idx]$. In that case, $\{i, idx\}$ cannot be an edge for $1 \le i < idx - 1$ and only the edge $\{idx - 1, idx\}$ will be appended to the list *edges*. Otherwise, the *else*-case is executed: We loop through a reversed version of *decreasing* and append the edge between the current element and idx. We continue this as long as $series[idx]$ is greater than the current element and increment the value of *counter* every time by 1. This variable stores the number of elements in *decreasing*, which are smaller than or equal to $series[idx]$. If we come to an element in $reversed(decreasing)$ that is greater than or equal to $series[idx]$, the *break* statement stops the inner for-loop. Since the last *counter* elements in *decreasing* are smaller than or equal to $series[idx]$ and are therefore not visible for $series[j]$ with $j > idx$, they get deleted from *decreasing*. Finally, $series[idx]$ is appended to *decreasing*. Note, *decreasing* now contains every $series[i]$ with $i \le idx$ that could be visible for the next element $series[idx + 1]$ and nothing more. From a computational perspective, it is very advantageous that all elements $series[i] \in decreasing$, which $series[idx]$ can see, are also those that are deleted from *decreasing* except the last one if it is strictly greater than $series[idx]$. Thus, *decreasing* is simultaneously updated such that it contains all elements that $series[idx + 1]$ could theoretically see omitting redundant data. This will be the main reason that the algorithm will run in linear time for any type of time series. Finally, when the outer for-loop is finished, *edges* is returned.

3.2.1 Correctness of the algorithm

In the following, we prove the correctness of the LT-algorithm. The algorithm is equivalent to the FHVG algorithm [LWZ12] when applied to a single time series (no

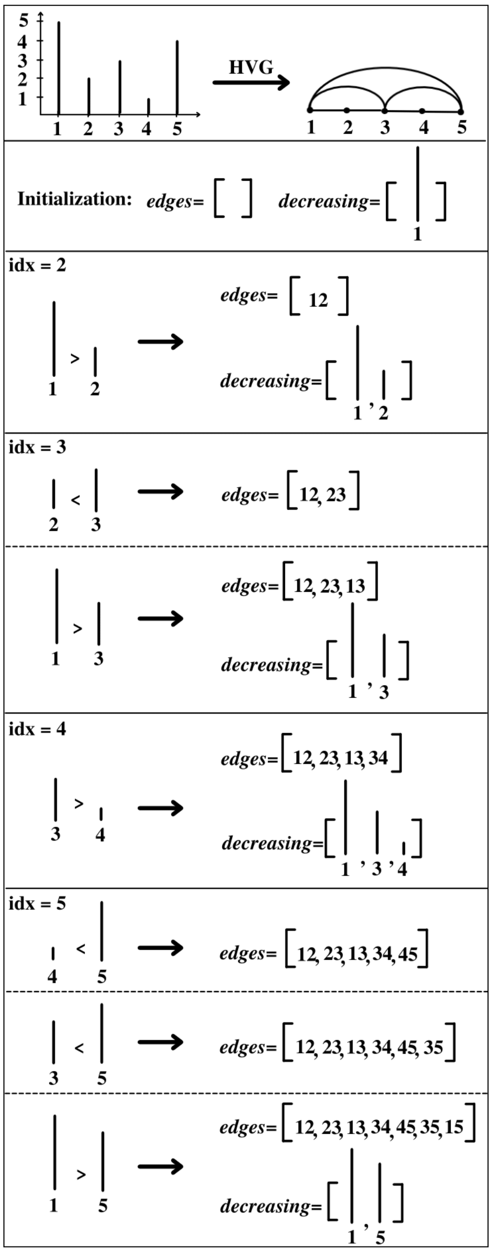

FIGURE 3.3: Illustration of the LT-algorithm for the time series $S = (5, 2, 3, 1, 4)$. If the algorithm is stopped at $idx = i, 2 \le i \le 5$, the current set *edges* matches the set of edges of the HVG$((s_1, \dots, s_i))$.

streamed data or multi-processing). However, in [LWZ12], no formal proof was given that shows the correctness of this algorithm. Thus, we close this gap in the chain of reasoning for the FHVG algorithm. We refer to a specific line x in the LT-algorithm by (l.x).

Theorem 3.2.1. *If the input of the LT-algorithm is the time series $S = (s_1, ..., s_N)$, then the output equals $E(\mathrm{HVG}(S))$.*

Proof. Let $G = \mathrm{HVG}(S)$, $H = (\{1, \dots, N\}, edges)$, where *edges* is the output of the LT-algorithm and D_k be the list *decreasing* in LT-algorithm at the time when $idx = k$. Note that, in this case, s_{k-1} is the last element of *decreasing* (l.7). We first show that $G \subseteq H$. Let $ij \in E(G)$. Then we must have

$$s_i > s_k < s_j \quad \forall k : i < k < j. \tag{3.1}$$

First, we show $s_i \in D_j$. Since $i < j$, the element s_i must have been added to the list *decreasing* after completing the for-loop (l.7) with $idx = i$. The element s_i only gets deleted from the list decreasing if there is an element s_k with $k > i$ such that $s_k \geq s_i$. But due to (3.1), this can only be s_j at earliest. Thus, $s_i \in D_j$.

Now, assume $ij \notin E(H)$. Then $i < j-1$ since otherwise ij must be in $E(H)$ because edges between neighbors are always included. Thus, there must exist an $i < l < j$ such that $s_j \leq s_l$. Otherwise, we do not get to a *break* command in the algorithm and the edge ij would be included. Thus, we have a contradiction to equation (3.1) and every edge of G is also in H.

We now show that $H \subseteq G$. Let $ij \in E(H)$ and assume $ij \notin E(G)$. This implies that i and j are not neighbors, since these are in $E(G)$. Then there exists an $i < l < j$ such that either $s_i \leq s_l$ or $s_j \leq s_l$. In the first case, $s_i \notin D_j$ and the edge ij is not generated. In the second case, the inner for-loop for $idx = j$ stops at element s_l which is reached before s_i. Thus, ij is not generated. This is a contradiction to the initial assumption that $ij \in E(H)$. □

3.2.2 Time complexity

The time complexity of algorithms is of special interest in many use cases. For the LT-algorithm, we can prove in our second main theorem that it runs worst-case in linear time. For other algorithms like FHVG or DTHVG the authors used the fact that the maximum number of edges in an HVG with N vertices is less than or equal to $2N-3$ to determine the time complexity class [GMS11]. We do not need this in our approach.

Theorem 3.2.2. *The LT-algorithm has worst-case time complexity $O(N)$.*

Proof. To determine the complexity class of the LT-algorithm, the runtimes of the individual parts are analyzed . The expressions in lines 1 to 6 are executed in $O(1)$ and are not relevant for calculating the complexity class, as they do not depend on the input length N of the time series. The key is to analyze the outer for-loop.
We will calculate how often which parts that run in $O(1)$ are executed in this for-loop. The initialization of *counter* (l.8) and the appending of the current element to the list *decreasing* (l.24) are carried out in constant time and can be neglected since the *if-else* case (l.9 and 11) is also executed in $O(1)$. It is necessary to examine this *if-else* case in more detail: If the *if*-case (l.9) occurs, this block is also finished in constant time. However, when the *else*-case (l.11) occurs, a for-loop is executed that passes through the elements from the *decreasing* list, whose length may vary. Several statements (l.13 – 22) are processed in $O(1)$, but possibly not for all elements in *decreasing* since it can also stop early. However, using the value of *counter*, we can count how many loop passes were executed. Also, the sum of all *counter* values can be used to determine how many times these $O(1)$ blocks were carried out in total. The same sum can also be taken to calculate the total number of delete operations from the *decreasing* list (l.23), for which a single one is also in $O(1)$. Because both parts depend on the sum of the *counter* values and are executed one after the other, i.e., their runtimes are only added, the complexity class does not change. So it follows that the growth behavior of the sum of the *counter* values alone determines the complexity class.

Now, we explain in greater detail how the value of *counter* can be used to estimate the runtime for the *if*-*else* case (l.9 and 11). If the *if*-case occurs, the inner statement is executed exactly ones, which is equal to *counter* + 1, where we consider the value of *counter* after one loop pass of the outer for-loop. For the *else*-case, we distinguish two cases. If the inner for-loop runs through the entire list *decreasing* or stops due to the *if*-case in line 18, then the value of *counter* after the loop corresponds to the number of loop passes. Otherwise, the *else*-case with *break* is executed so that *counter* is not incremented for the last iteration of the loop, resulting in *counter* + 1 iterations. Note that the inner for-loop is executed at most *counter* + 1 many times for $2 \le idx \le N$. Hence, we get the time complexity by calculating $\sum_{i=2}^{N}(c_i + 1)$, where $c_i, 2 \le i \le n$, is the value of *counter* after the loop pass with $idx = i$. Let D_j be the list *decreasing* in LT-algorithm after the loop pass with $idx = j$. Then for $2 \le j \le N$, $|D_j|$ can be computed recursively via

$$|D_j| = |D_{j-1}| - (c_j - 1). \tag{3.2}$$

The expression (3.2) is equivalent to $c_j = |D_{j-1}| - |D_j| + 1$ and summing over $2 \le j \le N$ gives

$$\begin{aligned}\sum_{j=2}^{N}(c_j + 1) &= \sum_{j=2}^{N}(|D_{j-1}| - |D_j| + 2) \\ &= |D_1| - |D_N| + 2(N-1) = 2N - 1 - |D_N|,\end{aligned} \tag{3.3}$$

where $|D_1|$ is the length of list *decreasing* at the start of the LT-algorithm, which is 1. Noteworthy is the fact that this applies to the best, average, and worst-case, as can be seen directly from the equation (3.3), where we have not made any prerequisites for the time series. We can minimize $2N - 1 - |D_N|$ by choosing $|D_N|$ to be maximal, that is, equal to N, which occurs only when the time series S is strictly monotone decreasing. Thus, in the minimal case, $\sum_{j=2}^{N}(c_j + 1) = n - 1$. The sum is maximized if $|D_N| = 1$, for which there are different possibilities, e.g., if S is strictly monotone decreasing for $s_1, \dots, s_{N-1}$ and $s_N = s_1$. Then $\sum_{j=2}^{N}(c_j + 1) = 2(N-1)$. This shows that there is only a factor of 2 between the upper bound for the number of times constant blocks are executed in the best and worst-cases. This proves that the LT-algorithm is in $O(N)$ and this visualizes how close even the worst and best cases are. □

3.2.3 Online version

Suppose we want to analyze a time series over a longer period of time and calculate an HVG from it at regular intervals. In that case, it is very important that we do not have to recalculate the HVG on all data, but reuse the results of the previous calculations to reduce the runtime. This is called the *online* functionality of an HVG algorithm [Yel+20]. The proposed method enables exactly that. If we want to apply the LT-algorithm on streamed data, we proceed as follows: Consider a time series S with the values $(s_1, \dots, s_M)$ as input for the LT-algorithm, then the output *edges* and *decreasing* must be saved. If new values of the time series come in, whereby $S = (s_1, \dots, s_M, \dots, s_N)$ with $N > M$, the LT-algorithm can be used again, with *series* = $(s_{M+1}, \dots, s_N)$, *edges* and *decreasing* as inputs. In this case, the index of every entry in *series* is shifted by 1 and the last element of *decreasing* (which is s_M) is added as the first element to this list (l.5–6).

Note, with this procedure we carry out the same steps as if we had given $(s_1, \dots, s_N)$ directly as input and stopped after $idx = M$ and started the algorithm again. Since we have already proven that the algorithm returns the correct set of edges, we know that this is also the case here since we are performing the same steps as for $\mathrm{HVG}(s_1, \ldots, s_N)$.

This shows further advantages of our algorithm, which are exemplarily shown in Figure 3.3. If the LT-algorithm receives $S = (s_1, \ldots, s_N)$ as input, then the algorithm can be stopped after $idx = i$, $2 \leq i \leq N$ and the current list *edges* exactly contains the edges of $\mathrm{HVG}(s_1, \ldots, s_i)$. The LT-algorithm thus not only generates $\mathrm{HVG}(S)$, but also implicitly $\mathrm{HVG}(s_1, \ldots, s_i)$ for every time series that starts at s_1 and ends at s_i, $2 \leq i \leq N$ and that without additional effort.

3.2.4 Multi-processing

In general, given a very long time series, it is desirable to be able to parallelize the proposed algorithm such that we can benefit from multi-processing to potentially speed up the runtime. For this purpose, we suggest dividing the time series into shorter sections to calculate the corresponding HVGs in parallel and combine these at the end to a single HVG. The BST [Yel+20] and DTHVG [Ste21] approaches make it possible to divide the time series at any point, where the merge operation for a constant number of HVGs is in $O(N \log N)$ or $O(N)$, respectively. We follow a different approach, which also admits a complexity in $O(N)$ and works with a constant-time merge on specifically chosen points of the time series. To ensure that the HVG created by merging the individual HVGs also contains all the desired edges, we need to split the time series at points corresponding to non-nested vertices. The approach is based on Lemma 1.1.3 (vi), which states that we can derive $\mathrm{HVG}(S)$ as 1-sums of the HVGs induced on non-nested-vertices $\mathcal{N} = \{i_1 < \ldots < i_k\}$. Note that, computationally, the 1-sum operation of two HVGs is performed in constant time since we only identify two vertices. Moreover, the set of non-nested vertices can be determined in linear time. This can, e.g., be done by first traversing the time series S of length N from left to right and creating a list *increasing*. This list is initialized by setting *increasing* $= (s_1)$. A data point s_i is added to *increasing* if for the last to *increasing* added element s_j holds $s_i \geq s_j$. After completely traversing S, the last element s_m in *increasing* is the global maximum of S. Then we reverse S, add s_N to *inceasing* and continue with this procedure up to s_m. Then *increasing* contains all non-nested vertices and the complexity is bounded by $2N$. So, in total, the parallel computation is also in $O(N)$ as in Stephen's approach.

However, in general, it is unclear how many non-nested vertices there are and in how many parts the time series can therefore be divided into. This question is hard to answer. But in the case of identically independent distributed (i.i.d.) data points, we give evidence that there is a sufficient number of non-nested vertices by computing its expectation.

Proposition 3.2.3. *Let $S = (s_1, \ldots, s_N)$ be a time series with s_i i.i.d. for $1 \leq i \leq N$, $2 \leq N$, $G = \mathrm{HVG}(S)$ and $\mathcal{N}(G)$ the set of non-nested vertices of G. Then*

$$\mathbb{E}[|\mathcal{N}(G)|] = 2 \cdot \sum_{i=1}^{N-1} \frac{1}{i} - \frac{N-2}{N}.$$

Proof. Given a time series $S = (s_1, \ldots, s_N)$, a vertex i of $G = \mathrm{HVG}(S)$ is non-nested if and only if $s_1, \ldots, s_{i-1} \leq s_i$ or $s_{i+1}, \ldots s_N \leq s_i$. Since the data points of S are i.i.d., direct computation yields

$$\begin{aligned}
\mathbb{E}[|\mathcal{N}(G)|] &= \mathbb{E}\left[\sum_{i=1}^{N} \mathbb{1}(i \text{ is non-nested})\right] \\
&= 2 + \mathbb{E}\left[\sum_{i=2}^{N-1} \mathbb{1}(i \text{ is non-nested})\right] = 2 + \sum_{i=2}^{N-1} \mathbb{P}(i \text{ is non-nested}) \\
&= 2 + \sum_{i=2}^{N-1} \Big(\mathbb{P}(s_1, \dots, s_{i-1} \le s_i) + \mathbb{P}(s_{i+1}, \dots, s_N \le s_i) \\
&\quad -\mathbb{P}(s_1, \dots, s_{i-1} \le s_i \ge s_{i+1}, \dots, s_N)\Big) \\
&= 2 + \sum_{i=2}^{N-1} \left(\frac{1}{i} + \frac{1}{N-i+1} - \frac{1}{N}\right) \\
&= 2 + \sum_{i=1}^{N-1} \frac{1}{i} - 1 + \sum_{i=1}^{N-1} \frac{1}{N-i} - 1 - \frac{N-2}{N} \\
&= 2 \cdot \sum_{i=1}^{N-1} \frac{1}{i} - \frac{N-2}{N}.
\end{aligned}$$

□

We can bound $\mathbb{E}[|\mathcal{N}(G)|]$ from below by

$$\mathbb{E}[|\mathcal{N}(G)|] = 2 \cdot \sum_{i=1}^{N-1} \frac{1}{i} - \frac{N-2}{N} \ge 2 \cdot \sum_{i=1}^{N-1} \frac{1}{i} - 1 \ge 2 \int_0^{N-1} \frac{1}{x+1} dx - 1 = 2 \cdot \ln(N) - 1.$$

Since the expectation is not guaranteed to be met, theoretically, this is not enough to conclude anything about the values of $|\mathcal{N}(G)|$. But numerical experiments have shown for large N, although $|\mathcal{N}(G)|$ can range from 2 to N, that it seems to be distributed closely around $2 \cdot \ln(N)$ in most cases (see Figure 3.4). Thus, for a time

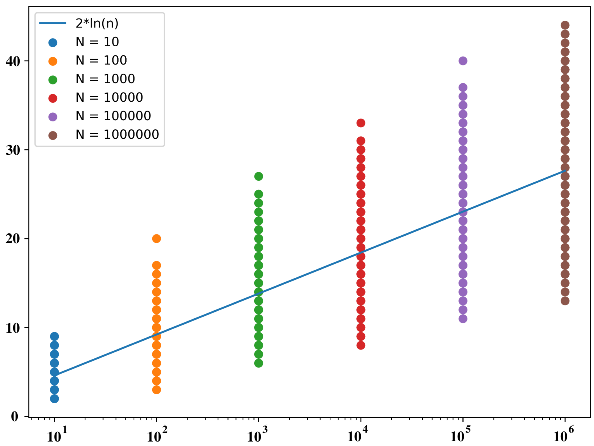

FIGURE 3.4: For each $N = 10, 10^1, \dots, 10^6$, we generated 100 time series of length N by uniformly and independently choosing N points out of $[0, 1]$. The number of the non-nested vertices of the corresponding HVGs is displayed on the y-axis.

series with i.i.d data, we conjecture that in the average case, the number of non-nested vertices is close to $\ln(N)$. This would confirm that we can divide a long time series into sufficient sections for parallelization.

But in fact, it is not always useful to divide at every non-nested vertex but to choose a fixed number r such that we divide the time series into r sections of roughly the same size. Note, the number r also depends on how the multi-processing is executed, i.e., e.g., how many kernels one can use for parallel computations. The prime example for not choosing all non-nested vertices is P_N which would result in $N-1$ many P_1 where nothing is gained. But, unfortunately, deciding which non-nested vertices to choose can increase the runtime. There are different approaches which can be executed fast but cannot guarantee that the r parts are almost of the same size. Thus, it should be investigated what the right choice is, in practice. We leave this as an open problem.

In Subsection 3.3.4, we compare the run times of the LT-algorithm with the parallelized version of the DTHVG algorithm. There, we try to divide the given i.i.d. time series S into $r \leq |\mathcal{N}(\mathrm{HVG}(S))| - 1$ parts of roughly similar size. We achieve this by iteratively removing from $\mathcal{N}(\mathrm{HVG}(S))$ the nodes i_j for $2 \leq j \leq N-1$ for which $i_{j+1} - i_j$ is minimal until only $r+1$ nodes are left. Then we split the time series into r parts, calculate the HVGs in parallel and join them to one HVG. It turns out, although in theory, the process of finding these non-nested vertices is in $O(|\mathcal{N}(\mathrm{HVG}(S))| \cdot (|\mathcal{N}(\mathrm{HVG}(S))| - r - 1))$, there seems to be no large disadvantage concerning the runtime. Moreover, experiments have shown that it is still more efficient than the parallelized version of the DTHVG algorithm (see Figure 3.9).

3.3 Numerical experiments

In this section, we show empirical results of our algorithm compared to the current state-of-the-art. The experiments were carried out on an OpenStack virtual machine with 8 VCPUs and 32 GB of RAM. The source code was implemented in Python 3.7 and can be freely accessed online [Sch22a].

3.3.1 Synthetic time series

In the same way as [Yel+20], we test our algorithm on synthetic time series and measure the time to calculate HVGs with increasing number of vertices. We consider three different types of synthetic time series, where we analyze how the time series' structure influences the HVG algorithms' runtime. The results can be seen in Figure 3.5. We define a time series $S = (s_1, \dots, s_N)$ with uniformly random noise of length N via $s_t = u$, $t \in [N]$, where u is a uniformly distributed random variable on the interval $[0,1]$ and is independently drawn for every t. For a normally distributed time series X of length N, we define analogously $x_t = y$, $t \in [N]$, where y is normally distributed with mean 0 and variance 1. The third type of time series W is based on a random walk. Unlike the other time series, the current value w_t depends on its previous values, i.e., $w_t = w_{t-1} + \epsilon$, $t \in [N]$, where the start value w_0 is 0 and ϵ is a Bernoulli distributed random variable with $P(\epsilon = 1) = P(\epsilon = 0) = \frac{1}{2}$.

Figure 3.5 shows the runtime of the Python implementation of the proposed method (the LT-algorithm called LT), Lacasa's approach, Stephen's dual tree HVG algorithm (DTHVG) and the binary search tree (BST) approach from Fano Yela in comparison. A naive implementation with a running time of $O(N^2)$ is not shown because it is too slow in comparison. Otherwise the difference between the proposed method and all other methods would no longer be recognizable in a single figure. The runtime for the HVGs was calculated up to a number of 10^5 vertices starting at 10^4 at intervals of $5 \cdot 10^3$. For each number, the computation time shows the minimum of 100 calculations since the minimum always contains the slightest temporal measurement error.

It is, first of all, apparent that the LT and DTHVG approaches can calculate the HVGs much faster, which confirms the theoretical runtime analysis of $O(N)$ compared to $O(N \log N)$ for BST. With the proposed method, it is possible to calculate HVGs with more than 10^7 vertices without much computing power. When looking at the time scales, it is noticeable that for all algorithms, the runtimes are very similar for uniform random noise and for the normally distributed time series. Note that with the random walk, the time scale deviates very strongly from the other two and the BST and Lacasa's algorithm take significantly longer to calculate the HVGs. The impact on the proposed method and the DTHVG algorithm is minimal. However, behavior like that of the random walks is rather comparable with an empirical time series pattern. This is a further argument in favor for the LT approach. Also note that a new stack frame in Python is allocated for a recursive call, which worsens the runtime of recursive functions like BST. On the other hand, the LT and BST approaches remain in different time complexity classes, which also explains the large discrepancy.

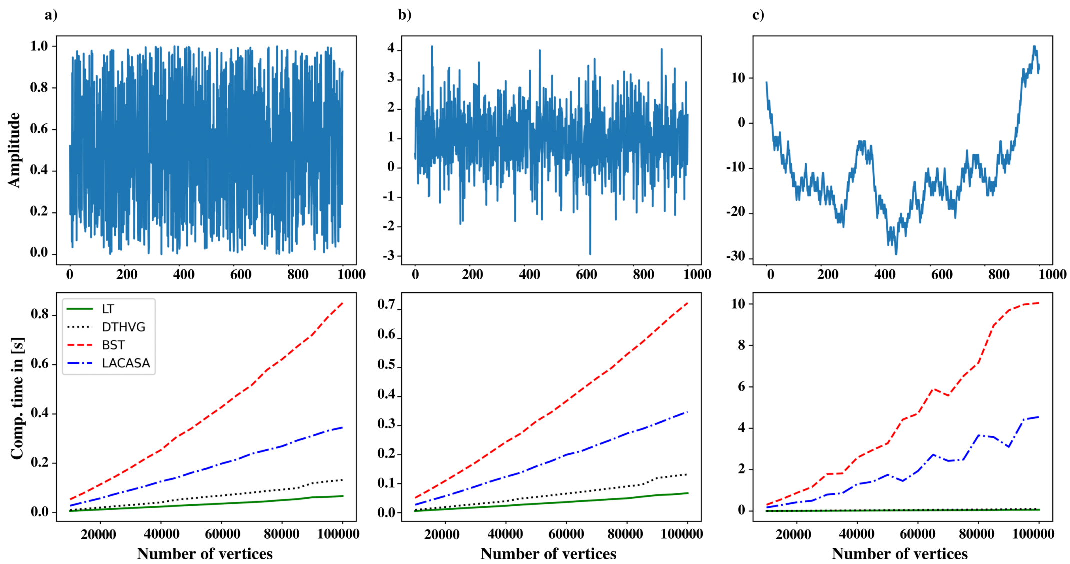

FIGURE 3.5: The first row shows examples of (a) random uniform noise, (b) random normal noise, and (c) a random walk. The second row illustrates the computation time for the HVGs for these types of synthetic time series with an increasing number of vertices. Each time value shown is the minimum of 100 runs with this number of vertices.

3.3.2 Audio and financial time series

To test the behavior of the HVG algorithms on empirical data, we calculate the computation time for an audio and a financial data set. The results are shown in Figure 3.6. The runtime is determined for each sample and the distribution for the different data sets is shown as a box plot. For each time series, the minimum runtime of 20 runs is chosen for calculating the boxplot because the minimal runtime for one sample is the one with the smallest error rate. The yellow line in the box plot is the median of the runtimes. The lower and upper edges of the box represent the 1st and 3rd quartiles, respectively. The upper and lower whiskers are the 5% and 95% quantiles, respectively. All 160 samples of speech files from the TIMIT acoustic-phonetic continuous speech corpus were used, in which several English speakers pronounce phonetically different sentences [Gar+93]. The data was recorded at 16 kHz and the first 20.000 data points were used to build the HVGs. This corresponds to 1.25 seconds per audio file. The financial data set are intraday share prices of 46 shares of the S&P 500 in the period from May to August 2021. The time interval between two share prices is 5 minutes to also receive 20.000 points for this time series.

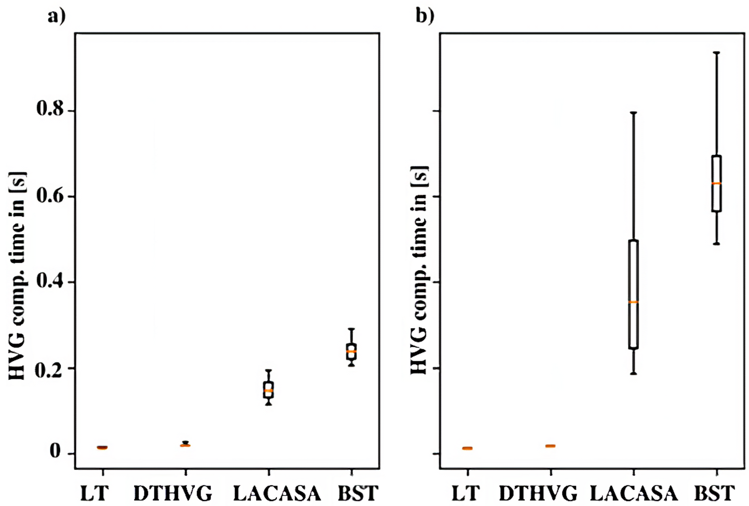

FIGURE 3.6: Representation of the HVG computation time as a box plot of the TIMIT audio data set in (a) and the intraday prices of S&P 500 stocks in (b) for the different algorithms.

An analysis of the box plots shows that the BST algorithm has significant runtime differences for the audio and financial data. In the median, it takes twice and a half as long on the financial data set (see Table 3.1).

Algorithm	Audio Data Set $Q_{5\%}$	$Q_{50\%}$	$Q_{95\%}$	Financial Data Set $Q_{5\%}$	$Q_{50\%}$	$Q_{95\%}$
BST	0.205	0.238	0.290	0.472	0.631	0.972
Lacasa	0.114	0.147	0.194	0.183	0.353	0.825
DTHVG	0.0178	0.0181	0.0271	0.0162	0.0170	0.0176
LT	0.0114	0.0118	0.0143	0.0113	0.0114	0.0117

TABLE 3.1: HVG computation times in seconds for the TIMIT audio data set and intraday prices of S&P 500 stocks for the different algorithms.

It is also noticeable that the running time is more scattered here because the whiskers are more distant. In this case, the binary search tree seems more unbalanced, increasing the computation time. For Lacasa's approach it can also be observed that the median runtime on the financial data set is more than twice as large as on the audio data set. There are also stronger outliers in terms of runtime. Both approaches are heavily dependent on the structure of the time series.

The LT approach has similar runtimes for the audio and financial data sets. Here, the different structure of the audio and financial data records seems not to influence the runtime. The LT-algorithm runs about 50% faster on the audio and financial data set than the DTHVG algorithm. Recalling that the given 20.000 data points were generated by only 1.25 seconds of audio data, the runtime improvement makes a significant difference when analyzing longer audio data with a high sampling rate. In contrast to the BST approach and Lacasa's, both are slightly faster on the financial data set. However, their running time is almost unaffected by the type of time series. The DTHVG algorithm stores additional information during the construction of the HVG, which is only needed if the HVG is subsequently merged with another HVG, e.g., in the case of multi-processing. This worsens its runtime compared to the LT algorithm, which only stores the necessary information about the time series in the *decreasing* list to calculate the HVG correctly.

From the determination of the complexity class of the LT-algorithm, we know that we can specify an upper bound for the number of executions of iterations of the for-loop using $2N - 1 - |D_N|$, where N is the number of data points in the time series and $|D_N|$ describes the number of elements at the end of the loop iteration from the list *decreasing*. Our runtime experiments confirm the theoretical justification that the runtimes for the LT approach cannot vary widely since there is an upper limit for the LT approach that is only twice that of the best case. Especially the application to empirical data shows the strength of the proposed method, that it runs in the best, average, and worst-case in $O(N)$. Of course, the measured computation time may differ more than a factor of two, because the runtime measurements are always noisy and delays occur due to other tasks being carried out by the system.

3.3.3 Acceleration time series

New efficient HVG algorithms open up fields of applications for HVGs that previously would only have been feasible with a great amount of computing capacity. This includes the analysis of structure-borne sound data. Besides classical airborne sound data, very high sampling rates in the kilohertz range are often used for structure-borne sound analysis. We analyze a data set provided by ZF Friedrichshafen AG, in which test drives with low and normal tire pressure were carried out. During the drive, tri-axial acceleration sensors were attached to the upper right control arm recording the accelerations with 50 kHz in a range of $\pm 50g$. We use a version of the data set downsampled to 8 kHz, analog to [Sch22b]. The drives with low and normal tire pressure lasted approximately 1000 seconds and were carried out on the same route with various road conditions. For further analysis, we only use the acceleration in the Z-direction. Examining the time signal shows no significant differences in the observed amplitudes (see Figure 3.7). Therefore, we test whether there are differences between the data sets when we convert them into HVGs. First, we divide both data sets into windows of length 2000. Then we calculate for each window its HVG. We compare the runtime of the LT-algorithm and the DTHVG for the transformation into HVGs for one test drive. The proposed algorithm takes 5.8 seconds and the DTHVG 8.8 seconds. From the HVGs, we extract several statistical properties. These include the average node degree, the standard deviation of the node degree, the diameter of the HVG, and other graph-specific properties that describe the local and global topology of the graph. A detailed description of the 15 properties and their definitions are given in [Sch22b]. In order to visualize these features, they are projected into a two-dimensional space using the UMAP algorithm [HMM18]. UMAP is an unsupervised dimensionality reduction technique. Figure 3.8 shows the result.

It can be seen that the data sets of normal and low tire pressure form clusters. Both data sets are nearly separable. There is only a small area where the projections of the features of both classes overlap. How an XGBoost classifier can be trained

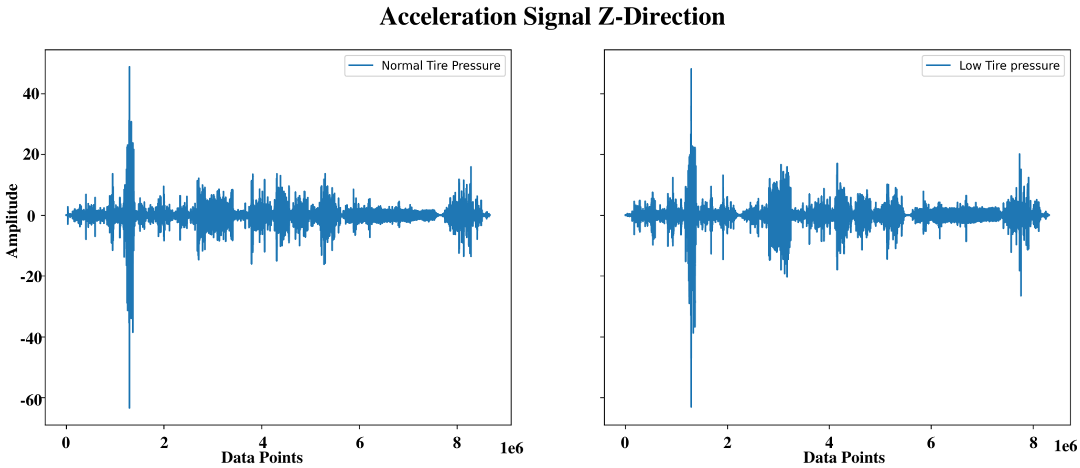

FIGURE 3.7: In the time domain, the amplitudes of the acceleration signal of normal and low tire pressure are very similar.

to classify the HVG features into normal or low tire pressure is shown in [Sch22b]. Analyzing the acceleration data using HVGs as preprocessing shows that they are a powerful tool for classifying time series and that efficient algorithms are beneficial for sound data measured at high sampling rates.

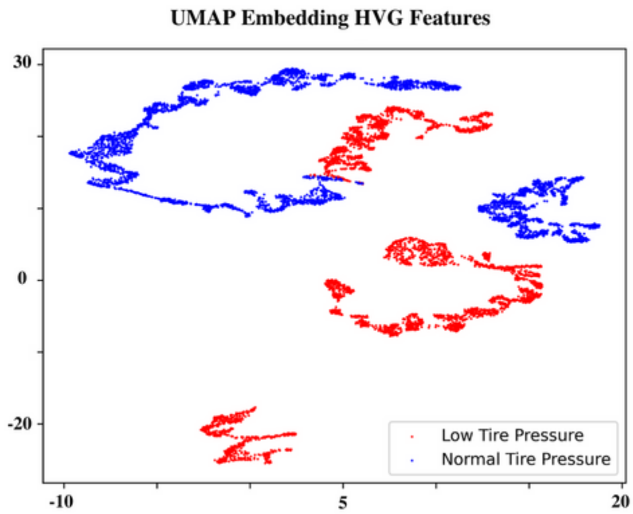

FIGURE 3.8: The projection of the HVG features shows a clustering that allows a distinction between the two classes.

3.3.4 Multi-processing

The DTHVG algorithm is faster than the BST in computing HVGs whose time series has been previously split to compute the smaller HVGs in parallel and then merge them into one HVG [Ste21]. This is because the DTHVG, in particular, allows merging in $O(N)$ compared to $O(N \log N)$ from the BST approach. Therefore, we only compare the proposed method with the DTHVG algorithm for multi-processing applications. Figure 3.9 shows the computation times for the HVGs with 2^{10} to 2^{26} vertices of the different algorithms in a parallelizable version for random uniform noise. For this purpose, each time series was split into eight shorter time series. For the curves with the LT and DTHVG NN labels, the non-nested vertices were calculated and the eight partial time series were determined according to the described strategy in Subsection 3.2.4. Afterwards, the HVG is calculated for each shorter time series and the HVGs are merged at the end. To exclude an additional source of error in the runtime determination, the calculation was performed sequentially since the parallelization process may also lead to runtime differences. However, since the DTHVG allows splitting the time series at arbitrary points, we also compare this variant. In this case, corresponding to the curve labeled DTHVG, the time series is divided into eight partial time series of equal size. The runtime for a given number of vertices is the minimum of 100 executions. With the scalable variant of the LT-algorithm, we achieve a runtime of about 69 seconds for 2^{26} vertices compared to 128 for the DTHVG NN and 148 for the DTHVG approach. The DTHVG algorithm does allow the time series to be split at arbitrary points, but more complicated merge operations must then be performed. The proposed method always splits the time series so that individual HVGs are created, which only have to be concatenated. The comparison shows that the computation of the non-nested vertices in advance is computationally more favorable than separating the time series at arbitrary points and to carry out more expensive merge operations for it.

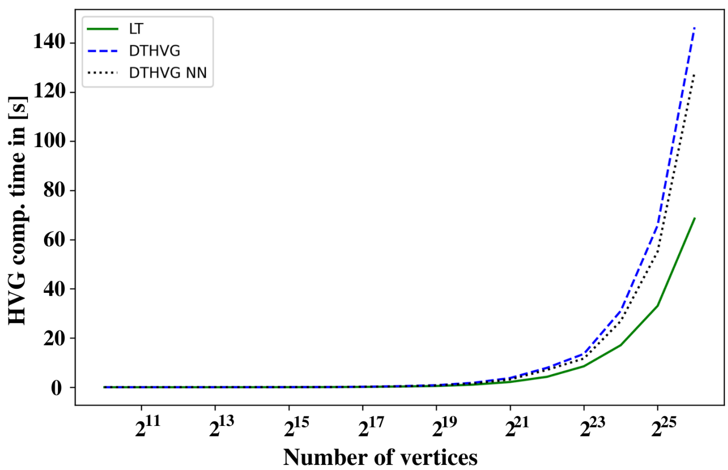

FIGURE 3.9: Parallizable versions of the DTHVG and LT-algorithm in comparison. For DTHVG the time series were splitted equally in 8 parts. DTHVG NN and LT werde splitted into 8 parts at non-nested vertices.

Chapter 4

On the gamma vector of symmetric edge polytopes

Symmetric edge polytopes are a family of lattice polytopes associated to simple graphs. They were first introduced in [Hib+10] and are defined as follows.

Definition 4.0.1. *Given a simple graph $G = ([n], E)$, the associated* symmetric edge polytope $\mathcal{P}_G$ *is defined as*

$$\mathcal{P}_G = \operatorname{conv}(\pm(e_i - e_j) \ : \ ij \in E) \subseteq \mathbb{R}^{|V|}.$$

On the one hand, the dependence on a graph allows for graph-theoretical characterizations of some polytopal properties: for instance, for a connected graph, $\dim \mathcal{P}_G$ only depends on the number of vertices and equals $n-1$ [Hib+10, Proposition 3.1]. Moreover, Higashitani proved in [Hig15, Corollary 2.3] that a symmetric edge polytope $\mathcal{P}_G$ arising from a connected graph G is simplicial if and only if G contains no even cycles. This is equivalent to $\mathcal{P}_G$ being smooth. While this result gives the existence of infinitely many simplicial symmetric edge polytopes, only a finite list of graphs yield symmetric edge polytopes that are simple (see Proposition 4.1.5). On the other hand, there are several pleasant properties that are shared by any symmetric edge polytope, independent of the underlying graph: all of these polytopes are known to admit a regular unimodular triangulation [HO14; HJM19] and to be centrally symmetric, terminal and reflexive [Hig15]. In particular, by this latter property, it follows from work of Hibi [Hib92] that their h^*-vectors are palindromic. Thus, given the h^*-vector $h^*(\mathcal{P}_G) = (h^*_0, \dots, h^*_d)$ of a symmetric edge polytope, we can apply (1.2) to get the γ-vector $\gamma(\mathcal{P}_G) = (\gamma_0, \dots, \gamma_{\lfloor \frac{d}{2} \rfloor})$ of $\mathcal{P}_G$. Since $\mathcal{P}_G$ is reflexive and admits a regular unimodular triangulation Δ, the restriction of Δ yields a unimodular triangulation of $\partial\mathcal{P}_G$ and the h^*-vector of $\mathcal{P}_G$ equals the h-vector of the restriction, which, in particular, is a simplicial sphere. This provides a link between the study of the γ-vector of $\mathcal{P}_G$ and the rich world of conjectures on the γ-non-negativity of simplicial spheres; however, note that the objects we are interested in will *not* be flag in general. Despite the lack of flagness, in all currently known cases, the γ-vector of $\mathcal{P}_G$ is non-negative. This lead Ohsugi and Tsuchiya to formulate the following conjecture, which is the starting point of this chapter:

Non-negativity conjecture for γ-vectors of symmetric edge polytopes. *[OT21b, Conjecture 5.11] Let G be a graph. Then $\gamma_i(\mathcal{P}_G) \geq 0$ for every $i \geq 0$.*

Moreover, it is already known and follows, e.g., from [BR07], that a weaker property, namely, unimodality of the h^*-vector holds. On the other hand, though it is tempting to hope that even the stronger property of the h^*-polynomial being real-rooted is true, this is not the case in general; the 5-cycle is a counterexample.

The main goal of this chapter is to provide some supporting evidence to the γ-non-negativity conjecture, independent of the graph.

4.1 Basic properties of symmetric edge polytopes

Though, a priori, all graphs in this chapter and especially in Definition 4.0.1 are undirected, we often consider different orientations of the edges. We then write $v \to w$ and $w \to v$ for the directed edges going from v to w and w to v, respectively. For $ij \in E$, we will call the vertices $e_i - e_j$ and $e_j - e_i$ of $\mathcal{P}_G$ an *antipodal pair*. In the following, we will always identify a vertex $e_i - e_j$ of $\mathcal{P}_G$ with the directed edge $i \to j$ and use the short-hand notation $e_{i,j} := e_i - e_j$. Though G is undirected, we can naturally direct each cycle of G by directing its edges either clockwise or counter-clockwise. By abuse of notation, we refer to those cycles as the *oriented* cycles of G.

Turning to triangulations of symmetric edge polytopes, we recall that it was shown in [HO14] that $\mathcal{P}_G$ admits a regular unimodular triangulation. It is well known (see, e.g., [Stu96, Corollary 8.9]) that such a triangulation can be obtained from the Gröbner basis of the toric ideal of $\mathcal{P}_G$ (with respect to the degrevlex order), provided in [HJM19, Proposition 3.8], as follows:

Lemma 4.1.1. *Let $<$ be a total order on the edges E of G. Then there exists a regular unimodular triangulation $\Delta_<$ of $\partial\mathcal{P}_G$ such that F is a non-face of $\Delta_<$ if and only if it contains at least one subset of the following form:*

(i) an antipodal pair;

(ii) an ℓ-element subset of a directed $(2\ell-1)$-cycle of G;

(iii) an ℓ-element subset of a directed 2ℓ-cycle of G not containing its $<$-minimal edge.

Example 4.1.2. *Given the graph $C_4 = ([4], \{12, 23, 34, 14\})$, the symmetric edge polytope is a cube (see Figure 4.1 (left)). Moreover, fixing the order $12 < 23 < 34 < 14$ on the edges, via Lemma 4.1.1, the minimal non-faces of $\Delta_<$ are the convex hulls of all antipodal pairs and of the pairs $e_{1,4}e_{3,2}$, $e_{1,4}e_{4,3}$, $e_{4,1}e_{3,4}$, $e_{4,1}e_{2,3}$, $e_{3,2}e_{4,3}$ and $e_{2,3}e_{3,4}$. Thus, a triangulation of the boundary is given as visualized in Figure 4.1 on the right-hand side.*

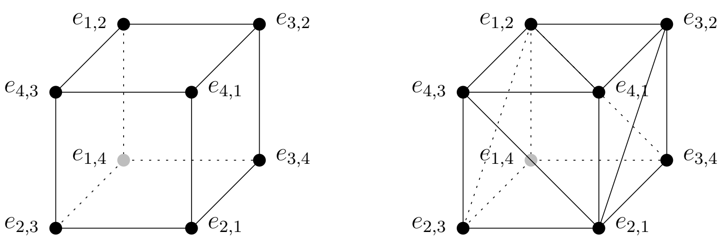

FIGURE 4.1: $\mathcal{P}_{C_4}$ (left) and a triangulation of its boundary (right) constructed via Lemma 4.1.1.

We remark that the triangulation $\Delta_<$ extends to a regular unimodular triangulation of $\mathcal{P}_G$ by coning over the origin. In (iii), a directed edge $i \to j$ of a directed cycle C is called *$<$-minimal* if ij is minimal with respect to $<$ among $\{k\ell \ : \ k \to \ell \in E(C)\}$. It is apparent that the triangulation of Lemma 4.1.1 depends on the chosen ordering $<$. However, any edge of $\mathcal{P}_G$ is necessarily a face of any such triangulation.

Complementing [HJM19, Theorem 3.1], which characterizes facets of symmetric edge polytopes, we provide the following characterization of their edges:

Theorem 4.1.3. *Let $G = ([n], E)$ be a graph. Two directed edges of G form an edge of $\mathcal{P}_G$ if and only if they are not antipodal and not contained in a directed 3- or 4-cycle of G.*

Proof. The "only if"-part directly follows from Lemma 4.1.1 and the paragraph preceding this theorem. For the reverse statement, note that the origin can be written as a convex combination of any antipodal pair and thus an antipodal pair can't form an edge. Let $i \to j, k \to \ell$ be directed non-antipodal edges of G lying neither in a directed 3- nor in a directed 4-cycle of G. The aim is to construct a supporting hyperplane of $\mathcal{P}_G$ only containing the vertices $e_{i,j}$ and $e_{k,\ell}$. More precisely, we construct $a \in \mathbb{R}^n$ such that $a^T e_{i,j} = a^T e_{k,\ell} > a^T y$ for every vertex y of $\mathcal{P}_G$ different from $e_{i,j}$ and $e_{k,\ell}$. We distinguish different cases.

Case 1: $\{i,j\} \cap \{k,\ell\} = \emptyset$. Since $i \to j$ and $k \to \ell$ do not lie in a directed 4-cycle, we have $|\{i\ell, jk\} \cap E| \leq 1$. If $|\{i\ell, jk\} \cap E| = 0$ then it is easy to verify that setting $a_i = a_k = 1$, $a_j = a_\ell = -1$ and $a_m = 0$, otherwise, works. If $|\{i\ell, jk\} \cap E| = 1$, then without loss of generality assume $i\ell \in E$. In this case setting $a_i = 1$, $a_j = -2$, $a_k = 2$, $a_\ell = -1$ and $a_m = 0$, otherwise, has the required properties.

Case 2: $\{i,j\} \cap \{k,\ell\} \neq \emptyset$. First assume $i = k$. In this case, we set $a_i = 1$, $a_j = a_\ell = -1$ and $a_m = 0$, otherwise. Similarly, if $j = \ell$, setting $a_j = -1$, $a_i = a_k = 1$ and $a_m = 0$, otherwise, works. Finally assume that $i = \ell$ or $j = k$. By symmetry, we only need to consider the case $i = \ell$. Since $i \to j$ and $k \to i$ do not lie in a directed 3-cycle, it follows that $jk \notin E$. Similarly, as $i \to j$ and $k \to i$ do not lie in a directed 4-cycle, the vertices j and k do not have common neighbors other than i. We can then set $a_j = -2$, $a_k = 2$, $a_i = 0$, $a_p = -1$ if $jp \in E$, $a_q = 1$ if $kq \in E$ and $a_m = 0$, otherwise and this is well-defined by the previous arguments. It is again easy to see that this choice of a works. □

Proposition 4.1.4. *Let $G = G_1 \oplus_1 \cdots \oplus_1 G_k$ be a graph which is given as 1-sums of the graphs $G_1, \dots, G_k$. Then*

$$\mathcal{P}_G \cong \mathcal{P}_{G_1} \oplus \cdots \oplus \mathcal{P}_{G_k}.$$

Proof. Let $G = ([n], E) = G_1 \oplus_1 \cdots \oplus_1 G_k$. We prove the claim via induction on k. If $k = 2$, we have $G = G_1 \oplus_1 G_2$. Let $m \in \mathbb{N}$, $G_1 = ([m], E_1)$ and $G_2 = ([m+1, n+1], E_2)$ such that the 1-sum is taken along m and $m+1$. We set Q_1 and Q_2 as the projection of $\mathcal{P}_{G_1}$ and $\mathcal{P}_{G_2}$ onto the $m-1$ and $n-m$ last coordinates, respectively. Since every symmetric edge polytope lies in the hyperplane where all coordinates sum up to 0, $\mathcal{P}_{G_1} \cong Q_1$ and $\mathcal{P}_{G_2} \cong Q_2$. Moreover, let φ be the linear map given by the matrix

$$(U)_{ij} = \begin{cases} 1, & \text{if } i = j, \text{ or} \\ & \text{if } i = 1, \text{ or} \\ & \text{if } i = m \text{ and } j > m, \\ 0, & \text{otherwise} \end{cases} \in \mathbb{Z}^{n \times n}.$$

Since U is unimodular, $\mathcal{P}_G \cong \varphi(\mathcal{P}_G)$. From an easy computation follows $\varphi(\mathcal{P}_G) = \{0\} \times \{Q_1 \oplus Q_2\}$. Thus, $\mathcal{P}_G \cong \mathcal{P}_{G_1} \oplus \mathcal{P}_{G_2}$.

Now, let $k \geq 3$, and we assume that the claim holds for a particular $k-1$. Let $G = G_1 \oplus_1 \cdots \oplus_1 G_k$ and $H = G_1 \oplus_1 \cdots \oplus_1 G_{k-1}$. Then $G = H \oplus_1 G_k$, and by applying the induction hypothesis twice, the claim follows. □

Theorem 4.1.3 allows us to characterize simple symmetric edge polytopes in terms of their graphs.

Proposition 4.1.5. *Let $G = ([n], E)$ be a graph with $E \neq \varnothing$. Then $\mathcal{P}_G$ is simple if and only if, after removing isolated vertices, $G \in \{P_2, 2P_2, P_3, C_3, C_4\}$.*

Proof. It follows by direct computation that $\mathcal{P}_G$ is a 1-simplex, a 4-gon, a 4-gon, a 6-gon, or a 3-cube if G is equal to P_2, $2P_2$, P_3, C_3 or C_4, respectively.
Assume that G is connected and fix a directed edge $i \to j$. Observe that if there exists an edge $k\ell$ such that both $k \to \ell$ and $\ell \to k$ lie in a directed 3- or 4-cycle together with $i \to j$, then the subgraph of G induced by the vertices i, j, k, ℓ (which must be all distinct) is isomorphic to K_4. Then consider the connected subgraph H of G obtained by removing all edges st such that the induced subgraph of G on the vertex set $\{i, j, s, t\}$ is isomorphic to K_4. By construction, for every edge $k\ell$ of H different from ij, at least one of the directed edges $k \to \ell$ and $\ell \to k$ does not lie in a 3- or 4-cycle with $i \to j$. By Theorem 4.1.3, this implies that at least one of the vertices $e_{k,\ell}$ or $e_{\ell,k}$ is adjacent to $e_{i,j}$ both in $\mathcal{P}_H$ and in $\mathcal{P}_G$. As all edges of $\mathcal{P}_H$ containing the vertex $e_{i,j}$ are also edges of $\mathcal{P}_G$ (and vice versa), we conclude that the number of edges containing $e_{i,j}$ in $\mathcal{P}_G$ is greater than or equal to $|E(H)| - 1$. Hence, $\mathcal{P}_G$ cannot be simple if $|E(H)| > \dim(\mathcal{P}_G) + 1 = n$. In order for $\mathcal{P}_G$ to be simple, we must hence have $|E(H)| \in \{n-1, n\}$. If $|E(H)| = n-1$, then H is a tree, while if $|E(H)| = n$, then H can be built starting from a cycle and taking successive 1-clique sums with single edges. Both cases can only happen if $G = H$, since otherwise H would contain at least two distinct 3-cycles. Using Proposition 4.1.4, it follows that if G is connected and $\mathcal{P}_G$ is simple, then $\mathcal{P}_G$ is unimodular equivalent to the free sum of the symmetric edge polytope of a cycle and some segments (since the symmetric edge polytope of P_1 is a segment). Since the free sum of two polytopes of dimension greater than zero is simple if and only if the polytopes are segments, we are left with the following possibilities: either $G \in \{P_2, P_3\}$ or $G \cong C_k$, for some $k \geq 3$. For analogous reasons, if G is not connected and $\mathcal{P}_G$ is simple, $\mathcal{P}_G$ must be the free sum of two segments, i.e., $G \cong 2P_2$, the disjoint union of two edges. Finally, assume that $G \cong C_k$, for some $k \geq 5$. Applying again Theorem 4.1.3, we conclude that the number of edges of $\mathcal{P}_G$ containing $e_{i,j}$ equals $2(k-1) > k-1 = \dim(\mathcal{P}_G)$ and hence $\mathcal{P}_G$ is not simple. □

4.2 Non-negativity of γ_2

The aim of this section is to prove that $\gamma_2(\mathcal{P}_G)$ is non-negative for any graph G, and to characterize which graphs attain the equality $\gamma_2(\mathcal{P}_G) = 0$. In [HO14, Corollary 3.1], the authors prove that, when G is connected, $\mathcal{P}_G$ has a unimodular triangulation, and this was made more explicit in [HJM19] by providing a Gröbner basis. This triangulation depends on an order $<$ on the set of edges E, and, in particular, different orders might yield non-isomorphic simplicial complexes. However, all of them are cones over the corresponding triangulation $\Delta_<$ of the boundary of $\mathcal{P}_G$ (see Lemma 4.1.1). As the h^*-vector of a lattice polytope which admits a unimodular triangulation is equal to the h-vector of such a triangulation, we can write $\gamma_2(\mathcal{P}_G)$ in terms of the number of vertices and edges of $\Delta_<$, and these numbers do not depend on the order $<$. Our first goal is to write the number $\gamma_2(\mathcal{P}_G)$ as a function of certain invariants of the graph. For this aim, given a graph $G = ([n], E)$ and a fixed total order $<$ on E, let

$$n_1(G) := \binom{2|E|}{2} - |E| - f_1(\Delta_<).$$

Let $\blacklozenge_{|E|}$ be the $|E|$-dimensional cross-polytope with vertex labeled by the vertices of $\mathcal{P}_G$ such that antipodal vertices in $\blacklozenge_{|E|}$ correspond to antipodal pairs of $\mathcal{P}_G$. Then in other words, $n_1(G)$ equals the number of edges of $\blacklozenge_{|E|}$ that are non-edges of $\Delta_<$. By Lemma 4.1.1, $n_1(G)$ is equal to the number of pairs of directed edges of G where the two undirected edges are different and the pair satisfies at least one of the following:

(i) the pair is contained in a directed 3-cycle;

(ii) the pair is contained in a directed 4-cycle, and none of its edges is the $<$-minimal edge of such a cycle.

We call a pair of directed edges satisfying at least one of these two conditions a *bad pair* and say that it is *supported* on the corresponding pair of undirected edges. We use $n_1(G)$ to express $\gamma_2(\mathcal{P}_G)$ explicitly, as follows.

Lemma 4.2.1. *Let G be a connected graph. Then*

$$\gamma_1(\mathcal{P}_G) = 2\,\mathrm{cy}(G),$$

and

$$\gamma_2(\mathcal{P}_G) = 2\,\mathrm{cy}(G)(\mathrm{cy}(G)+2) - n_1(G). \tag{4.1}$$

Proof. Let $G = ([n], E)$. The next computation shows the first statement:

$$\begin{aligned}\gamma_1(\mathcal{P}_G) &= h_1^*(\mathcal{P}_G) - (n-1) = h_1(\Delta_<) - (n-1)\\ &= f_0(\Delta_<) - 2(n-1) = 2(|E| - n + 1) = 2\,\mathrm{cy}(G),\end{aligned}$$

where the first equality follows from Equation (1.2), the fact that $\mathcal{P}_G$ is $(n-1)$-dimensional and by comparing coefficients. The second equality holds since $\mathcal{P}_G$ admits a unimodular triangulation and the third follows from (1.1). Using the first statement and analogue arguments, we can further show (4.1):

$$\begin{aligned}\gamma_2(\mathcal{P}_G) &= h_2^*(\mathcal{P}_G) - \binom{n-1}{2} - (n-3)\gamma_1(\mathcal{P}_G)\\ &= h_2(\Delta_<) - \binom{n-1}{2} - 2(n-3)\,\mathrm{cy}(G)\\ &= f_1(\Delta_<) - (n-2)f_0(\Delta_<) + \binom{n-1}{2} - \binom{n-1}{2} - 2(n-3)\,\mathrm{cy}(G)\\ &= \binom{2|E|}{2} - |E| - n_1(G) - 2(n-2)|E| - 2(n-3)\,\mathrm{cy}(G)\\ &= 2|E|(|E| - n + 1) - n_1(G) - 2(n-3)\,\mathrm{cy}(G)\\ &= 2\,\mathrm{cy}(G)(|E| - n + 3) - n_1(G) = 2\,\mathrm{cy}(G)(\mathrm{cy}(G)+2) - n_1(G).\end{aligned}$$

□

Next, we present the main result of this section.

Theorem 4.2.2. *Let G be a graph. Then $\gamma_2(\mathcal{P}_G) \geq 0$.*

The proof of this theorem will require several lemmas and propositions. The strategy is to prove that there exists an edge $e \in E$ such that $\gamma_2(\mathcal{P}_G) \geq \gamma_2(\mathcal{P}_{G\setminus e})$, from which the claim follows inductively. We note that, if e is not a bridge of G, then $\mathrm{cy}(G\setminus e) = \mathrm{cy}(G) - 1$, and Lemma 4.2.1 directly yields

$$\gamma_2(\mathcal{P}_G) - \gamma_2(\mathcal{P}_{G\setminus e}) = 4\,\mathrm{cy}(G) + 2 - (n_1(G) - n_1(G\setminus e)). \tag{4.2}$$

By the following lemma, we can reduce to the case when G is 2-connected.

Lemma 4.2.3. *Let G be a graph, and let $G_1, \dots, G_k$ be its 2-connected components. Then $\gamma_1(\mathcal{P}_G) = \sum_{i=1}^k \gamma_1(\mathcal{P}_{G_i})$, and*

$$\gamma_2(\mathcal{P}_G) = \sum_{i=1}^k \gamma_2(\mathcal{P}_{G_i}) + 4 \sum_{1 \le i < j \le k} \operatorname{cy}(G_i) \operatorname{cy}(G_j) \ge \sum_{i=1}^k \gamma_2(\mathcal{P}_{G_i}).$$

Proof. By [OT21b, Proposition 5.2], the h^*-polynomial of $\mathcal{P}_G$ is the product of the h^*-polynomials of the polytopes $\mathcal{P}_{G_i}$. Then due to Lemma 1.2.1, the same holds for their γ-polynomials, and hence we obtain that

$$\gamma_1(\mathcal{P}_G) = \sum_{i=1}^k \Big(\prod_{j \ne i} \gamma_0(\mathcal{P}_{G_j})\Big) \gamma_1(\mathcal{P}_{G_i})$$

and

$$\gamma_2(\mathcal{P}_G) = \sum_{i=1}^k \Big(\prod_{j \ne i} \gamma_0(\mathcal{P}_{G_j})\Big) \gamma_2(\mathcal{P}_{G_i}) + \sum_{1 \le i < j \le k} \Big(\prod_{\ell \ne i,j} \gamma_0(\mathcal{P}_{G_\ell})\Big) \gamma_1(\mathcal{P}_{G_i}) \gamma_1(\mathcal{P}_{G_j}).$$

We conclude using $\gamma_0(\mathcal{P}_{G_i}) = 1$, from Lemma 4.2.1 that $\gamma_1(\mathcal{P}_{G_i}) = 2 \operatorname{cy}(G_i)$ hold for every i and the fact that the cyclomatic number is non-negative. □

Combining Lemma 4.2.1 and Lemma 4.2.3 with the non-negativity of the cyclomatic number, we get the following corollary.

Corollary 4.2.4. *Let G be a graph. Then $\gamma_1(\mathcal{P}_G) \ge 0$.*

In particular, proving non-negativity of $\gamma_2(\mathcal{P}_G)$ for every 2-connected graph G is sufficient to prove the statement for every graph. Our study is divided into cases, which we deal with in Propositions 4.2.5, 4.2.6 and 4.2.9. We start with the simplest case.

Proposition 4.2.5. *Let $G = ([n], E)$ be a 2-connected graph. Assume that there exists $e \in E$ which is not contained in any 3- or 4-cycle. Then*

$$\gamma_2(\mathcal{P}_G) = \gamma_2(\mathcal{P}_{G \smallsetminus e}) + 4 \operatorname{cy}(G) + 2 > \gamma_2(\mathcal{P}_{G \smallsetminus e}).$$

Proof. Since $e \in E$ is not contained in any 3- or 4-cycle of G, its deletion from G does not change the set of 3- and 4-cycles of G and, therefore, $n_1(G) = n_1(G \smallsetminus e)$. The claim now follows from (4.2). □

Next, we assume the existence of a vertex of degree 2. The reason why this case is taken care of separately is that it forces restrictions on which edges can be removed (see Remark 4.2.10).

Proposition 4.2.6. *Let $G = ([n], E)$ be a 2-connected graph. Assume that there exists $e = ij \in E$ such that $\delta_G(i) = 2$. Then*

$$\gamma_2(\mathcal{P}_G) \ge \gamma_2(\mathcal{P}_{G \smallsetminus e}).$$

Moreover, equality holds if and only if every edge of G lies in a 3- or 4-cycle together with e.

Proof. If e does not lie in any 3- or 4-cycle of G, the statement follows from Proposition 4.2.5.

Assume that e is contained in at least one 3- or 4-cycle. Let $f = ik$ be the unique edge adjacent to i other than e. As $\delta_G(i) = 2$, each 3- or 4-cycle containing e needs to contain f as well. Hence, if e is contained in some 3-cycle, then the one on the vertices i, j and k is the unique one. Let $s \in \{0,1\}$ and $r \in \mathbb{N}$ be the number of 3- and 4-cycles containing e (and hence f), respectively. Let $<$ be any order on E for which $e > f > h$ for every $h \in E \setminus \{e,f\}$. By the way $<$ is defined, the minimal element of each 4-cycle containing e and f is distinct from these.
We now list the bad pairs of G which are not bad pairs of $G \setminus e$. Their number is equal to $n_1(G) - n_1(G \setminus e)$, since every bad pair of $G \setminus e$ is a bad pair of G.

- As e is contained in some 3- or 4-cycle, and $e > f > h$ for every $h \in E \setminus \{e,f\}$, the pairs $\{j \to i, i \to k\}$ and $\{k \to i, i \to j\}$ are bad pairs.
- If $s = 1$, there are 4 additional bad pairs, which are contained in a directed 3-cycle of G, but which are not bad pairs for $G \setminus e$. Namely, the four pairs of directed edges $\{i \to j, j \to k\}$, $\{k \to j, j \to i\}$, $\{i \to k, k \to j\}$ and $\{j \to k, k \to i\}$. Note that the latter two are not bad pairs of $G \setminus e$ since they neither lie in a 3-cycle nor in a 4-cycle of $G \setminus e$ as $\delta_G(i) = 2$.
- For each 4-cycle containing e, there are 4 additional pairs. To see this, let $\{ij, j\ell, \ell k, ki\}$ be the edge set of such a 4-cycle. If the minimal element is $j\ell$, then we get $\{i \to j, \ell \to k\}$, $\{j \to i, k \to \ell\}$, $\{\ell \to k, k \to i\}$ and $\{k \to \ell, i \to k\}$. If instead the minimal element is ℓk, then we get $\{i \to j, j \to \ell\}$, $\{j \to i, \ell \to j\}$, $\{j \to \ell, k \to i\}$ and $\{\ell \to j, i \to k\}$. It follows from $\delta_G(i) = 2$, that all of these pairs are not bad pairs of $G \setminus e$.

We deduce that $n_1(G) - n_1(G \setminus e) = 4r + 4s + 2$ and hence (4.2) implies

$$\gamma_2(\mathcal{P}_G) - \gamma_2(\mathcal{P}_{G\setminus e}) = 4(\mathrm{cy}(G) - s - r). \tag{4.3}$$

To conclude, let H be the subgraph of G consisting of all edges of G which are contained in a 3- or 4-cycle together with e. By definition H is 2-connected and $s + r = \mathrm{cy}(H)$. Moreover, since H is a 2-connected subgraph of the 2-connected graph G, we have that $\mathrm{cy}(G) \geq \mathrm{cy}(H)$. This inequality holds since the cyclomatic number counts the number of ears in any ear decomposition of a graph, and any ear decomposition of H can be completed to one of G. Using (4.3) this implies $\gamma_2(\mathcal{P}_G) - \gamma_2(\mathcal{P}_{G\setminus e}) \geq 0$.

It remains to characterize the case when $\gamma_2(\mathcal{P}_G) = \gamma_2(\mathcal{P}_{G\setminus e})$. By the previous argument $\gamma_2(\mathcal{P}_G) - \gamma_2(\mathcal{P}_{G\setminus e}) = 0$ if and only if $\mathrm{cy}(G) = \mathrm{cy}(H)$. As the cyclomatic number of a proper 2-connected subgraph of G needs to be strictly smaller than $\mathrm{cy}(G)$, it follows that $\mathrm{cy}(G) = \mathrm{cy}(H)$ if and only if $G = H$, which proves the claim. □

Before proving the last and main proposition, we need a technical lemma.

Lemma 4.2.7. *Let $G = ([n], E)$ be a 2-connected graph without vertices of degree 2 and let H be a 2-connected subgraph with k vertices of degree 2. Then*

$$\mathrm{cy}(G) \geq \mathrm{cy}(H) + \frac{k}{2}.$$

Proof. Any ear decomposition of H can be completed to one of G by adding $(\mathrm{cy}(G) - \mathrm{cy}(H))$-many ears. Since G does not have vertices of degree 2, every vertex of degree

2 in H is adjacent to at least one new ear. Moreover, each new ear is adjacent to at most two such vertices. The number of new ears must then be at least equal to half the number of vertices of degree 2 in H. □

Before handling the remaining case towards the proof of Theorem 4.2.2, we need an additional definition.

Definition 4.2.8. *Let $G = ([n], E)$ be a graph and let i and j be two new vertices.*

(i) The double cone *of G with respect to i and j is the graph with vertex set $V \cup \{i, j\}$ and with edges*

$$E \cup (\{i, j\} \times V) \cup \{ij\}.$$

(ii) If G is bipartite with bipartition given by $V = V_1 \cup V_2$, then the bipartite cone *of G with respect to i and j is the bipartite graph with vertex set $V \cup \{i, j\}$ and with edges*

$$E \cup (\{i\} \times V_1) \cup (\{j\} \times V_2) \cup \{ij\}.$$

See Figure 4.2 for an example of Definition 4.2.8.

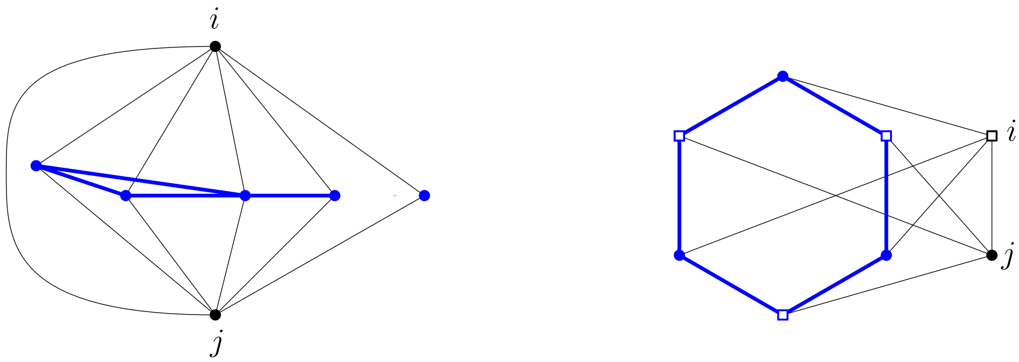

FIGURE 4.2: The double cone of a graph (left) and the bipartite cone of a 6-cycle (right).

Proposition 4.2.9. *Let $G = ([n], E)$ be a 2-connected graph. Assume that every edge of G is contained in some 3- or 4-cycle, and that $\min_{i \in [n]} \delta_G(i) \geq 3$. Then for every $e \in E$,*

$$\gamma_2(\mathcal{P}_G) \geq \gamma_2(\mathcal{P}_{G \setminus e}).$$

Moreover, equality holds if and only if $G = G_1 \oplus_2 \cdots \oplus_2 G_m$, where $m \geq 1$, all the 2-clique sums are taken along $e = ij$, G_1 is the double cone w.r.t. i and j over a connected graph G_1' with $|E(G_1')| \geq 1$, and for every $2 \leq \ell \leq m$ either:

- *G_ℓ is the double cone w.r.t. i and j over any connected graph G_ℓ' with $|E(G_\ell')| \geq 1$, or*

- *G_ℓ is the bipartite cone w.r.t. i and j over an even cycle.*

Proof. Let $e = ij$ be any edge. We define $H = (W, F)$ to be the subgraph induced by all edges of G which lie in a 3- or 4-cycle together with e. We now give an iterative procedure to construct H in a sequence of steps, yielding a partition of F. We use $H' = (W', F')$ to denote the current graph in the procedure. Set $E' = E$.

Step 0: Set $H' = (\{i, j\}, \{ij\})$, namely H' is the graph consisting of the edge e alone.

Step 1: For every pair of edges $f, g \in E'$ such that $\{e, f, g\}$ is a 3-cycle, add f, g to F' and delete them from E'. This step adds to H' a number r_1 of ears of length 2.

Step 2: Add to F' every edge $k\ell \in E'$ such that k and ℓ are vertices of H', and delete these edges from E'. This step adds to H' a number r_2 of ears of length 1;

Step 3: If there is a 4-cycle C in G with $E(C) \cap F' = \{e\}$, add the three edges in $E(C) \smallsetminus \{e\}$ to F', and delete them from E'. Update H' and repeat this procedure as often as possible. In this step, r_3 many ears of length 3 are added to H'.

Step 4: If there is a 4-cycle C in G with $E(C) \cap F' = \{e, g\}$ for some edge g, add $E(C) \smallsetminus \{e, g\}$ to F' and delete these edges from E'. Update H' and iterate this procedure as long as possible. This step adds to H' a number r_4 of ears of length 2;

Step 5: Add to F' the edges $f \in E'$ such that e and f are contained in a 4-cycle C with $E(C) \smallsetminus F' = \{f\}$. This step adds to H' a number r_5 of ears of length 1.

(See Figure 4.3 for an example of how this algorithm works.)

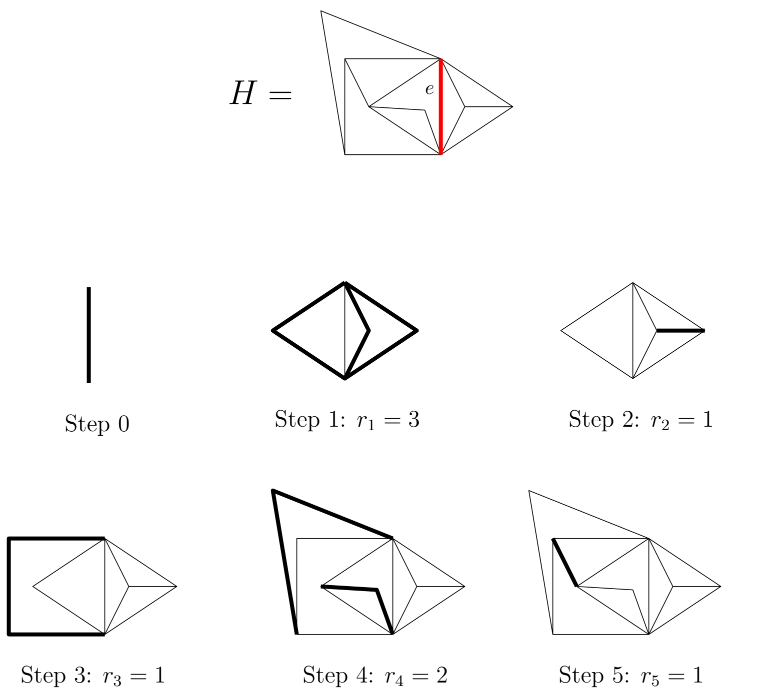

FIGURE 4.3: The construction of the graph H as in the proof of Proposition 4.2.9.

It is obvious that this procedure indeed yields an open ear decomposition of H (the closed ear being the first cycle that is constructed either in Step 1 or 3). Hence,

$$\mathrm{cy}(H) = \sum_{i=1}^{5} r_i. \tag{4.4}$$

Observe that we make multiple choices in Steps 3 and 4 and hence neither the decomposition nor the numbers r_3, r_4 and r_5 are uniquely determined. Fix now any linear order on F such that:

- g is bigger than f if g has been added to F before f;
- if f, g, h are edges added in an iteration of Step 3, then the smallest of the three is the one not incident to e;
- if f, g are edges added in an iteration of Step 4, then the smallest of the two is the one not incident to e.

Consider an extension $<$ of this linear order to E such that any edge of $E \smallsetminus F$ is smaller than any edge of F. In particular, e is the $<$-maximal edge.

We now describe the bad pairs of G which are not bad pairs of $G \smallsetminus e$. We will use the fact that any pair of disjoint directed edges determines a unique directed 4-cycle. In the following, let $\mathbb{1}_C$ be the indicator function which equals 1 if condition C holds and 0 otherwise.

- For every edge f lying in a 3-cycle with e, there are 2 bad pairs supported on $\{e, f\}$. As there are $2r_1$ such edges f, this gives rise to $4r_1$ bad pairs.
- There are 2 bad pairs supported on the set $\{f, g\}$, where $\{e, f, g\}$ is the last 3-cycle added in Step 1. As these pairs only occur if $r_1 \geq 1$, their number is $2 \cdot \mathbb{1}_{r_1 \geq 1}$.
- Each edge h added in Step 2 lies in a subgraph of H isomorphic to K_4 that also contains e. In particular, there are two 4-cycles containing e and h, and in both cycles h is the minimal element. For each cycle, only the two edges different from e and h give rise to 2 new bad pairs. Therefore, for each edge h added in Step 2 we get 4 new bad pairs, and hence we obtain $4r_2$ many.
- If f, g and h have been added in the same iteration of Step 3 with $\min_<\{e, f, g, h\} = h$, then there are 2 bad pairs supported on each of $\{e, f\}$, $\{e, g\}$ and $\{f, g\}$. This yields $6r_3$ such bad pairs.
- If $\{e, f, g, h\}$ lie in a 4-cycle such that g and h have been added in the same iteration of Step 4 and $h < g$, then there are 2 bad pairs supported on each of $\{e, g\}$ and $\{f, g\}$. Note that f is incident to e and has been added either in Step 1 or in Step 3. This implies that the two bad pairs supported on $\{e, f\}$ have already been counted in the previous discussion. Hence there are $4r_4$ new bad pairs.
- If $\{e, f, g, h\}$ is a 4-cycle such that h has been added in Step 5, then there are 2 bad pairs supported on $\{f, g\}$. These are new, since f and g did not lie in a 4-cycle with e before Step 5. There are $2r_5$ such bad pairs.

Figure 4.4 shows all bad pairs for the graph H in Figure 4.3. For the total number of bad pairs in G that are not bad pairs of $G \smallsetminus e$ we hence get

$$\begin{aligned} n_1(G) - n_1(G \smallsetminus e) &= 4r_1 + 2 \cdot \mathbb{1}_{r_1 \geq 1} + 4r_2 + 6r_3 + 4r_4 + 2r_5 \\ &= 4\,\mathrm{cy}(H) + 2(r_3 - r_5) + 2 \cdot \mathbb{1}_{r_1 \geq 1}, \end{aligned}$$

where the second equality follows from (4.4). Hence, (4.2) implies

$$\gamma_2(\mathcal{P}_G) - \gamma_2(\mathcal{P}_{G \smallsetminus e}) = 4(\mathrm{cy}(G) - \mathrm{cy}(H)) - 2(r_3 - r_5) + 2(1 - \mathbb{1}_{r_1 \geq 1}). \tag{4.5}$$

As H is 2-connected, we have that $\mathrm{cy}(G) - \mathrm{cy}(H) \geq 0$, and hence the only possibly negative term in the last equation is $-2(r_3 - r_5)$. In particular, if $r_3 - r_5 \leq 0$, it follows

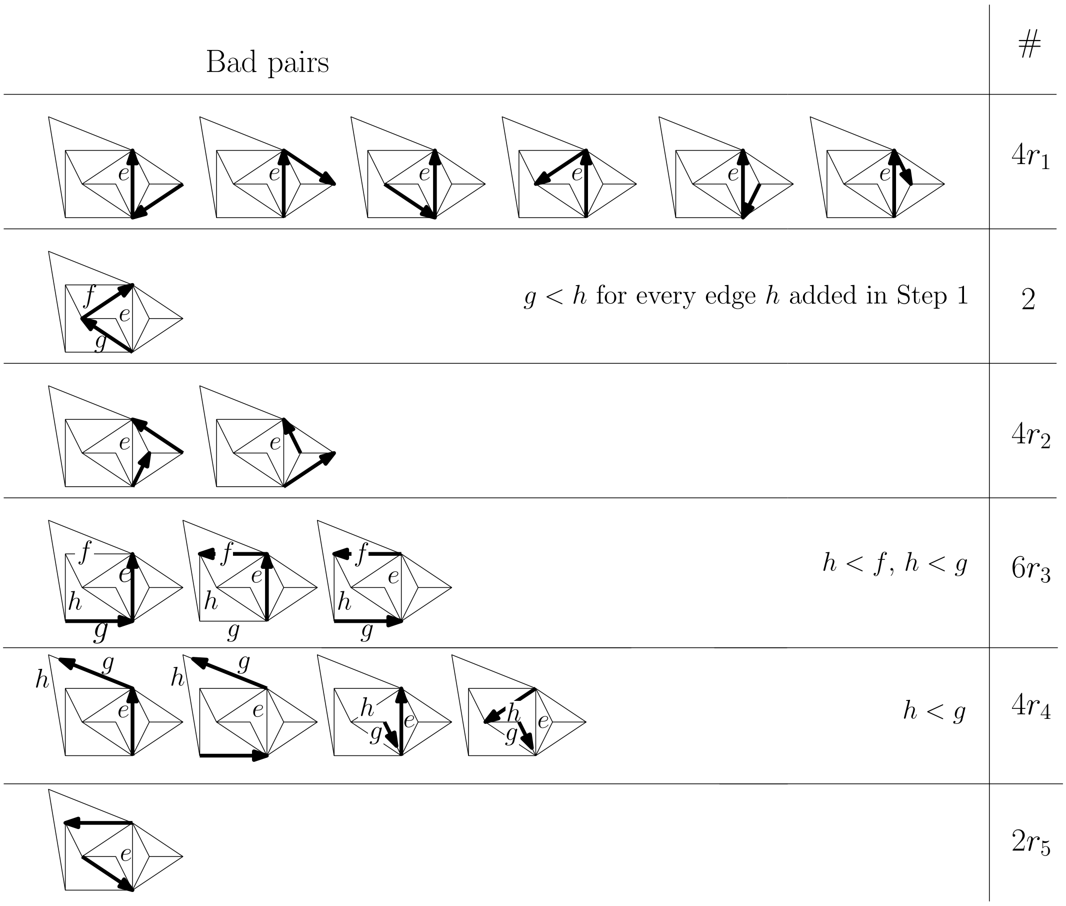

FIGURE 4.4: The bad pairs of edges as in Proposition 4.2.9 for the graph H in Figure 4.3.

that $\gamma_2(\mathcal{P}_G) - \gamma_2(\mathcal{P}_{G\smallsetminus e}) \geq 0$. Now assume $r_3 - r_5 \geq 0$. We claim that in this case

$$\mathrm{cy}(G) \geq \mathrm{cy}(H) + (r_3 - r_5). \tag{4.6}$$

Note that using (4.5) it then follows that

$$\gamma_2(\mathcal{P}_G) - \gamma_2(\mathcal{P}_{G\smallsetminus e}) \geq 2(r_3 - r_5) + 2(1 - \mathbb{1}_{r_1 \geq 1}), \tag{4.7}$$

which is even stronger than $\gamma_2(\mathcal{P}_G) - \gamma_2(\mathcal{P}_{G\smallsetminus e}) \geq 0$.

To show (4.6), let $J = H \smallsetminus \{i, j\}$ (i.e., J is the graph obtained by removing the vertices i and j from H). The vertex set of J can be partitioned as $V(J) = V_1 \cup V_3 \cup V_4$, where V_ℓ is the set of vertices that have been added to H during Step ℓ of the described procedure. Since Steps 2 and 5 add ears of length 1, no new vertices are introduced during these steps. Note that $|E(J)| = r_2 + r_3 + r_4 + r_5$. For each connected component J_ℓ of J, we let $r_{k,\ell}$ be the number of edges of J_ℓ added to H in Step k, for $k = 1, \dots, 5$. We distinguish between two cases:

Case 1: If $V(J_\ell) \cap V_1 \neq \varnothing$, then we consider an auxiliary graph J'_ℓ with vertex set $V(J'_\ell) = (V(J_\ell) \smallsetminus V_1) \cup \{v\}$, where v is a new vertex. Two vertices $a, b \in V(J'_\ell)$ form an edge of J'_ℓ if either $ab \in E(J_\ell)$ or $a = v$ and $wb \in E(J_\ell)$, for some $w \in V(J_\ell) \cap V_1$. Then J'_ℓ is connected. Hence,

$$r_{3,\ell} + r_{4,\ell} + r_{5,\ell} \geq |E(J'_\ell)| \geq |V(J'_\ell)| - 1 = 2r_{3,\ell} + r_{4,\ell} + 1 - 1, \tag{4.8}$$

where the first inequality follows from the fact that the edges in J_ℓ between two vertices in V_1 do not appear in J'_ℓ. We obtain that $r_{3,\ell} - r_{5,\ell} \leq 0$.

Case 2: If $V(J_\ell) \cap V_1 = \varnothing$, then

$$r_{3,\ell} + r_{4,\ell} + r_{5,\ell} = |E(J_\ell)| \geq |V(J_\ell)| - 1 = 2r_{3,\ell} + r_{4,\ell} - 1. \tag{4.9}$$

This implies $r_{3,\ell} - r_{5,\ell} \leq 1$, with equality attained if and only if $|E(J_\ell)| = |V(J_\ell)| - 1$, i.e., if J_ℓ is a tree (with at least one edge, since $r_{3,\ell} = r_{5,\ell} + 1 \geq 1$). In this case, J_ℓ has at least 2 leaves. Since each leaf of J_ℓ corresponds to a vertex of degree 2 in H, one has that

$$|\{v \in H \;:\; \delta_H(v) = 2\}| \geq 2 \cdot |\{\ell \;:\; J_\ell \text{ is a tree with } |V(J_\ell)| \geq 2 \text{ and } V(J_\ell) \cap V_1 = \varnothing\}|.$$

Combining the two cases above and using the identities $\sum_\ell r_{k,\ell} = r_k$, we obtain that

$$r_3 - r_5 \leq |\{\ell \;:\; J_\ell \text{ is a tree with } |V(J_\ell)| \geq 2,\ V(J_\ell) \cap V_1 = \varnothing\}| \leq \frac{|\{v \in H \;:\; \delta_H(v) = 2\}|}{2}. \tag{4.10}$$

Using Lemma 4.2.7, we conclude that

$$\mathrm{cy}(G) \geq \mathrm{cy}(H) + \frac{|\{v \in H \;:\; \delta_H(v) = 2\}|}{2} \geq \mathrm{cy}(H) + (r_3 - r_5),$$

which proves (4.6) and hence the inequality $\gamma_2(\mathcal{P}_G) - \gamma_2(\mathcal{P}_{G \smallsetminus e}) \geq 0$.

We now study the case when $\gamma_2(\mathcal{P}_G) - \gamma_2(\mathcal{P}_{G \smallsetminus e}) = 0$. It follows from (4.5), (4.6) and (4.7) that $\gamma_2(\mathcal{P}_G) - \gamma_2(\mathcal{P}_{G \smallsetminus e}) = 0$ if and only if $r_3 = r_5$, $r_1 \geq 1$ and $\mathrm{cy}(G) = \mathrm{cy}(H)$. The last equality implies that $G = H$. In particular, since we assumed that every vertex in G has degree at least 3, the same holds for H. It follows from (4.10) that there is no component J_ℓ with $V(J_\ell) \cap V_1 = \varnothing$ that is a tree with at least one edge. In particular, we have that $r_{3,\ell} - r_{5,\ell} \leq 0$ for any component J_ℓ and, as $r_3 = r_5$, all of these inequalities are in fact equalities. The idea now is to analyze what the components J_ℓ can look like.

If $V(J_\ell) \cap V_1 \neq \varnothing$, then it follows from (4.8) that J'_ℓ has to be a tree and that we have $|E(J'_\ell)| = r_{3,\ell} + r_{4,\ell} + r_{5,\ell}$. It follows from these two conditions that for every $w \in V(J_\ell) \cap (V_3 \cup V_4)$ there is at most one edge of the form wz for some $z \in V(J_\ell) \cap V_1$. This implies that every vertex of degree 1 in J'_ℓ (other than v) corresponds to a vertex of degree 2 in H. As there are none such vertices, we conclude that J'_ℓ is just an isolated vertex, namely v. Hence, $r_{3,\ell} = r_{4,\ell} = r_{5,\ell} = 0$ and J_ℓ is an arbitrary graph on $r_{1,\ell}$ vertices, where each vertex is connected to both i and j in G. This implies that the subgraph of G induced on $V(J_\ell) \cup \{i, j\}$ is the double cone over J_ℓ w.r.t. i and j.

If $V(J_\ell) \cap V_1 = \varnothing$, then by (4.9) we have that $r_{3,\ell} - r_{5,\ell} = 0$ if and only if $|E(J_\ell)| = |V(J_\ell)|$. By the same argument as above, J_ℓ cannot have vertices of degree 1 and must hence be a cycle. Since all vertices of J_ℓ have been added in an iteration of Step 3 or 4, each vertex of J_ℓ is connected to either i or j in G, but not to both. Consider an edge $vw \in E(J_\ell)$ and assume that $vi \in E(G)$. As vw lies in a 4-cycle together with e by assumption and there is a unique such, namely the one with edges $\{vw, vi, e, wj\}$, it follows that $wj \in E$. This shows that J_ℓ is a bipartite graph with vertex partition $\{v \in V(J_\ell) \;:\; vi \in E\} \cup \{v \in V(J_\ell) \;:\; vj \in E\}$. Hence, J_ℓ is an even cycle, and the subgraph of G induced on $V(J_\ell) \cup \{i, j\}$ is the bipartite cone of J_ℓ w.r.t. i and j.

□

We can finally provide the proof of Theorem 4.2.2.

Proof of Theorem 4.2.2. Let $G = ([n], E)$ be a graph. We show the claim by induction on $|E|$. If $|E| = 1$, the claim is trivially true. Assume that $|E| > 1$. Without loss of generality, we can assume that G is connected since taking 1-sums of its connected components does not change the symmetric edge polytope [DDM22, Remark 35] and, in particular, its γ-vector due to [OT21b, Proposition 5.2] and Lemma 1.2.1. If G is not 2-connected, then let $G_1, \dots, G_s$ be its 2-connected components, where $s \geq 2$. As $|E(G_i)| < |E(G)|$, it follows from the induction hypothesis and Lemma 4.2.3 that $\gamma_2(\mathcal{P}_G) \geq 0$. Assume that G is 2-connected. Applying Propositions 4.2.5, 4.2.6 and 4.2.9, it follows that there exists $e \in E$ with $\gamma_2(\mathcal{P}_G) \geq \gamma_2(\mathcal{P}_{G\smallsetminus e})$. Since, by the induction hypothesis, the latter expression is non-negative, this finishes the proof. $\square$

Remark 4.2.10. *We remark that in the proof of Theorem 4.2.2, we do not claim that $\gamma_2(\mathcal{P}_G) \geq \gamma_2(\mathcal{P}_{G\smallsetminus e})$ for every edge $e \in E$. This statement is indeed false. For a small counterexample, let G be the 2-connected graph on 5 vertices with $E = \{12, 23, 34, 45, 15, 35\}$. Then $\gamma_2(\mathcal{P}_G) = 4$ and $\gamma_2(\mathcal{P}_{G\smallsetminus 35}) = 6$, so γ_2 increases when removing the edge 35. However, $\delta_G(3) = \delta_G(5) = 3$ and $\delta_G(1) = \delta_G(2) = \delta_G(4) = 2$ in G, so this is the setting from Proposition 4.2.6. In particular, the proof states that we should choose e to be adjacent to one of the vertices of degree 2, a condition that the edge 35 does not satisfy.*

In the remaining part of this section, we focus on the problem of when $\gamma_2(\mathcal{P}_G) = 0$.

Definition 4.2.11. *Let $n \geq 3$. Let G_n be the graph on n vertices obtained from the complete bipartite graph $K_{2,n-2}$, considered with bipartition $[n] = [2] \cup \{3, \dots, n\}$, by adding the edge 12.*

We note that G_n has $2n-3$ edges. See Figure 4.5 for an example of Definition 4.2.11 for $n = 6$.

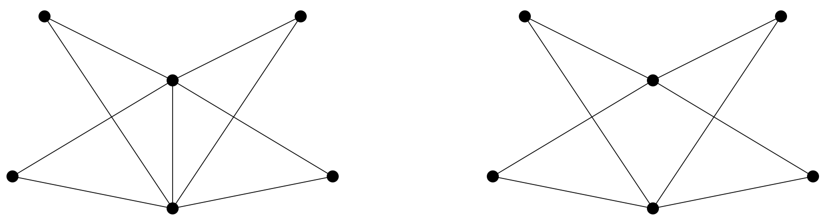

FIGURE 4.5: The graphs G_6 and $K_{2,4}$.

Theorem 4.2.12. *Let $G = ([n], E)$ be a 2-connected graph. Then $\gamma_2(\mathcal{P}_G) = 0$ if and only if either $n < 5$, or $n \geq 5$ and $G \cong G_n$ or $G \cong K_{2,n-2}$.*

Proof. By [OT21b, Example 5.9], we have that $\gamma_i(\mathcal{P}_{K_n}) = \binom{n-1}{2i}\binom{2i}{i}$, and in [HJM19] it is proved that $\gamma_i(\mathcal{P}_{K_{m,n}}) = \binom{m-1}{2i}\binom{n-1}{2i}\binom{2i}{i}$. Moreover, $\gamma_i(\mathcal{P}_{G_n}) = \gamma_i(\mathcal{P}_{K_{2,n-1}})$ for every $i \geq 0$ by [OT21b, Proposition 5.4]. This proves the "if" statement, which can be also verified directly using Lemma 4.2.1, (4.12) and (4.13).

We prove the claim by double induction on the pairs (n, k), with $n = |V(G)|$ and $k = |E(G)|$. The base case is given by any graph with $n < 5$, as $\gamma_2(\mathcal{P}_G) = 0$ for every graph G with less than 5 vertices.

Let $n \geq 5$. First assume that G has a vertex i of degree 2. Let $e = ij$ be any of the two edges incident with i. Being 2-connected, G is either a cycle (in which case

Theorem 4.2.2 and Proposition 4.2.6 imply that $n \in \{3,4\}$) or can be obtained from a 2-connected graph G' by adding an open ear P of length $\ell \geq 2$ containing e. Assume the latter. We then have that

$$0 = \gamma_2(\mathcal{P}_G) \geq \gamma_2(\mathcal{P}_{G \setminus e}) = \gamma_2(\mathcal{P}_{G'}) \geq 0,$$

where the first inequality follows from Proposition 4.2.6, the last equality from (4.1) in Lemma 4.2.1, and the last inequality from Theorem 4.2.2.

Hence $\gamma_2(\mathcal{P}_{G'}) = 0$ and, by induction, $G' \in \{G_{n'} : n' \geq 3\} \cup \{K_{2,n'-2} : n' \geq 4\} \cup \{K_4\}$. We claim that the length ℓ of the ear P must be 2. Indeed, consider any edge f in G' different from the one (if it exists) connecting the two endpoints of P. Then every cycle containing both e and f has length at least $\ell + 2$, and Proposition 4.2.6 forces $\ell = 2$. Let then $e = ij$, ik be the edges in P. Note that G' cannot be a K_4, as otherwise the edge of K_4 opposite to jk would not be contained in any 3- or 4-cycle together with e. Then either $G' \cong G_{n-1}$ or $G' \cong K_{2,n-3}$, and thus $G \cong G_n$ (if $jk \in E$) or $G \cong K_{2,n-2}$ (otherwise).

If $\min \delta_G(v) \geq 3$, we choose e to be the unique edge in the last ear of any ear decomposition of G. We then have that $G \setminus e$ is 2-connected and has $n \geq 5$ vertices. As $\gamma_2(\mathcal{P}_{G \setminus e}) = 0$, we conclude by induction that $G \setminus e \cong K_{2,n-2}$ or $G \setminus e \cong G_n$. In both cases, $G \setminus e$ has at least 3 vertices of degree 2. Hence G has at least one degree 2 vertex, which contradicts the assumption $\min \delta_G(v) \geq 3$. □

The characterization of the equality case $\gamma_2 = 0$ can be extended to all graphs as follows.

Corollary 4.2.13. *Let $G = ([n], E)$ be a graph. Then $\gamma_2(\mathcal{P}_G) = 0$ if and only if either*

(i) G is a forest, or,

(ii) all but one of the 2-connected components of G are edges and the remaining component is isomorphic to one of K_4, G_ℓ for some $\ell \geq 3$, and $K_{2,\ell}$ for some $\ell \geq 2$.

Proof. Assume $\gamma_2(\mathcal{P}_G) = 0$. If G has at least two 2-connected components that are not edges, then the product of their cyclomatic numbers is positive, as the cyclomatic number of any 2-connected graph is strictly positive. By Lemma 4.2.3 and Theorem 4.2.2, this implies that $\gamma_2(\mathcal{P}_G) > 0$. Hence, G has at most one 2-connected component that is not an edge. Let us denote this component by H, if it exists. Again using Lemma 4.2.3, we observe that if $\gamma_2(\mathcal{P}_H) > 0$, then $\gamma_2(\mathcal{P}_G) > 0$. The claim now follows from Theorem 4.2.12 by noting that the only 2-connected graphs on less than 5 vertices are K_4, $C_3 = G_3$, $C_4 = K_{2,2}$ and G_4. □

We close this section with a conjecture that extends Theorem 4.2.12. To state the conjecture, for $k \geq 2$, let $G_{n,k}$ be the graph that is obtained from $K_{k,n-k}$ by adding all edges between the vertices on the side of the vertex partition with k elements. In other words, $G_{n,k}$ can be thought of as the *k-fold cone* over a set of $n-k$ isolated vertices. In particular, for $k = 2$ we have $G_{n,2} = G_n$. The following conjecture naturally generalizes Theorem 4.2.12 and has been verified computationally for small values of k and n.

Conjecture 4.2.14. *Let $k \in \mathbb{N}$ and let G be a k-connected graph on n vertices. Then $\gamma_k(\mathcal{P}_G) = 0$ if and only if $n < 2k + 1$ or, $n \geq 2k + 1$ and $K_{k,n-k} \subseteq G \subseteq G_{n,k}$.*

4.3 On a conjecture of Lutz and Nevo

In this section, our focus lies on a conjecture by Lutz and Nevo [LN16, Conjecture 6.1], which characterizes flag PL-spheres Δ with $\gamma_2(\Delta) = 0$. Our goal is to show that symmetric edge polytopes with $\gamma_2 = 0$ admit a triangulation of their boundary with the properties predicted by [LN16, Conjecture 6.1]. Let us denote by $\Diamond_d$ the boundary complex of the $(d+1)$-dimensional cross-polytope.

Conjecture 4.3.1. *[LN16, Conjecture 6.1] Let Δ be a $(d-1)$-dimensional flag piecewise linear sphere, with $d \geq 4$. Then the following are equivalent:*

(i) $\gamma_2(\Delta) = 0$*;*

(ii) There exists a sequence of edge contractions

$$\Delta = \Delta_0 \to \Delta_1 = \Delta_0/F_1 \to \cdots \to \Delta_{k-1}/F_k \cong \Diamond_{d-1},$$

such that each Δ_i is a $(d-1)$-dimensional flag PL-sphere, and $\mathrm{lk}_{\Delta_{i-1}}(F_i) \cong \Diamond_{d-3}$, for every $1 \leq i \leq k$.

The implication "(ii)⇒(i)" follows from the fact that $\gamma_1 = \gamma_2 = 0$ for the boundary of any cross-polytope [LN17, Lemma 2.4] combined with the following relation between the γ-vectors of Δ and of an edge contraction Δ/F [LN17, Lemma 2.3 (ii)]:

$$\gamma_2(\Delta) = \gamma_2(\Delta/F) + \gamma_1(\mathrm{lk}_\Delta(F)). \tag{4.11}$$

The remaining implication has been proven for the subclass of (dual complexes) of flag nestohedra (see [LN16, Section 6] and [Vol10]) and has been tested computationally by Lutz and Nevo [LN16, Section 6], but is open in general.

In the following, we show that the boundary complexes of the symmetric edge polytopes of the graphs $K_{2,n-2}$ and G_n admit a triangulation satisfying (i) and (ii) above. We start by fixing labelings on $K_{2,n-2}$ and G_n. We label the vertices of $K_{2,n-2}$ and G_n so that $E(K_{2,n-2}) = \{1,2\} \times \{3,\ldots,n\}$ and $E(G_n) = E(K_{2,n-2}) \cup \{12\}$. Let further $<$ be a total order on the edges of both graphs such that $2n < 2(n-1) < \cdots < 23$ are the smallest edges and let $\Delta_{K_{2,n-2}}$ and Δ_{G_n} be the corresponding unimodular triangulations of $\partial\mathcal{P}_{K_{2,n-2}}$ and $\partial\mathcal{P}_{G_n}$, respectively, provided by Lemma 4.1.1. The $6n^2 - 28n + 34$ edges of $\Delta_{K_{2,n-2}}$ and the $6n^2 - 24n + 24$ edges of Δ_{G_n} can then be listed as follows:

$$\begin{aligned} E(\Delta_{K_{2,n-2}}) = &\{\pm\{e_{i,a}, e_{i,b}\} \ : \ 1 \leq i \leq 2, 3 \leq a < b \leq n\} \cup \\ &\{\pm\{e_{1,a}, e_{b,2}\} \ : \ 3 \leq a \neq b \leq n\} \cup \\ &\{\pm\{e_{1,a}, e_{2,a}\} \ : \ 3 \leq a \leq n\} \cup \\ &\{\pm\{e_{2,b}, e_{1,a}\} \ : \ 3 \leq a < b \leq n\} \cup \\ &\{\pm\{e_{2,a}, e_{b,2}\} \ : \ 3 \leq a < b \leq n\} \cup \\ &\{\pm\{e_{1,n}, e_{n,2}\}\}. \end{aligned} \tag{4.12}$$

$$
\begin{aligned}
E(\Delta_{G_n}) = &\{\pm\{e_{i,a}, e_{i,b}\} \ : \ 1 \le i \le 2, 3 \le a < b \le n\} \cup \\
&\{\pm\{e_{1,a}, e_{b,2}\} \ : \ 3 \le a \ne b \le n\} \cup \\
&\{\pm\{e_{1,a}, e_{2,a}\} \ : \ 3 \le a \le n\} \cup \\
&\{\pm\{e_{2,b}, e_{1,a}\} \ : \ 3 \le a < b \le n\} \cup \\
&\{\pm\{e_{2,a}, e_{b,2}\} \ : \ 3 \le a < b \le n\} \cup \\
&\{\pm\{e_{1,2}, e_{1,a}\}, \pm\{e_{1,2}, e_{a,2}\} \ : \ 3 \le a \le n\}.
\end{aligned} \tag{4.13}
$$

In particular, we get that $E(\Delta_{K_{2,n-2}}) \smallsetminus E(\Delta_{G_n}) = \{\pm\{e_{1,n}, e_{n,2}\}\}$, and the only edges of Δ_{G_n} that are non-edges of $\Delta_{K_{2,n-2}}$ are those containing $e_{1,2}$ or $e_{2,1}$.

Lemma 4.3.2. *For every $n \ge 3$, we have:*

(i) $\Delta_{K_{2,n-2}} \cong \langle e_{2,n}, e_{n,2} \rangle * \Delta_{G_{n-1}}$,

(ii) $(\Delta_{G_n}/\{e_{1,2}, e_{1,n}\})/\{e_{2,1}, e_{n,1}\} \cong \Delta_{K_{2,n-2}}$.

Observe that $\{e_{1,2}, e_{1,n}\}$ is an edge of Δ_{G_n} and $\{e_{2,1}, e_{n,1}\}$ is an edge of $\Delta_{G_n}/\{e_{1,2}, e_{1,n}\}$. Hence it makes sense to consider the corresponding edge contractions in (ii).

Proof. To prove (i), we first note that, since by Lemma 4.1.1 both complexes involved in the statement are flag spheres, it suffices to provide an isomorphism between the 1-skeleta of the corresponding complexes. For this aim, let $\varphi : \Delta_{K_{2,n-2}} \to \langle e_{2,n}, e_{n,2} \rangle * \Delta_{G_{n-1}}$ be the simplicial map induced by $\varphi(\pm e_{1,n}) = \pm e_{1,2}$ and $\varphi(e) = e$ for any other vertex $e \in \Delta_{K_{2,n-2}}$. By comparing (4.12) and (4.13), it is easily seen that φ is a simplicial isomorphism between the 1-skeleta of $\Delta_{K_{2,n-2}}$ and $\langle e_{2,n}, e_{n,2} \rangle * \Delta_{G_{n-1}}$.

To show (ii), observe that by Lemma 4.1.1 $\Delta_{K_{2,n-2}}$ and Δ_{G_n} are flag simplicial complexes. We first show that so is $(\Delta_{G_n}/\{e_{1,2}, e_{1,n}\})/\{e_{2,1}, e_{n,1}\}$. For this it is enough to show that $\{e_{1,2}, e_{1,n}\}$ and $\{e_{2,1}, e_{n,1}\}$ are not contained in any induced subcomplex of Δ_{G_n} and $\Delta_{G_n}/\{e_{1,2}, e_{1,n}\}$, respectively, that is isomorphic to a 4-cycle (see [LN17, Lemma 2.1 (ii)]). If, by contradiction, such a subcomplex exists in Δ_{G_n}, then it has to contain the vertex $e_{2,n}$ (respectively, $e_{n,2}$) since $e_{2,n}$ (respectively, $e_{n,2}$) is the only vertex lying in an edge with $e_{1,n}$ but not $e_{1,2}$ (respectively, vice versa). As $\{e_{2,n}, e_{n,2}\}$ is not an edge of Δ_{G_n}, such a subcomplex cannot exist. The same reasoning shows the corresponding statement for $\Delta_{G_n}/\{e_{1,2}, e_{1,n}\}$ and $\{e_{2,1}, e_{n,1}\}$. In particular, it follows that $(\Delta_{G_n}/\{e_{1,2}, e_{1,n}\})/\{e_{2,1}, e_{n,1}\}$ is flag. We consider the simplicial map $\xi : (\Delta_{G_n}/\{e_{1,2}, e_{1,n}\})/\{e_{2,1}, e_{n,1}\} \to \Delta_{K_{2,n-2}}$, defined by $\xi(\pm e_{1,2}) = \pm e_{1,n}$ and $\xi(e) = e$ for any other vertex of $(\Delta_{G_n}/\{e_{1,2}, e_{1,n}\})/\{e_{2,1}, e_{n,1}\}$. Using (4.12), (4.13) and the definition of edge contraction it is easy to check that ξ induces a simplicial isomorphism between the 1-skeleta of $(\Delta_{G_n}/\{e_{1,2}, e_{1,n}\})/\{e_{2,1}, e_{n,1}\}$ and $\Delta_{K_{2,n-2}}$, which shows the claim. □

We record here an explicit computation that will come in handy in the proof of Theorem 4.3.4 below.

Example 4.3.3. *Consider the graphs K_4 and G_4 (with the labeling described previously) and order their edges so that $34 < 24 < 23 < 14 < 13 < 12$. Let Δ_{K_4} and Δ_{G_4} be the respective (flag) unimodular triangulations of $\partial\mathcal{P}_{K_4}$ and $\partial\mathcal{P}_{G_4}$ induced by this choice.*

Consider the sequence of edge contractions

$$\Delta_{K_4} =: \Delta_0 \to \Delta_1 := (\Delta_{K_4}/\{e_{1,4}, e_{3,4}\}) \to \Delta_2 := (\Delta_{K_4}/\{e_{1,4}, e_{3,4}\})/\{e_{4,1}, e_{4,3}\}.$$

One can check that Δ_1 and Δ_2 are flag spheres and, since Δ_0 is 2-dimensional, both $\mathrm{lk}_{\Delta_0}(\{e_{1,4}, e_{3,4}\})$ and $\mathrm{lk}_{\Delta_1}(\{e_{4,1}, e_{4,3}\})$ consist of two vertices. We claim that Δ_2 is isomorphic to Δ_{G_4}: since both complexes are flag, this can be verified by exhibiting a simplicial map between Δ_2 and Δ_{G_4} which is an isomorphism on the 1-skeleton. The map $\varphi\colon \Delta_2 \to \Delta_{G_4}$ defined by $\varphi(\pm e_{1,2}) = \pm e_{1,3}$, $\varphi(\pm e_{1,3}) = \pm e_{2,3}$, $\varphi(\pm e_{1,4}) = \pm e_{4,2}$, $\varphi(\pm e_{2,3}) = \pm e_{2,1}$, $\varphi(\pm e_{2,4}) = \pm e_{4,1}$ gives the desired result.

We can now state the main result of this section.

Theorem 4.3.4. *Let G be a connected graph on $n \geq 5$ vertices. Then $\gamma_2(\mathcal{P}_G) = 0$ if and only if there exist a flag unimodular triangulation Δ_G of $\partial\mathcal{P}_G$ and a sequence of edge contractions $\Delta_G =: \Delta_0 \to \Delta_1 := \Delta_0/F_1 \to \Delta_2 := \Delta_1/F_2 \to \cdots \to \Delta_{2k} := \Delta_{2k-1}/F_k$ such that*

(i) Δ_i is a flag sphere for every $0 \leq i \leq 2k$;

(ii) $\Delta_{2k} \cong \Diamond_{n-2}$;

(iii) $\mathrm{lk}_{\Delta_{i-1}}(F_i) \cong \Diamond_{n-4}$ for every $1 \leq i \leq 2k$.

Moreover, if the conditions above are met, for every $0 \leq i \leq k$ the complex Δ_{2i} is a unimodular triangulation of the boundary of some symmetric edge polytope.

Proof. The validity of the "if"-part has already been observed for general flag PL-spheres at the beginning of this section.

For the other direction assume first that G is 2-connected. By Theorem 4.2.12, we know that $\gamma_2(\mathcal{P}_G) = 0$ if and only if either $G \cong K_{2,n-2}$ or $G \cong G_n$. Iteratively applying Lemma 4.3.2 and recalling that $(\Delta * \Gamma)/F = \Delta * (\Gamma/F)$ whenever F is a face of Γ, we obtain the following chain of edge contractions and isomorphisms:

$$\begin{aligned}
\Delta_{G_n} = \Delta_0 \to \Delta_1 &= (\Delta_{G_n}/\{e_{1,2}, e_{1,n}\}) \to \Delta_2 = (\Delta_{G_n}/\{e_{1,2}, e_{1,n}\})/\{e_{2,1}, e_{n,1}\} \\
&\overset{(ii)}{\cong} \Delta_{K_{2,n-2}} \overset{(i)}{\cong} \langle e_{2,n}, e_{n,2}\rangle * \Delta_{G_{n-1}} \\
&\to \Delta_3 = \langle e_{2,n}, e_{n,2}\rangle * (\Delta_{G_{n-1}}/\{e_{1,2}, e_{1,n-1}\}) \\
&\to \Delta_4 = \langle e_{2,n}, e_{n,2}\rangle * (\Delta_{G_{n-1}}/\{e_{1,2}, e_{1,n-1}\})/\{e_{2,1}, e_{n-1,1}\} \\
&\overset{(ii)}{\cong} \langle e_{2,n}, e_{n,2}\rangle * \Delta_{K_{2,n-3}} \overset{(i)}{\cong} \langle e_{2,n}, e_{n,2}\rangle * \langle e_{2,n-1}, e_{n-1,2}\rangle * \Delta_{G_{n-2}} \\
&\qquad\qquad \vdots \\
\Delta_{2n} &\overset{(ii)}{\cong} \langle e_{2,n}, e_{n,2}\rangle * \cdots * \langle e_{2,4}, e_{4,2}\rangle * \Delta_{K_{2,1}} \cong \Diamond_{n-2},
\end{aligned}$$

where the last isomorphism holds as $\Delta_{K_{2,1}} \cong \Diamond_1$, and the $(n-3)$-fold suspension over $\Diamond_1$ is isomorphic to $\Diamond_{n-2}$. It follows from Lemma 4.3.2 that all complexes in this sequence are flag. Moreover, the proof of Lemma 4.3.2 (ii) shows that the links of the contracted edges need to satisfy the link condition, implying that all complexes in the sequence are triangulations of spheres (see [LN16, Section 6] and [Nev07]). Since the link of a simplex in a flag sphere is again a flag sphere, and $\gamma_1 \geq 0$ for all flag spheres [Gal05; Mes03], a double application of (4.11) together with Theorem 4.2.12 implies that $\gamma_1 = 0$ for every link of an edge that is contracted. As the only flag spheres with $\gamma_1 = 0$ are the boundaries of cross-polytopes (see [Gal05; Mes03]), (iii) follows.

The "Moreover"-statement follows from the above sequence of contractions and the fact that adding a leaf to a graph corresponds to taking the suspension of the corresponding symmetric edge polytope.

Finally, assume G is not 2-connected. Let $G = H_1 \cup \cdots \cup H_k$ be its decomposition in the 2-connected components H_i. Then $\Delta_G = \Delta_{H_1} * \cdots * \Delta_{H_k}$. Corollary 4.2.13 implies that there exists at most one i such that H_i is not a single edge. If all H_i are edges, then $\mathcal{P}_G$ is a cross-polytope and there is nothing to show in this case. Otherwise, without loss of generality, we can assume that H_1 is not an edge. It follows from the above proof and Example 4.3.3 that H_1 admits edge contractions as required. As all $\mathcal{P}_{H_i}$ are line segments for any $2 \le i \le k$ and since edge contractions and taking links commute with taking joins, the claim follows. □

4.4 Symmetric edge polytopes for Erdős-Rényi random graphs

In this section, we consider symmetric edge polytopes for random graphs generated by the Erdős-Rényi model. The ultimate goal is to prove the following main results:

Theorem A (Theorems 4.4.5 and 4.4.12)**.** *Let k be a positive integer. For the Erdős-Rényi model $G(n, p(n))$, where $p(n) = n^{-\beta}$ for some $\beta > 0$, $\beta \neq 1$, the following statements hold:*

- (subcritical regime) *if $\beta > 1$, then asymptotically almost surely $\gamma_\ell = 0$ for all $\ell \geq 1$;*
- (supercritical regime) *if $0 < \beta < 1$, then asymptotically almost surely $\gamma_\ell \in \Theta(n^{(2-\beta)\ell})$ for every $0 < \ell \leq k$.*

We try to keep this section self-contained and tailored for a reader without much knowledge of random graphs. However, we recommend [AS16; Bol01] and [FK16] for more background on Erdős-Rényi random graphs.

4.4.1 Edges and cycles in Erdős-Rényi graphs

We write $G(n,p)$ for the Erdős-Rényi probability model of random graphs on vertex set $[n]$, where edges are chosen independently with probability $p \in [0,1]$. Usually, $p : \mathbb{N} \to [0,1]$ is a function depending on n that tends to 0 at some rate as n goes to infinity. For ease of notation, we mostly just write p. We will say that a graph property $\mathcal{A}$, i.e., a family of graphs closed under isomorphism, holds *asymptotically almost surely* (a.a.s. for short) or *with high probability* if the probability that $G \in G(n,p)$ has property $\mathcal{A}$ tends to 1 as n goes to infinity, i.e.,

$$\lim_{n\to\infty} \mathbb{P}(G \in \mathcal{A}) = 1 \qquad \text{for } G \in G(n,p).$$

In the following, given $G \in G(n,p)$, we will consider the symmetric edge polytope $\mathcal{P}_G$ of G. It follows from (4.19) and Lemma 4.1.1 that the γ-vector of $\mathcal{P}_G$ is independent of the vertex and edge labels of G. Hence, in particular, properties such as $\gamma(\mathcal{P}_G)$ being non-negative or exhibiting a certain growth are graph properties as defined above. For the study of $\gamma_k(\mathcal{P}_G)$, the key idea is that its growth is governed by the number of cycles of length at most $2k$ in G. Therefore, we will take a detour through studying the number of cycles of length smaller than or equal to $2k$ in G for $G \in G(n,p)$. Most of the results we need can be found somewhere in the literature (most often in more general form) and are probably well-known to the stochastics community.

We start by considering the number $X_E(G)$ of edges of $G \in G(n,p)$. This random variable is highly concentrated around its expectation.

Lemma 4.4.1. *(i)* $\mathbb{E}(X_E) = \binom{n}{2}p$,

(ii) $\mathrm{Var}(X_E) = \binom{n}{2}(p - p^2)$,

(iii) $\lim_{n\to\infty} \mathbb{P}(|X_E - \mathbb{E}(X_E)| \leq A\mathbb{E}(X_E)) = 1$ *for any* $A \in \mathbb{R}_{>0}$ *and* $p(n) = n^{-\beta}$ *with* $0 \leq \beta \leq 1$.

Proof. (i) and (ii) follow from an easy computation. For (iii) Chebyshev's inequality implies

$$\mathbb{P}(|X_E - \mathbb{E}(X_E)| > A\mathbb{E}(X_E)) \leq \frac{\mathrm{Var}(X_E)}{A^2\mathbb{E}(X_E)^2} = \frac{p - p^2}{A^2\binom{n}{2}p^2} \leq \frac{1}{Bn^{2-\beta}},$$

where $B \in \mathbb{R}$ is a positive constant. Since $\beta \leq 1$, the above expression tends to 0 as n goes to infinity, which shows the claim. □

For $G \in G(n,p)$ and $k \in \mathbb{N}$, we denote by $X_k(G)$ and $X(G)$ the number of k-cycles and cycles of any length in G, respectively. If G is clear from context, we use X_k and X, respectively. Moreover, based on the following lemma (see e.g. [FK16, Theorem 5.3]) we will divide our study of $\gamma_\ell(\mathcal{P}_G)$, where $G \in G(n,p)$, into two cases.

Lemma 4.4.2. *Let* $k \geq 3$ *and let* $G \in G(n,p)$*. Then*

$$\lim_{n\to\infty} \mathbb{P}(X_k > 0) = \begin{cases} 0 & \text{if } \lim_{n\to\infty} np(n) = 0 \\ 1 & \text{if } \lim_{n\to\infty} np(n) = \infty. \end{cases}.$$

In the following sections, we will distinguish between

- the *subcritical* regime, i.e., $\lim_{n\to\infty} np(n) = 0$,
- the *supercritical* regime, i.e., $\lim_{n\to\infty} np(n) = \infty$.

4.4.2 The subcritical regime

We start by proving a strengthening of Lemma 4.4.2.

Lemma 4.4.3. *Let* $G \in G(n,p)$ *and* $p(n)$ *be such that* $\lim_{n\to\infty} np(n) = 0$*. Then*

$$\lim_{n\to\infty} \mathbb{P}(X > 0) = 0.$$

Proof. By Markov's inequality we have

$$\mathbb{P}(X \geq 1) \leq \mathbb{E}(X). \tag{4.14}$$

For an ℓ-cycle C in K_n, let X_C be the indicator variable on $G(n,p)$ with $X_C(G) = 1$ if $C \subseteq G$ and $X_C(G) = 0$, otherwise. Then $\mathbb{E}(X_C) = \mathbb{P}(X_C = 1) = p^\ell$ and since there are $\binom{n}{\ell}$ ways to choose ℓ vertices in K_n out of which $\frac{(\ell-1)!}{2}$ different cycles can be built, we conclude

$$\mathbb{E}(X_\ell) = \binom{n}{\ell}\frac{(\ell-1)!}{2}p^\ell. \tag{4.15}$$

Using the linearity of expectation and (4.14), we further obtain

$$\mathbb{P}(X > 0) \leq \sum_{\ell=3}^{n} \mathbb{E}(X_\ell) = \sum_{\ell=3}^{n} \binom{n}{\ell}\frac{(\ell-1)!}{2}p^\ell \leq \frac{1}{2}\sum_{\ell=3}^{n} \frac{(pn)^\ell}{\ell} \leq \frac{1}{2}\sum_{\ell=1}^{\infty} \frac{(pn)^\ell}{\ell}$$

As $\lim_{n\to\infty} np(n) = 0$, we have $0 < np(n) < 1$ for n large enough and hence the above series is convergent and equals $-\ln(1-pn)$. Taking the limit we obtain

$$\lim_{n\to\infty} \mathbb{P}(X > 0) \le \lim_{n\to\infty} -\ln(1-pn) = -\ln(1) = 0.$$

□

Remark 4.4.4. *We want to point out that Lemma 4.4.3 implies that, in the subcritical regime, a.a.s. the symmetric edge polytope is a free sum of cross-polytopes, the number of summands being the number of components of the graph, and as such a cross-polytope itself.*

The next theorem describes the behavior of the γ-vector in the subcritical regime.

Theorem 4.4.5. *Let $G \in G(n,p)$ and $p(n)$ be such that $\lim_{n\to\infty} np(n) = 0$. Then*

$$\lim_{n\to\infty} \mathbb{P}(\gamma_k(\mathcal{P}_G) = 0 \textit{ for all } k \ge 1) = 1.$$

Proof. Lemma 4.4.3 implies that a.a.s. $G \in G(n,p)$ is a forest. As the γ-vector of the symmetric edge polytope of a forest equals $(1,0,\dots,0)$, the claim follows. □

4.4.3 The supercritical regime

We now consider the situation where $\lim_{n\to\infty} np(n) = \infty$. We start by computing the variance of the number X_k of k-cycles.

Proposition 4.4.6. *Let $G \in G(n,p)$ and $p(n)$ be such that $\lim_{n\to\infty} np(n) = \infty$. For $k \in \mathbb{N}$, $k \ge 3$ and n large enough we have*

$$\mathrm{Var}(X_k) \le A \cdot \mathbb{E}(X_k)^2 \cdot (np(n))^{-1},$$

where $A \in \mathbb{R}$ is a positive constant.

Proof. We need to compute $\mathrm{Var}(X_k) = \mathbb{E}(X_k^2) - \mathbb{E}(X_k)^2$. As in the proof of Lemma 4.4.3, for a k-cycle $C \subseteq K_n$, we denote by X_C the corresponding indicator variable. Moreover, we use $\mathcal{H}$ to denote the set of all k-cycles in K_n. By linearity of expectation, it follows that

$$\mathbb{E}(X_k^2) = \sum_{C,C'\in\mathcal{H}} \mathbb{E}(X_C \cdot X_{C'}) = \sum_{C,C'\in\mathcal{H}} p^{2k-|E(C\cap C')|} \le \sum_{C,C'\in\mathcal{H}} p^{2k-|V(C\cap C')|}, \tag{4.16}$$

where for the last inequality we use that $C \cap C'$ is a subgraph of a cycle and hence $|E(C\cap C')| \le |V(C\cap C')|$. For $0 \le \ell \le k$, we set $\mathcal{H}_\ell = \{(C,C') \in \mathcal{H}^2 \,:\, |V(C\cap C')| = \ell\}$. If $(C,C') \in \mathcal{H}_0$, the random variables X_C and $X_{C'}$ are independent and we have

$$\begin{aligned}\sum_{(C,C')\in\mathcal{H}_0} \mathbb{P}(C\cup C' \subseteq G) &= \sum_{(C,C')\in\mathcal{H}_0} \mathbb{P}(C\subseteq G)\mathbb{P}(C'\subseteq G)\\ &\le \left(\sum_{C\in\mathcal{H}} \mathbb{P}(C\subseteq G)\right)\left(\sum_{C\in\mathcal{H}} \mathbb{P}(C\subseteq G)\right) = \mathbb{E}(X_k)^2.\end{aligned}$$

For $\ell \ge 1$ a simple counting argument shows that

$$|\mathcal{H}_\ell| = \binom{n}{k}\frac{(k-1)!}{2}\binom{k}{\ell}\binom{n-k}{k-\ell}\frac{(k-1)!}{2}.$$

This together with (4.16) yields

$$
\begin{aligned}
\mathbb{E}(X_k^2) &\le \mathbb{E}(X_k)^2 + \sum_{\ell=1}^{k} \binom{n}{k} \frac{(k-1)!}{2} \binom{k}{\ell} \binom{n-k}{k-\ell} \frac{(k-1)!}{2} p^{2k-\ell} \\
&= \mathbb{E}(X_k)^2 + \binom{n}{k} \frac{(k-1)!}{2} p^k \sum_{\ell=1}^{k} \binom{k}{\ell} \binom{n-k}{k-\ell} \frac{(k-1)!}{2} p^{k-\ell} \\
&\le \mathbb{E}(X_k)^2 + \mathbb{E}(X_k) \sum_{\ell=1}^{k} A_{1,\ell} \binom{k}{\ell} n^{k-\ell} \frac{(k-1)!}{2} n^{\ell} p^k (np)^{-\ell} \\
&\le \mathbb{E}(X_k)^2 + \mathbb{E}(X_k) \sum_{\ell=1}^{k} A_{2,\ell} \binom{k}{\ell} \binom{n}{k} \frac{(k-1)!}{2} p^k (np)^{-\ell} \\
&= \mathbb{E}(X_k)^2 + \mathbb{E}(X_k) \sum_{\ell=1}^{k} A_{2,\ell} \binom{k}{\ell} \mathbb{E}(X_k) (np)^{-\ell} \\
&= \mathbb{E}(X_k)^2 + \mathbb{E}(X_k)^2 \sum_{\ell=1}^{k} A_{2,\ell} \binom{k}{\ell} (np)^{-\ell},
\end{aligned}
$$

where $A_{1,\ell}, A_{2,\ell} \in \mathbb{R}$ are positive constants. If $\lim_{n\to\infty} np(n) = \infty$, then $(np)^{-\ell} \le (np)^{-1}$ for large n and hence

$$
\mathbb{E}(X_k^2) \le \mathbb{E}(X_k)^2 + \mathbb{E}(X_k)^2 \sum_{\ell=1}^{k} A_{2,\ell} \binom{k}{\ell} (np)^{-1} = \mathbb{E}(X_k)^2 + \mathbb{E}(X_k)^2 \cdot A \cdot (np)^{-1}
$$

for large n, where $A = \sum_{\ell=1}^{k} A_{2,\ell} \binom{k}{\ell}$. The claim now follows from the definition of the variance. □

Using Chebyshev's inequality, Proposition 4.4.6 implies the following concentration inequalities for X_k.

Corollary 4.4.7. *Let $G \in G(n,p)$ and $p(n)$ be such that $\lim_{n\to\infty} np(n) = \infty$. For $k \in \mathbb{N}$, $k \ge 3$ and $A \in \mathbb{R}_{>0}$ we have*

$$
\lim_{n\to\infty} \mathbb{P}(|X_k - \mathbb{E}(X_k)| \le A\mathbb{E}(X_k)) = 1.
$$

In the following, we assume that $p(n) = n^{-\beta}$ for some $0 < \beta < 1$. Using Corollary 4.4.7, we show different concentration inequalities which are more convenient for our purposes.

Lemma 4.4.8. *Let $G \in G(n,p)$, $0 < \beta < 1$, $p(n) = n^{-\beta}$, $\alpha = \min(\frac{1}{2}, \frac{\beta}{2-\beta})$ and $k \in \mathbb{N}$, $k \ge 3$. Then for $A \in \mathbb{R}_{>0}$ large enough, we have*

$$
\lim_{n\to\infty} \mathbb{P}\left(\frac{1}{2}\mathbb{E}(X_\ell) \le X_\ell \le A\mathbb{E}(X_E)^{\lceil \ell/2 \rceil - \alpha} \text{ for all } 3 \le \ell \le k\right) = 1.
$$

Proof. We note, it suffices to show the existence of some constant A satisfying the claimed statement, since then every $A' \ge A$ satisfies it, as well.

By (4.15) and Lemma 4.4.1, for n large enough, it holds that

$$
\begin{aligned}
\mathbb{E}(X_{2\ell}) \le& A_1 \left(\binom{n}{2} p\right)^{\ell} p^{\ell} = A_1 \mathbb{E}(X_E)^{\ell} (n^{2-\beta})^{\frac{-\beta\ell}{2-\beta}} \\
\le& A_2 \mathbb{E}(X_E)^{\ell} \left(\binom{n}{2} p\right)^{\frac{-\beta\ell}{2-\beta}} \le A_2 \mathbb{E}(X_E)^{\ell} \cdot \mathbb{E}(X_E)^{\frac{-\beta}{2-\beta}} \le A_2 \mathbb{E}(X_E)^{\ell-\alpha},
\end{aligned}
$$

where for the last two inequalities we use that $\mathbb{E}(X_E) \geq 1$ for n large enough and $A_1, A_2 \in \mathbb{R}$ are positive constants. This yields for $A \in \mathbb{R}_{>0}$ and n large enough

$$\mathbb{P}(X_{2\ell} < (1+A)\mathbb{E}(X_{2\ell})) \leq \mathbb{P}(X_{2\ell} < (1+A)A_2\mathbb{E}(X_E)^{\ell-\alpha}).$$

Setting $A_3 = (1+A)A_2$, we infer from Corollary 4.4.7 that

$$\lim_{n\to\infty} \mathbb{P}(X_{2\ell} < A_3\mathbb{E}(X_E)^{\ell-\alpha}) = 1.$$

Since, again by Corollary 4.4.7,

$$\lim_{n\to\infty} \mathbb{P}(X_{2\ell} < \frac{1}{2}\mathbb{E}(X_{2\ell})) \leq \lim_{n\to\infty} \mathbb{P}(|X_{2\ell} - \mathbb{E}(X_{2\ell})| > \frac{1}{2}\mathbb{E}(X_{2\ell})) = 0,$$

we obtain

$$\lim_{n\to\infty} \mathbb{P}(X_{2\ell} < \frac{1}{2}\mathbb{E}(X_{2\ell}) \text{ or } X_{2\ell} > A_3\mathbb{E}(X_E)^{\ell-\alpha}) = 0. \tag{4.17}$$

For odd cycles, a similar computation as for even cycles shows that for n large enough

$$\mathbb{E}(X_{2\ell-1}) \leq A_4 \cdot \mathbb{E}(X_E)^{\ell-\frac{1}{2}} \cdot n^{-\beta\ell+\frac{1}{2}\beta} \leq A_4 \cdot \mathbb{E}(X_E)^{\ell-\frac{1}{2}} \leq A_4 \cdot \mathbb{E}(X_E)^{\ell-\alpha},$$

where $A_4 \in \mathbb{R}$ is a positive constant and for the last inequality we use that $\mathbb{E}(X_E) \geq 1$ for n large enough. Almost the same argument as for even cycles implies

$$\lim_{n\to\infty} \mathbb{P}(X_{2\ell-1} < \frac{1}{2}\mathbb{E}(X_{2\ell-1}) \text{ or } X_{2\ell-1} > A_4\mathbb{E}(X_E)^{\ell-\alpha}) = 0. \tag{4.18}$$

Combining (4.17) and (4.18), we finally get

$$\begin{aligned}
&\lim_{n\to\infty} \mathbb{P}\left(\frac{1}{2}\mathbb{E}(X_\ell) \leq X_\ell \leq A\mathbb{E}(X_E)^{\lceil \ell/2\rceil-\alpha} \text{ for all } 3 \leq \ell \leq k\right) \\
&\geq 1 - \sum_{\ell=3}^{k} \lim_{n\to\infty} \mathbb{P}(X_\ell < \frac{1}{2}\mathbb{E}(X_\ell) \text{ or } X_\ell > A\mathbb{E}(X_E)^{\lceil \frac{\ell}{2}\rceil-\alpha}) = 1,
\end{aligned}$$

where A is taken as the maximal constant appearing in (4.17) and (4.18) for $3 \leq \ell \leq k$. $\square$

To get information about the γ-vector of the symmetric edge polytope of a random graph $G \in G(n,p)$, we want to use Lemma 4.1.1. The first part of our strategy consists in turning the concentration inequalities of Lemma 4.4.8 into concentration inequalities for the number of non-faces and faces of bounded cardinality. In a second step, we use the latter to infer concentration inequalities for the γ-vector up to a fixed entry. We now make this idea more precise. Given a graph G on n vertices, we let Δ_G be a unimodular triangulation of $\partial\mathcal{P}_G$ as described in Lemma 4.1.1. Since $\mathcal{P}_G$ is reflexive and Δ_G is unimodular, we have $h_j^*(\mathcal{P}_G) = h_j(\Delta_G)$ for every j. Using the symmetry of $h(\Delta_G)$ and the definition of the γ-vector, we further know

$$\sum_{i=0}^{\lfloor \frac{\dim \mathcal{P}_G}{2}\rfloor} \gamma_i(\mathcal{P}_G)t^i(t+1)^{\dim \mathcal{P}_G - 2i} = \sum_{j=0}^{\dim \mathcal{P}_G} h_j^*(\mathcal{P}_G)t^{\dim \mathcal{P}_G - j}.$$

The usual relation between the f- and h-vector of a simplicial complex together with the substitution of t by $t+1$ implies

$$\sum_{j=0}^{\dim \mathcal{P}_G} f_{j-1}(\Delta_G) t^{\dim \mathcal{P}_G - j} = \sum_{i=0}^{\lfloor \frac{\dim \mathcal{P}_G}{2} \rfloor} \gamma_i(\mathcal{P}_G)(t+1)^i (t+2)^{\dim \mathcal{P}_G - 2i}.$$

Note, with increasing index i the degree of each summand on the right is decreasing. Thus, the last summand which contributes to the coefficient of $t^{\dim \mathcal{P}_G - k}$ is when $i = k$. For a polynomial $p(t)$, we denote by $[t^i]p(t)$ the coefficient of t^i in $p(t)$. In particular, evaluating the coefficient of $t^{\dim \mathcal{P}_G - k}$ yields

$$\gamma_k(\mathcal{P}_G) = f_{k-1}(\Delta_G) - [t^{\dim \mathcal{P}_G - k}] \sum_{i=0}^{k-1} \gamma_i(\mathcal{P}_G)(t+1)^i (t+2)^{\dim \mathcal{P}_G - 2i}. \tag{4.19}$$

In order to be able to make sense out of (4.19), we need to know what the dimension of $\mathcal{P}_G$ is for "most" Erdős-Rényi graphs $G \in G(n,p)$ in the supercritical regime. Denoting by $X_{\dim \mathcal{P}}$ the corresponding random variable, we have:

Lemma 4.4.9. *Let $G \in G(n,p)$, $0 < \beta < 1$ and $p(n) = n^{-\beta}$. Then we have*

$$\lim_{n\to\infty} \mathbb{P}(X_{\dim \mathcal{P}_G} = n-1) = 1.$$

Proof. Since for any graph G on n vertices $\dim \mathcal{P}_G = n-1$ if and only if G is connected, the result follows e.g. from [FK16, Theorem 4.1] using the fact that $n^{-\beta}$ grows faster than $\frac{\log(n)}{n}$ for any $0 < \beta < 1$. □

In order to use (4.19) to show concentration inequalities for the γ-vector of $\mathcal{P}_G$, we need to study the random variables f_{k-1} or equivalently the number of non-faces of Δ_G. For $G \in G(n,p)$, we denote by $n_{k-1}(G)$ the number of $(k-1)$-dimensional non-faces of Δ_G that do not contain antipodal vertices. Note that $n_1(G)$ equals the number of bad pairs of G as in Section 4.2.

Theorem 4.4.10. *Let $G \in G(n,p)$, $0 < \beta < 1$, $p(n) = n^{-\beta}$, $\alpha = \min(\frac{1}{2}, \frac{\beta}{2-\beta})$ and $k \in \mathbb{N}$, $k \geq 1$. Then for $B \in \mathbb{R}_{>0}$ large enough, we have*

$$\lim_{n\to\infty} \mathbb{P}(n_{\ell-1} \leq B\mathbb{E}(X_E)^{\ell-\alpha} \text{ for all } 2 \leq \ell \leq k+1) = 1.$$

Proof. As in the proof of Lemma 4.4.8, it suffices to show the existence of some constant B satisfying the claimed statement.

Let $G \in G(n,p)$ and let $2 \leq \ell \leq k+1$. On the one hand, any $(\ell-1)$-non-face of Δ_G contains a minimal (not necessarily unique) r-non-face of Δ_G for some $1 \leq r \leq \ell-1$. On the other hand, any such minimal r-non-face of Δ_G can be extended to an $(\ell-1)$-non-face of Δ_G by adding $\ell-1-r$ non-antipodal vertices to it, for which there are $\binom{X_E(G)-(r+1)}{\ell-1-r} \cdot 2^{\ell-1-r}$ possibilities. Hence, denoting by $N_r(G)$ the number of minimal r-non-faces of Δ_G, we conclude

$$n_{\ell-1}(G) \leq \sum_{r=1}^{\ell-1} \binom{X_E(G)-(r+1)}{\ell-1-r} \cdot 2^{\ell-1-r} \cdot N_r(G) \leq \sum_{r=2}^{\ell} B_{r,\ell} X_E(G)^{\ell-r} N_{r-1}(G),$$

where $B_{r,\ell} \in \mathbb{R}$ are positive constants. Let $A_1 \in \mathbb{R}$ such that Lemma 4.4.8 holds. As, by Lemma 4.1.1, for $G \in G(n,p)$ we have $N_{r-1}(G) \leq 2 \cdot \binom{2r-1}{r}(X_{2r}(G) + X_{2r-1}(G))$, it follows that

$$\begin{aligned} & \mathbb{P}\left(N_{r-1} \leq 4 \cdot \binom{2r-1}{r} \cdot A_1 \cdot \mathbb{E}(X_E)^{r-\alpha}\right) \\ \geq\ & \mathbb{P}\left(X_{2r} \leq A_1 \mathbb{E}(X_E)^{r-\alpha} \text{ and } X_{2r-1} \leq A_1 \mathbb{E}(X_E)^{r-\alpha}\right). \end{aligned}$$

By the choice of A_1, we have $\lim_{n\to\infty} \mathbb{P}(N_{r-1} \leq 4 \cdot \binom{2r-1}{r} \cdot A_1 \cdot \mathbb{E}(X_E)^{r-\alpha}) = 1$. As, by Lemma 4.4.1 (iii), we also have $\lim_{n\to\infty} \mathbb{P}(X_E \leq (1+A_2)\mathbb{E}(X_E)) = 1$ for any $A_2 \in \mathbb{R}_{>0}$, we conclude that a.a.s. it holds that

$$\begin{aligned} n_{\ell-1} &\leq \sum_{r=2}^{\ell} B_{r,\ell}(1+A_2)^{\ell-r}\mathbb{E}(X_E)^{\ell-r} \cdot 4 \cdot \binom{2r-1}{r} \cdot A_1 \cdot \mathbb{E}(X_E)^{r-\alpha} \\ &= \left(\sum_{r=2}^{\ell} B_{r,\ell}(1+A_2)^{\ell-r} \cdot 4 \cdot \binom{2r-1}{r} \cdot A_1 \right) \mathbb{E}(X_E)^{\ell-\alpha} = B \cdot \mathbb{E}(X_E)^{\ell-\alpha} \end{aligned}$$

with $B = \sum_{r=2}^{\ell} B_{r,\ell}(1+A_2)^{\ell-r} \cdot 4 \cdot \binom{2r-1}{r} \cdot A_1$. The claim follows. □

For $G \in G(n,p)$ we denote by $f_{k-1}(G)$ the number of $(k-1)$-faces of Δ_G. From Theorem 4.4.10, we can deduce concentration inequalities for these random variables.

Theorem 4.4.11. *Let $0 < \beta < 1$, $p(n) = n^{-\beta}$, $\alpha = \min(\frac{1}{2}, \frac{\beta}{2-\beta})$ and $k \in \mathbb{N}$, $k \geq 1$. Then for $G \in G(n,p)$ and $\epsilon > 0$ and $B \in \mathbb{R}_{>0}$ large enough, we have*

$$\lim_{n\to\infty} \mathbb{P}\left(2^{\ell-\epsilon}\binom{\mathbb{E}(X_E)}{\ell} - B\mathbb{E}(X_E)^{\ell-\alpha} \leq f_{\ell-1} \leq 2^{\ell+\epsilon}\binom{\mathbb{E}(X_E)}{\ell} \text{ for all } 1 \leq \ell \leq k \right) = 1.$$

In particular,

$$\lim_{n\to\infty} \mathbb{P}\left(f_{\ell-1} \in \Theta(n^{(2-\beta)\ell}) \text{ for all } 1 \leq \ell \leq k \right) = 1. \tag{4.20}$$

Proof. The statement trivially holds for $k=1$ since $f_0 = 2X_E$. Let $k \geq 2$ and $1 \leq \ell \leq k$. For $G \in G(n,p)$, we have

$$f_{\ell-1}(G) = 2^{\ell}\binom{X_E(G)}{\ell} - n_{\ell-1}(G).$$

Let $0 < A_1 < 1$ be such that $\binom{(1-A_1)\mathbb{E}(X_E)}{\ell} = 2^{-\epsilon}\binom{\mathbb{E}(X_E)}{\ell}$.

It follows from Theorem 4.4.10 and Lemma 4.4.1 (iii) that for large enough $B \in \mathbb{R}_{>0}$

$$\lim_{n\to\infty} \mathbb{P}\left(f_{\ell-1} \geq 2^{\ell-\epsilon}\binom{\mathbb{E}(X_E)}{\ell} - B\mathbb{E}(X_E)^{\ell-\alpha} \right) = 1. \tag{4.21}$$

Finally, let $A_2 > 0$ be such that $\binom{(1+A_2)\mathbb{E}(X_E)}{\ell} = 2^{\epsilon}\binom{\mathbb{E}(X_E)}{\ell}$. As for $G \in G(n,p)$ the triangulation Δ_G is a subcomplex of a cross-polytope of dimension $X_E(G)$, we can bound $f_{\ell-1}(G)$ from above by $2^{\ell}\binom{X_E(G)}{\ell}$. Using Lemma 4.4.1 (iii), we conclude that

$$\lim_{n\to\infty} \mathbb{P}\left(f_{\ell-1} \leq 2^{\ell+\epsilon}\binom{\mathbb{E}(X_E)}{\ell} \right) = 1. \tag{4.22}$$

Combining (4.21) and (4.22) for any $1 \leq \ell \leq k$ finishes the proof of the first statement.

For the "In particular"-part it suffices to note that, since $\mathbb{E}(X_E) \in \Theta(n^{2-\beta})$, the upper and lower bounds for $f_{\ell-1}$ both lie in $\Theta(n^{(2-\beta)\ell})$. □

We are now ready to state the main result of this subsection.

Theorem 4.4.12. *Let $0 < \beta < 1$, $p(n) = n^{-\beta}$ and $k \in \mathbb{N}$. Then for $G \in G(n,p)$,*

$$\lim_{n\to\infty} \mathbb{P}(\gamma_\ell(\mathcal{P}_G) \in \Theta(n^{(2-\beta)\ell}) \text{ for all } 0 \leq \ell \leq k) = 1.$$

Proof. We show the statement by induction on k. Since $\gamma_0 = 1$ is constant, the statement holds for $k = 0$.

Now assume $k \geq 1$. Since by the induction hypothesis we have

$$\lim_{n\to\infty} \mathbb{P}(\gamma_\ell \geq 0 \text{ for all } 0 \leq \ell \leq k-1) = 1, \tag{4.23}$$

it follows from (4.19) that

$$\lim_{n\to\infty} \mathbb{P}(\gamma_\ell \leq f_{\ell-1} \text{ for all } 0 \leq \ell \leq k) = 1. \tag{4.24}$$

Thus, we have an upper bound for γ_ℓ, which a.a.s. lies in $\Theta(n^{(2-\beta)\ell})$ by (4.20). Combining this upper bound with a more detailed analysis of (4.19) will enable us to prove that γ_ℓ can be bounded asymptotically always surely by a lower bound that also lies in $\Theta(n^{(2-\beta)\ell})$. Lemma 4.4.9 implies that $X_{\dim \mathcal{P}} = n-1$ a.a.s.; hence, by (4.24) and (4.19) we have a.a.s.

$$\begin{aligned}\gamma_\ell \geq & f_{\ell-1} - [t^{n-1-\ell}]\sum_{i=0}^{\ell-1} f_{i-1}(t+1)^i(t+2)^{n-1-2i} \\ =& f_{\ell-1} - \sum_{i=0}^{\ell-1} f_{i-1}\left(\sum_{j=n-1-\ell-i}^{n-1-\ell} 2^{n-1-2i-j}\binom{i}{n-1-\ell-j}\binom{n-1-2i}{j}\right).\end{aligned} \tag{4.25}$$

Using Theorem 4.4.11, we conclude that for large enough $B \in \mathbb{R}_{>0}$ it holds a.a.s. that

$$\begin{aligned}\gamma_\ell \quad \geq \quad & 2^{\ell-\epsilon}\binom{\mathbb{E}(X_E)}{\ell} - B\mathbb{E}(X_E)^{\ell-\alpha} \\ & -\sum_{i=0}^{\ell-1} 2^{i+\epsilon}\binom{\mathbb{E}(X_E)}{i}\left(\sum_{j=n-1-\ell-i}^{n-1-\ell} 2^{n-1-2i-j}\binom{i}{n-1-\ell-j}\binom{n-1-2i}{j}\right).\end{aligned}$$

Since for $n \geq 2\ell+1$ one has $n-1-\ell-i \geq \frac{n-1-2i}{2}$, the expression $\binom{n-1-2i}{j}$ in the last sum is maximal for $j = n-1-\ell-i$. As also $2^{n-1-2i-j}$ is maximal in this case and $\binom{i}{n-1-\ell-j} \leq \binom{\ell-1}{\lfloor(\ell-1)/2\rfloor}$ for $0 \leq i \leq \ell-1$ and any j, it follows that a.a.s. γ_ℓ is greater or equal to

$$\begin{aligned}& 2^{\ell-\epsilon}\binom{\mathbb{E}(X_E)}{\ell} - B\mathbb{E}(X_E)^{\ell-\alpha} - \binom{\ell-1}{\lfloor(\ell-1)/2\rfloor}\sum_{i=0}^{\ell-1} 2^{i+\epsilon}\binom{\mathbb{E}(X_E)}{i}(i+1)2^{\ell-i}\binom{n-1-2i}{n-1-\ell-i} \\ =\ & 2^{\ell-\epsilon}\binom{\mathbb{E}(X_E)}{\ell} - B\mathbb{E}(X_E)^{\ell-\alpha} - \binom{\ell-1}{\lfloor(\ell-1)/2\rfloor}\sum_{i=0}^{\ell-1} 2^{\ell+\epsilon}\binom{\mathbb{E}(X_E)}{i}(i+1)\binom{n-1-2i}{\ell-i}.\end{aligned}$$

Analysing the expressions in the last equation, we see that

$$2^{\ell-\epsilon}\binom{\mathbb{E}(X_E)}{\ell} - B\mathbb{E}(X_E)^{\ell-\alpha} \in \Theta(n^{(2-\beta)\ell})$$

and

$$2^{\ell+\epsilon}\binom{\mathbb{E}(X_E)}{i}(i+1)\binom{n-1-2i}{\ell-i} \in \Theta(n^{(2-\beta)i}\cdot n^{\ell-i}) = \Theta(n^{i+\ell-i\beta}).$$

As $(2-\beta)\ell > i+\ell-i\beta$ for $\ell > i$, this implies

$$2^{\ell-\epsilon}\binom{\mathbb{E}(X_E)}{\ell} - B\mathbb{E}(X_E)^{\ell-\alpha} - \sum_{i=0}^{\ell-1} 2^{\ell+\epsilon}\binom{\mathbb{E}(X_E)}{i}(i+1)\binom{n-1-2i}{\ell-i} \in \Theta(n^{(2-\beta)\ell}).$$

As a consequence, we have found that γ_ℓ can a.a.s. be bounded from below by an expression in $\Theta(n^{(2-\beta)\ell})$. Combining this with the previously shown upper bound completes the proof. □

Remark 4.4.13. *It is natural to ask if the results for γ_k we obtained in the subcritical and the supercritical regime (Theorems 4.4.5 and 4.4.12) can be extended to the critical regime, i.e., $p(n) = \frac{c}{n}$ for a constant $c > 0$. Indeed, using that in this regime X_ℓ converges in distribution to a Poisson distribution with mean and variance $\frac{c^\ell}{2\ell}$ (see e.g., [AS16, Theorem 10.1.1]), one can show that X_ℓ is highly concentrated around its mean. More precisely,*

$$\lim_{n\to\infty} \mathbb{P}\left(|X_\ell - \mathbb{E}(X_\ell)| \leq \omega(n)\right) = 1$$

for any arbitrarily slowly increasing function $\omega : \mathbb{N} \to \mathbb{R}$. By similar arguments as in the proof of Theorem 4.4.10, this gives rise to the following concentration inequality for the non-faces:

$$\lim_{n\to\infty} \mathbb{P}(n_{\ell-1} \leq n^\kappa \mathbb{E}(n_{\ell-1})) = 1. \tag{4.26}$$

By the same method as in the proof of Theorem 4.4.11, one can show that

$$\lim_{n\to\infty} \mathbb{P}(f_{\ell-1} \in \Theta(n^\ell)) = 1. \tag{4.27}$$

Unfortunately, the arguments from the proof of Theorem 4.4.12 only allow us to bound the double sum in the second row of (4.25) by an expression in $\Theta(n^\ell)$. Hence, in order to be able to turn (4.27) into concentration inequalities for γ_ℓ, different arguments or at least a more refined analysis including the leading coefficients would be needed. It is reasonable to believe that, analogously to the variety of behaviors of the largest component of an Erdős-Rényi graph (see e.g. [AS16, Chapter 11]), one would also get different behaviors for γ_ℓ depending on whether $c < 1$, $c = 1$ or $c > 1$. We leave this as an open problem.

Chapter 5

Laplacian polytopes of simplicial complexes

It was shown in [BM17] that Laplacian simplices have unimodal h^*-vectors for certain classes of graphs, including trees, odd cycles and complete graphs. Inspired by these results, we study properties of the h^*-vectors of general Laplacian polytopes. This is further motivated by the general question under which conditions a lattice polytope has a unimodal h^*-vector. It was conjectured by Hibi and Ohsugi that this is true for reflexive lattice polytopes that have the integer decomposition property (IDP) [HO06], and, recently, Adiprasito, Papadakis, Petrotou and Steinmeyer could confirm this conjecture in the positive [Adi+22]. However, it is still mysterious what happens if the polytope is not reflexive. We consider this question for the Laplacian polytope $P_{\partial(\sigma_{d+1})}$ of the boundary of the $(d+1)$-simplex. Even in this seemingly most simple situation, $P_{\partial(\sigma_{d+1})}$ turns out to be not reflexive and hence the mentioned results towards unimodality do not apply. However, the following result shows that $P_{\partial(\sigma_{d+1})}$ has at least the integer decomposition property.

Theorem B. *$P_{\partial(\sigma_{d+1})}$ has a regular unimodular triangulation for every integer $d \geq 0$.*

We note that, combined with [Ath04, Theorem 1.3], this result implies that the h^*-vector of $P_{\partial(\sigma_{d+1})}$ is decreasing in its second half which is obviously implied by but weaker than unimodality. The main ingredient for Theorem B is the so-called *interior polytope* of $P_{\partial(\sigma_{d+1})}$, that is defined as the convex hull of the interior lattice points of $P_{\partial(\sigma_{d+1})}$. Indeed, this polytope turns out to be reflexive (after translation to the origin) and miraculously, $P_{\partial(\sigma_{d+1})}$ happens to be the second dilation of it (after translating both polytopes to the origin). Using edgewise subdivisions, we provide an explicit construction of a regular unimodular triangulation for the interior polytope which then extends to such a triangulation of $P_{\partial(\sigma_{d+1})}$ by [Haa+14, Theorem 4.8]. As a byproduct, we can also compute the normalized volume of $P_{\partial(\sigma_{d+1})}$ (see Corollary 5.4.7). Theorem B combined with the results on the interior polytope enables us to show the following statement:

Theorem C. *(a) $h^*\left(P_{\partial(\sigma_{d+1})}; t\right)$ has only real roots if $d \in \mathbb{N}$ is odd.*

(b) $h^*\left(P_{\partial(\sigma_{d+1})}\right)$ is unimodal with peak in the middle for every $d \in \mathbb{N}$.

We note that if d is odd, then the statement in (b) is just an easy consequence of the one in (a). We conjecture (a) to be true also if d is even.

5.1 Laplacian matrices of boundaries of simplices

In this section, we investigate basic properties of the Laplacian matrix of the boundary of a simplex that will be useful for deriving properties of the corresponding Laplacian polytope in Section 5.2.

We start with an easy general statement.

Lemma 5.1.1. *Let Δ be a d-dimensional simplicial complex. Then*

$$\operatorname{rank} \mathcal{L}_d(\Delta) = f_d(\Delta) - \dim_{\mathbb{Q}} H_d(\Delta;\mathbb{Q}).$$

Proof. We have the following chain of equalities:

$$\operatorname{rank} \mathcal{L}_d(\Delta) = \operatorname{rank}(\partial_d^\top \partial_d) = f_d(\Delta) - \dim_{\mathbb{Q}} \ker(\partial_d^\top \partial_d) = f_d(\Delta) - \dim_{\mathbb{Q}} \ker(\partial_d),$$

where the last equality follows from the fact that $\ker(\partial_d) = \ker(\partial_d^\top \partial_d)$. Since $\dim \Delta = d$, we also have $H_d(\Delta;\mathbb{Q}) = \ker(\partial_d)$, which shows the claim. □

Let $F_i = [d+2] \smallsetminus \{d+3-i\}$ for $1 \le i \le d+2$ and order the columns and rows of $\mathcal{L}_d(\partial(\sigma_{d+1}))$ according to $F_1, \ldots, F_{d+2}$. We first provide an explicit description of the d^{th} Laplacian matrix in this case.

Theorem 5.1.2. *Let $\Delta = \partial(\sigma_{d+1})$. Then $\mathcal{L}_d(\Delta) \in \mathbb{Z}^{(d+2)\times(d+2)}$, $\mathcal{L}_0(\Delta) = \begin{pmatrix} 0 & 0 \\ 0 & 0 \end{pmatrix}$ and, for $d \ge 1$, $1 \le i,j \le d+2$, we have*

$$\mathcal{L}_d(\Delta)_{ij} = \begin{cases} d+1, & \textit{if } i = j, \\ (-1)^{i+j-1}, & \textit{otherwise.} \end{cases}$$

Proof. Since $f_d(\partial(\sigma_{d+1})) = d+2$, we have $\mathcal{L}_d(\Delta) \in \mathbb{Z}^{(d+2)\times(d+2)}$.

Assume $d = 0$. As ∂_0 is the zero map, the statement is immediate.

Now let $d \ge 1$. Since $\dim \Delta = d$, it follows that $\deg_U(F) = 0$ for any d-face F of Δ. Using Theorem 1.2.2, this implies that $\mathcal{L}_d(\Delta)_{ii} = d+1$ for all $1 \le i \le d+2$.

Now, let $i \ne j$. Since $\mathcal{L}_d(\Delta)$ is symmetric, we can assume that $i < j$. F_i and F_j have the common lower simplex $F_i \cap F_j = [d+2] \smallsetminus \{d+3-i, d+3-j\} \ne \varnothing$. By Equation (1.3), $e_{F_i \cap F_j}$ appears with sign $(-1)^{d+2-j}$ in $\partial_d(e_{[d+2]\smallsetminus\{d+3-i\}})$ and it appears with sign $(-1)^{d+1-i}$ in $\partial_d(e_{[d+2]\smallsetminus\{d+3-j\}})$. These signs coincide, meaning that $F_i \cap F_j$ is a similar common lower simplex of F_i and F_j, if and only if $i+j$ is odd. The claim follows from Theorem 1.2.2. □

The next two lemmata will be crucial for determining the dimension of the Laplacian polytope of $\partial(\sigma_{d+1})$ in Proposition 5.2.6.

Lemma 5.1.3. *Let $\Delta = \partial(\sigma_{d+1})$. Then $\mathcal{L}_d(\Delta)$ has rank $d+1$ and every $(d+1)$-element subset of the columns (resp. rows) of $\mathcal{L}_d(\Delta)$ is linearly independent.*

Proof. The first statement follows from Lemma 5.1.1 and the fact that $H_d(\Delta;\mathbb{Q}) = \mathbb{Q}$. Let $1 \le i \le d+2$. Let A_i be the $(d+1)\times(d+1)$-matrix obtained from $\mathcal{L}_d(\Delta)$ by removing the i^{th} row and column. By definition, $A_i = \mathcal{L}_d(\Delta \smallsetminus \{F_i\})$. Since $H_d(\Delta \smallsetminus \{F_i\}), \mathbb{Q}) = 0$, by Lemma 5.1.1 again, this matrix has full rank. As adding any extra row or column to A_i does not change the rank, the claim follows.

□

Lemma 5.1.4. *Let $\Delta = \partial(\sigma_{d+1})$. Then*

$$\operatorname{rank} \begin{pmatrix} \mathcal{L}_d(\Delta) \\ 1 \cdots 1 \end{pmatrix} = \begin{cases} d+1, & \textit{if } d \textit{ is even,} \\ d+2, & \textit{if } d \textit{ is odd.} \end{cases}$$

Proof. First assume that d is even. We define $\lambda = (\lambda_1, ..., \lambda_{d+2})^\top \in \mathbb{R}^{d+2}$ by

$$\lambda_j = \begin{cases} 0, & \text{if } j \text{ is odd,} \\ \frac{2}{d+2}, & \text{if } j \text{ is even.} \end{cases}$$

Using Theorem 5.1.2, it is straight-forward to verify that $\mathcal{L}_d(\Delta) \cdot \lambda = \mathbb{1}$, which, combined with Lemma 5.1.3, shows the claim.

Now, let d be odd and assume by contradiction that $\operatorname{rank}\begin{pmatrix}\mathcal{L}_d(\Delta) \\ 1\cdots 1\end{pmatrix} < d+2$. Lemma 5.1.1 and Lemma 5.1.3 imply that $\operatorname{rank}\begin{pmatrix}\mathcal{L}_d(\Delta) \\ 1\cdots 1\end{pmatrix} = \operatorname{rank}\mathcal{L}_d(\Delta)$. Hence, there exists $\lambda = (\lambda_1, \ldots, \lambda_{d+2})^\top \in \mathbb{R}^{d+2}$, such that $\mathcal{L}_d(\Delta) \cdot \lambda = \mathbb{1}$. Let $\mathcal{L}_d(\Delta)_{[d+1]}$ be the matrix obtained from $\mathcal{L}_d(\Delta)$ by deleting the last row. Then we also have $\mathcal{L}_d(\Delta)_{[d+1]} \cdot \lambda = \mathbb{1}$ and it follows from Lemma 5.1.3 that, up to the choice of the last coordinate λ_{d+2}, the vector λ is unique. Indeed, a direct computation shows that, if $\lambda_{d+2} = \mu$ for some $\mu \in \mathbb{R}$, then we must have

$$\lambda_j = \begin{cases} \frac{(d+2)\cdot\mu+1}{d+2}, & \text{if } j \text{ is odd,} \\ \\ -\frac{(d+2)\cdot\mu-1}{d+2}, & \text{if } j \text{ is even.} \end{cases} \tag{5.1}$$

However, denoting by r_{d+2} the last row of $\mathcal{L}_d(\Delta)$, it holds that $r_{d+2} \cdot \lambda = 0 \neq 1$, which yields a contradiction. □

5.2 General properties of Laplacian polytopes

The goal of this section is to generalize Laplacian simplices – as introduced and studied in [BM17; MT18] – that are associated to a graph to arbitrary simplicial complexes and their Laplacian matrices. After stating some basic general properties of what we call Laplacian polytopes, we focus on boundaries of simplices and their highest Laplacians.

In the following, given a matrix M, we use $\operatorname{conv}(M)$ to denote the polytope given by the convex hull of the columns of M.

Definition 5.2.1. *Let Δ be a d-dimensional simplicial complex on $[n]$, ordered $1 < \cdots < n$, and let $0 \le k \le d$. The k^{th}* Laplacian polytope *of Δ is defined as the convex hull of the columns of $\mathcal{L}_k(\Delta)$, i.e.,*

$$P_\Delta^{(k)} := \operatorname{conv}(\mathcal{L}_k(\Delta)) \subseteq \mathbb{R}^{f_k(\Delta)}.$$

We want to remark that the 0^{th} Laplacian polytope of a simplicial complex coincides with the Laplacian simplex of its 1-skeleton, as defined in [BM17]. The next example shows that different orderings of the vertex set of Δ may result in polytopes of different dimensions.

Example 5.2.2. *Let G be the 4-cycle on $[4]$ with $E(G) = \{12, 23, 34, 14\}$. If the vertices of G are ordered $1 < 2 < 3 < 4$, then $P_G^{(1)}$ is a 3-simplex. If the vertices of G are ordered $1 < 2 < 4 < 3$, then $P_G^{(1)}$ is a 2-dimensional rectangle.*

Example 5.2.3. *$P^{(2)}_{\partial(\sigma_3)}$ is given by the convex hull of the columns of the following matrix:*

$$\mathcal{L}_2(\partial(\sigma_3)) = \begin{pmatrix} 3 & 1 & -1 & 1 \\ 1 & 3 & 1 & -1 \\ -1 & 1 & 3 & 1 \\ 1 & -1 & 1 & 3 \end{pmatrix}.$$

It will follow from Lemma 5.2.10 that $P^{(2)}_{\partial(\sigma_3)}$ is unimodular equivalent to the square in $\mathbb{R}^2$ with vertices $(-1,1),(1,-1),(3,1)$ and $(1,3)$.

We start by showing that every column of $\mathcal{L}_k(\Delta)$ yields a vertex of $P^{(k)}_\Delta$.

Proposition 5.2.4. *Let Δ be a d-dimensional simplicial complex and $0 \le k \le d$ an integer. Then $P^{(k)}_\Delta$ has $f_k(\Delta)$ many vertices.*

Proof. Set $m := f_k(\Delta)$ and let $v^{(i)}$ denote the i^{th} column of $\mathcal{L}_k(\Delta)$. We assume by contradiction that there exists $1 \le i \le m$, a set $S \subseteq [m] \setminus \{i\}$ and $\lambda_j \in \mathbb{R}$ with $\lambda_j > 0$ and $\sum_{j\in S} \lambda_j = 1$ such that $v^{(i)} = \sum_{j \in S} \lambda_j v^{(j)}$. Setting $\lambda_j = 0$ if $j \notin S \cup \{i\}$ and $\lambda_i = -1$, we see that $\lambda := (\lambda_1, \dots, \lambda_m)^\top \in \ker(\mathcal{L}_k(\Delta))$ and hence $\lambda \in \ker(\partial_k)$ by [MHJ22, Corollary 1.3.1]. Let $w^{(\ell)}$ denote the ℓ^{th} column of ∂_k. If $w^{(i)}_\ell = 1$, then since $w^{(j)}_\ell \in \{-1,0,1\}$, $\lambda_j > 0$ and $\sum_{j\in S}\lambda_j = 1$, we must have $w^{(j)}_\ell = 1$ for all $j \in S$. By the same reasoning, it follows that $w^{(j)}_\ell = -1$ for all $j \in S$ if $w^{(i)}_\ell = -1$. As all columns of ∂_k have the same number of non-zero entries, we conclude $w^{(i)} = w^{(\ell)}$ for all $\ell \in S$, which is a contradiction. □

The next proposition gives a sufficient criterion for $P^{(\dim\Delta)}_\Delta$ being a simplex.

Proposition 5.2.5. *Let Δ be a d-dimensional simplicial complex. If $H_d(\Delta;\mathbb{Q}) = 0$, then $P^{(\dim\Delta)}_\Delta$ is an $(f_d(\Delta)-1)$-simplex.*

Proof. Lemma 5.1.1 implies that $\operatorname{rank}\mathcal{L}_d(\Delta) = f_d(\Delta)$, and thus has full rank. Consequently, the columns of $\mathcal{L}_d(\Delta)$ are linearly independent which shows the claim. □

In the following, we focus on the d^{th} Laplacian polytope of $\partial(\sigma_{d+1})$. To simplify notation, we set $P_{\partial(\sigma_{d+1})} = P^{(d)}_{\partial(\sigma_{d+1})}$. We use $s^{(i)}$ to denote the i^{th} column of $\mathcal{L}_d(\partial(\sigma_{d+1}))$. Moreover, given a subset $S \subseteq [d+2]$, we denote by $\mathcal{L}_d(S)$ the matrix obtained from $\mathcal{L}_d(\partial(\sigma_{d+1}))$ by deleting the rows with indices in S.

Combining Lemma 5.1.4 and [Grü03, p. 4], the following formula for the dimension of $P_{\partial(\sigma_{d+1})}$ is immediate.

Proposition 5.2.6. *Let $\Delta = \partial(\sigma_{d+1})$. Then*

$$\dim P_\Delta = \begin{cases} d, & \text{if } d \text{ is even,} \\ d+1, & \text{if } d \text{ is odd.} \end{cases}$$

The previous statement together with Proposition 5.2.4 allows us to conclude:

Corollary 5.2.7. *Let $d \in \mathbb{N}$ with $d \ge 1$ and $\Delta = \partial(\sigma_{d+1})$. Then P_Δ has $d+2$ vertices. In particular, P_Δ is a $(d+1)$-simplex, if d is odd.*

Corollary 5.2.7 trivially implies that $P_{\partial(\sigma_{d+1})}$ is a simplicial polytope if d is odd. The same statement also turns out to be true for d even.

Theorem 5.2.8. *$P_{\partial(\sigma_{d+1})}$ is simplicial for every $d \in \mathbb{N}$.*

Proof. Let $\Delta = \partial(\sigma_{d+1})$. If d is odd, then the claim is trivially true by Corollary 5.2.7.

Now, let d be even. If $d = 0$, then P_Δ is just the origin and as such simplicial. Let $d \geq 2$ and let F be the vertices of a facet of P_Δ. Combining Proposition 5.2.6 and Corollary 5.2.7, it follows that $d \leq |F| \leq d+1$. If, by contradiction, $|F| = d+1$, then Lemma 5.1.3 implies that the convex hull of F is d-dimensional, i.e., F cannot be a facet. Consequently, F is a simplex, which finishes the proof. □

As, by Proposition 5.2.6, the Laplacian polytope of $\partial(\sigma_{d+1})$ is never full-dimensional, our next goal is to construct a polytope that is unimodular equivalent to $P_{\partial(\sigma_{d+1})}$ and full-dimensional with respect to its ambient space. We first need to introduce some further notation.

We let $\mathbb{1}_{\text{even}}$ and $\mathbb{1}_{\text{odd}}$ denote the $0-1$-vectors in $\mathbb{R}^{d+2}$ whose even and odd entries are equal to 1, respectively. Given these definitions, we can easily compute the affine hull of $P_{\partial(\sigma_{d+1})}$.

Lemma 5.2.9. *Let $d \in \mathbb{N}$ with $d \geq 1$ and $\Delta = \partial(\sigma_{d+1})$.*

$$\operatorname{aff}(P_\Delta) = \begin{cases} \left\{x \in \mathbb{R}^{d+2} \;:\; (\mathbb{1}_{\text{odd}} - \mathbb{1}_{\text{even}})^\top \cdot x = 0\right\}, & \text{if } d \text{ is odd,} \\ \left\{x \in \mathbb{R}^{d+2} \;:\; \mathbb{1}_{\text{odd}}^\top \cdot x = \mathbb{1}_{\text{even}}^\top \cdot x = \frac{d+2}{2}\right\}, & \text{if } d \text{ is even.} \end{cases}$$

Proof. By Proposition 5.2.6, it is enough to show that all vertices of P_Δ lie in the specified subspaces of dimension $d+1$ and d, respectively. This can be seen by a direct computation. □

The next lemma gives the desired unimodular equivalent polytopes.

Lemma 5.2.10. *Let $d \in \mathbb{N}$. The polytope $P_{\partial(\sigma_{d+1})}$ is unimodular equivalent to* $\operatorname{conv}(\mathcal{L}_d(\{1\}))$ *and* $\operatorname{conv}(\mathcal{L}_d(\{1,2\}))$ *if d is odd and even, respectively.*

Proof. Define matrices $A, B \in \mathbb{Z}^{(d+2)\times(d+2)}$ as follows:

$$A = \left(\begin{array}{c|c} \multicolumn{2}{c}{\mathbb{1}_{\text{odd}}^\top - \mathbb{1}_{\text{even}}^\top} \\ \hline 0 & \\ \vdots & E_{d+1} \\ 0 & \end{array}\right) \quad \text{and} \quad B = \left(\begin{array}{cc|c} \multicolumn{3}{c}{\mathbb{1}_{\text{odd}}^\top} \\ \multicolumn{3}{c}{\mathbb{1}_{\text{even}}^\top} \\ \hline 0 & 0 & \\ \vdots & \vdots & E_d \\ 0 & 0 & \end{array}\right),$$

where E_d and E_{d+1} denote identity matrices. Note that A and B are unimodular. By Lemma 5.2.9, we conclude that

$$A \cdot P_{\partial(\sigma_{d+1})} = \{0\} \times \operatorname{conv}(\mathcal{L}_d(\{1\})),$$

if d is odd and

$$B \cdot P_{\partial(\sigma_{d+1})} = \{((d+2)/2, (d+2)/2)\} \times \operatorname{conv}(\mathcal{L}_d(\{1,2\})),$$

if d is even. This finishes the proof. □

In the following, we use $\widetilde{P}_{\partial(\sigma_{d+1})}$ to denote the unimodular equivalent polytope to $P_{\partial(\sigma_{d+1})}$ as constructed in Lemma 5.2.10. By abuse of notation, we will also refer to $\widetilde{P}_{\partial(\sigma_{d+1})}$ as d^{th} Laplacian polytope of $\partial(\sigma_{d+1})$. We also want to remark that, if d is odd, we have the following, easy-to-show containment relation: $\widetilde{P}_{\partial(\sigma_{d+1})} \subseteq \widetilde{P}_{\partial(\sigma_{d+2})}$.

5.3 The facet description and the combinatorial type of $P_{\partial(\sigma_{d+1})}$

While, for odd d, we have already seen that $\widetilde{P}_{\partial(\sigma_{d+1})}$ is a simplex, the goal of this section is to determine the combinatorial type of $P_{\partial(\sigma_{d+1})}$ if d is even. To reach this goal, we will first provide a complete irredundant facet description of $P_{\partial(\sigma_{d+1})}$.

We fix some notation. Let $b^{(\ell)}$ denote the vertex of $\widetilde{P}_{\partial(\sigma_{d+1})}$, that is given by the ℓ^{th} column of $\mathcal{L}_d(\{1,2\})$. By Theorem 5.1.2, we have $b_k^{(\ell)} = d+1$ if $k = \ell - 2$ and $b_k^{(\ell)} = (-1)^{k+\ell-1}$, otherwise.

Proposition 5.3.1. *Let $d \geq 2$ be even. Then the following inequalities are facet-defining and irredundant for $\widetilde{P}_{\partial(\sigma_{d+1})}$:*

(i) $\mathbb{1}^\top \cdot x \leq d+2$,

(ii) $\mathbb{1}_{\text{odd}}^\top \cdot x - x_i \leq \frac{d+2}{2}$, *where $i \in [d]$ is even,*

(iii) $\mathbb{1}_{\text{even}}^\top \cdot x - x_j \leq \frac{d+2}{2}$, *where $j \in [d]$ is odd,*

(iv) $x_i + x_j \geq 0$, *where $1 \leq i < j \leq d$ such that $i+j$ is odd.*

Moreover, the vertices, which attain equality in (i)–(iv), are given by the sets $\{b^{(\ell)} : 3 \leq \ell \leq d+2\}$, $\{b^{(\ell)} : \ell \in [d+2] \setminus \{1, i+2\}\}$, $\{b^{(\ell)} : \ell \in [d+2] \setminus \{2, j+2\}\}$ and $\{b^{(\ell)} : \ell \in [d+2] \setminus \{i+2, j+2\}\}$, respectively.

Proof. We first consider the inequality in (i). If $\ell \in \{1,2\}$, then $b^{(\ell)} \in \{-1,1\}^d$ with alternating entries and hence $\mathbb{1}^\top \cdot b^{(\ell)} < d+2$. Let $3 \leq \ell \leq d+2$. As d is even, it follows from above that $b^{(\ell)}$ has one entry equal to $d+1$, $\frac{d}{2}$ entries equal to 1 and $\frac{d}{2}-1$ entries equal to -1. This implies $\mathbb{1}^\top \cdot b^{(\ell)} = d+2$. Hence, the inequality in (i) defines a facet, whose vertices are given by $\{b^{(\ell)} : 3 \leq \ell \leq d+2\}$, where we use that the affine hull of the latter set is $(d-1)$-dimensional by Lemma 5.1.3.

Similarly, it is straightforward to verify that the inequalities in (ii)–(iv) are valid for $\widetilde{P}_{\partial(\sigma_{d+1})}$ and that the given sets of vertices are the ones attaining equality. As those all differ and their affine hulls all have dimension $d-1$, it follows that the inequalities are irredundant. □

For the sake of completeness we add the description of the facets of $\widetilde{P}_{\partial(\sigma_{d+1})}$ for d odd.

Remark 5.3.2. *If $d \geq 3$ is odd, using Theorem 5.1.2, it is not hard to see that the following inequalities are facet-defining for $\widetilde{P}_{\partial(\sigma_{d+1})}$:*

(i) $\mathbb{1}^\top \cdot x \leq d+2$,

(ii) $2 \cdot \mathbb{1}_{\text{odd}}^\top \cdot x - x_i \leq \frac{d+2}{2}$, *where $i \in [d+1]$ is even,*

(iii) $2 \cdot \mathbb{1}_{\text{odd}}^\top \cdot x + x_j \leq d+2$, *where $j \in [d]$ is odd.*

It is easy to verify that these inequalities are irredundant and as, by Proposition 5.2.6, $\widetilde{P}_{\partial(\sigma_{d+1})}$ is a simplex, they provide the complete facet description of $\widetilde{P}_{\partial(\sigma_{d+1})}$. We omit an explicit proof since this description will not be needed.

We state the first main result of this section.

Theorem 5.3.3. *For d even, $\widetilde{P}_{\partial(\sigma_{d+1})}$ is completely described by the inequalities in Proposition 5.3.1. Moreover, this description is irredundant. In particular, $\widetilde{P}_{\partial(\sigma_{d+1})}$ has $\frac{(d+2)^2}{4}$ many facets.*

Proof. We let $\widetilde{\mathcal{F}}$ denote the set of facets of $\widetilde{P}_{\partial(\sigma_{d+1})}$ provided by Proposition 5.3.1, and we write $G_{\widetilde{\mathcal{F}}}$ for the subgraph of the facet-ridge graph of $\widetilde{P}_{\partial(\sigma_{d+1})}$ that is induced on vertex set $\widetilde{\mathcal{F}}$. It follows from Theorem 5.2.8, that the facet-ridge graph of $\widetilde{P}_{\partial(\sigma_{d+1})}$ is d-regular and connected. Since any d-regular subgraph does not have a proper d-regular subgraph, for the first statement, it suffices to show that $G_{\widetilde{\mathcal{F}}}$ is d-regular.

Since $G_{\widetilde{\mathcal{F}}}$ is a subgraph of $G(\widetilde{P}_{\partial(\sigma_{d+1})})$, its maximal degree is at most d. Hence, to show the claim, it suffices to show that $|E(G_{\widetilde{\mathcal{F}}})| = \frac{d\cdot|V(G_{\widetilde{\mathcal{F}}})|}{2}$.

We first count the vertices of G. Using Proposition 5.3.1, we get that

$$|V(G_{\widetilde{\mathcal{F}}})| = 1 + \frac{d}{2} + \frac{d}{2} + \left(\frac{d}{2}\right)^2 = \frac{(d+2)^2}{4}, \tag{5.2}$$

Here, the last term in the middle comes from the fact that the inequalities in (iv) are indexed by sets $\{i,j\}$ where $i \in \{2\ell \;:\; \ell \in [\frac{d}{2}]\}$ and $j \in \{2\ell - 1 \;:\; \ell \in [\frac{d}{2}]\}$.

It remains to count the number of edges of $G_{\widetilde{\mathcal{F}}}$. In the following, we identify a facet in $\widetilde{\mathcal{F}}$ with its set of vertices. Given this, we use the following short hand notation for the different types of facets in $\widetilde{\mathcal{F}}$.

(i) $F = \{b^{(\ell)} \;:\; 3 \le \ell \le d+2\}$;

(ii) $E_i = \{b^{(\ell)} \;:\; \ell \in [d+2] \setminus \{1, i+2\}\}$, where $i \in [d]$ is even;

(iii) $O_j = \{b^{(\ell)} \;:\; \ell \in [d+2] \setminus \{2, j+2\}\}$, where $j \in [d]$ is odd;

(iv) $F_{k,m} = \{b^{(\ell)} \;:\; \ell \in [d+2] \setminus \{k+2, m+2\}\}$ for $1 \le k < m \le d$ such that $k+m$ is odd.

We immediately get that

(a) $|F \cap E_i| = |F \cap O_j| = d-1$ for all even $i \in [d]$ and all odd $j \in [d]$;

(b) $|F \cap F_{k,m}| = d-2$ for all $1 \le k < m \le d$;

(c) $|E_i \cap E_j| = d-1$ for all odd $i, j \in [d]$ with $i \ne j$;

(d) $|E_i \cap O_j| = d-2$ for all even $i \in [d]$ and all odd $j \in [d]$;

(e) $|E_i \cap F_{k,m}| = d-1$ iff $i \in \{k,m\}$, i even, $k+m$ odd, and $|E_i \cap F_{k,m}| = d-2$, otherwise;

(f) $|O_i \cap O_j| = d-1$ for all even $i, j \in [d]$ with $i \ne j$;

(g) $|O_j \cap F_{k,m}| = d-1$ iff $j \in \{k,m\}$, j odd, $k+m$ odd, and $|O_j \cap F_{k,m}| = d-2$, otherwise.

(h) $|F_{i,j} \cap F_{k,m}| = d-1$ iff $|\{i,j,k,m\}| = 3$ and $|F_{i,j} \cap F_{k,m}| = d-2$, otherwise.

Since edges of $G_{\widetilde{\mathcal{F}}}$ are given by tuples of facets intersecting in $d-1$ vertices, we get d edges in (a), 0 edges in (b) and (d), $\binom{d/2}{2}$ edges in each of (c) and (f), $\left(\frac{d}{2}\right)^2$ edges in each of (e) and (g) and $2 \cdot \frac{d}{2} \cdot \binom{d/2}{2}$ edges in (h). This yields

$$|E(G_{\widetilde{\mathcal{F}}})| = d + 2\cdot\binom{d/2}{2} + 2\cdot\left(\frac{d}{2}\right)^2 + d\cdot\binom{d/2}{2} = \frac{d(d+2)^2}{8} = \frac{d\cdot|V(G_{\widetilde{\mathcal{F}}})|}{2}.$$

It follows that $G_{\widetilde{\mathcal{F}}}$ is d-regular. The *In particular*-statement follows from (5.2). $\square$

The previous theorem allows us to determine the combinatorial type of $\widetilde{P}_{\partial(\sigma_{d+1})}$ if d is even. It is well-known (see, e.g., [Grü03, Section 6.1]) that there are only finitely many combinatorial types of simplicial d-polytopes with $d+2$ vertices. More precisely, any simplicial d-polytope with $d+2$ vertices is obtained as the convex hull of a d-simplex T^d and a vertex v that is beyond k facets of T^d, where $1 \le k \le d-1$. It is easily seen that the combinatorial type of such a polytope only depends on k. Following Grünbaum, we use T_k^d to denote the corresponding combinatorial type. Given that we know the number of facets of $\widetilde{P}_{\partial(\sigma_{d+1})}$ (see Theorem 5.3.3), we can immediately determine its combinatorial type.

Theorem 5.3.4. *Let d be even. Then $\widetilde{P}_{\partial(\sigma_{d+1})}$ is of combinatorial type $T^d_{\frac{d}{2}}$. In particular, $\widetilde{P}_{\partial(\sigma_{d+1})}$ is combinatorially equivalent to a d-dimensional cyclic polytope on $d+2$ vertices.*

Proof. By Theorem 5.3.3, $\widetilde{P}_{\partial(\sigma_{d+1})}$ has $\frac{(d+2)^2}{4}$ facets. Using [Grü03, Section 6.1, Theorem 2], it follows that this number has to be equal to

$$\binom{d+2}{2} - \binom{k+1}{2} - \binom{d+1-k}{2},$$

where $\widetilde{P}_{\partial(\sigma_{d+1})}$ is of combinatorial type T_k^d. Solving for k yields $k = \frac{d}{2}$. The second statement follows from [Grü03, Section 6.1, Theorem 1]. $\square$

We remark that from the previous theorem, we also get a precise formula for the f- and h-vector of $\widetilde{P}_{\partial(\sigma_{d+1})}$ (see, e.g., [Grü03]).

Remark 5.3.5. *Given the precise description of the facets from the proof of Theorem 5.3.3, it is not hard to write down a shelling order for $\widetilde{P}_{\partial(\sigma_{d+1})}$ (d even). Namely, one particular shelling is given by*

$$F, E_2, E_4, \dots, E_d, O_1, O_3, \dots, O_{d-1}, F_{1,2}, F_{1,4}, \dots, F_{1,d}, F_{2,3}, F_{2,5}, \dots, F_{2,d-1}, \dots, F_{d-1,d}.$$

5.4 Regular unimodular triangulations and h^*-vectors

This section is divided into two parts. The goal of the first is to prove Theorem B, namely, that $\widetilde{P}_{\partial(\sigma_{d+1})}$ admits a regular unimodular triangulation . As a byproduct we will also be able to compute the normalized volume $\widetilde{P}_{\partial(\sigma_{d+1})}$. In the second part, we provide the proof of Theorem C.

5.4.1 Triangulations through interior polytopes

If d is even, one of our main tools towards the formulated goal is the so-called *interior polytope* $Q_{\partial(\sigma_{d+1})}$ of $\widetilde{P}_{\partial(\sigma_{d+1})}$, defined as follows:

$$Q_{\partial(\sigma_{d+1})} := \operatorname{conv}\left(\widetilde{P}_{\partial(\sigma_{d+1})} \setminus \partial\left(\widetilde{P}_{\partial(\sigma_{d+1})}\right) \cap \mathbb{Z}^d\right).$$

Figure 5.1 depicts $\widetilde{P}_{\partial(\sigma_3)}$ and its interior polytope $Q_{\partial(\sigma_3)}$, both translated to the origin.

Surprisingly, it turns out that $P_{\partial(\sigma_{d+1})}$ and its interior polytope are combinatorially equivalent. More precisely, the following stronger statement is true:

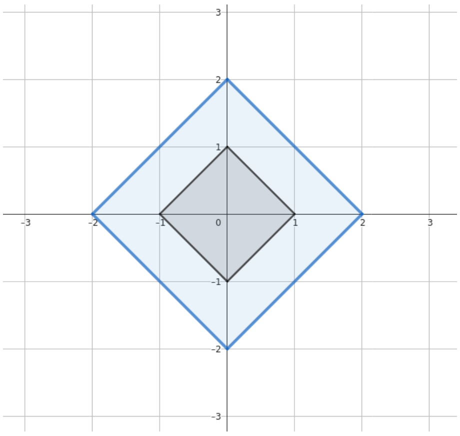

FIGURE 5.1: $\widetilde{P}_{\partial(\sigma_3)}$ and its interior polytope $Q_{\partial(\sigma_3)}$ translated to the origin.

Theorem 5.4.1. *Let $d \in \mathbb{N}$ be even. Then the following statements hold:*

(a) *The complete and irredundant facet description of $Q_{\partial(\sigma_{d+1})}$ is given by:*

  (i) $\mathbb{1}^\top \cdot x \le d+1$,

  (ii) $\mathbb{1}_{\text{odd}}^\top \cdot x - x_i \le \frac{d}{2}$ *for even* $i \in [d]$,

  (iii) $\mathbb{1}_{\text{even}}^\top \cdot x - x_j \le \frac{d}{2}$ *for odd* $j \in [d]$,

  (iv) $x_i + x_j \ge 1$ *for* $1 \le i < j \le d$ *such that* $i+j$ *is odd.*

(b) $Q_{\partial(\sigma_{d+1})} - \mathbb{1}$ *is reflexive. In particular,* $\mathbb{1}$ *is the unique interior lattice point of* $Q_{\partial(\sigma_{d+1})}$.

(c) $2 \cdot \left(Q_{\partial(\sigma_{d+1})} - \mathbb{1}\right) = \widetilde{P}_{\partial(\sigma_{d+1})} - \mathbb{1}$.

Proof. We let $Q = \widetilde{P}_{\partial(\sigma_{d+1})} - \mathbb{1}$. The vertices of Q are given by $u^{(\ell)} \coloneqq b^{(\ell)} - \mathbb{1}$ for $1 \le \ell \le d+2$. It is immediate that all coordinates of $u^{(\ell)}$ are divisible by 2. Hence, $\frac{1}{2}Q$ is a lattice polytope. Using Theorem 5.3.3, it follows that the facets of $\frac{1}{2}Q$ are given by

- $\mathbb{1}^\top \cdot x \le 1$,
- $\mathbb{1}_{\text{odd}}^\top \cdot x - x_i \le 1$ for even $i \in [d]$,
- $\mathbb{1}_{\text{even}}^\top \cdot x - x_j \le 1$ for odd $j \in [d]$,
- $x_i + x_j \ge -1$ for $1 \le i < j \le d$ such that $i+j$ is odd,

which shows that $\frac{1}{2}Q$ is reflexive. It remains to show that $\frac{1}{2}Q + \mathbb{1} = Q_{\partial(\sigma_{d+1})}$. Since $\frac{1}{2}Q + \mathbb{1}$ is a lattice polytope, it follows that $\frac{1}{2}Q + \mathbb{1} \subseteq Q_{\partial(\sigma_{d+1})}$. For the other inclusion it suffices to note that the facets of $\frac{1}{2}Q + \mathbb{1}$ and $\widetilde{P}_{\partial(\sigma_{d+1})}$ are parallel and that they have distance $\frac{1}{\sqrt{d}}$, $\frac{\sqrt{2}}{\sqrt{d+2}}$, $\frac{\sqrt{2}}{\sqrt{d+2}}$ and $\frac{1}{\sqrt{2}}$ to each other for facets of the form in (i), (ii), (iii) and (iv), respectively. This implies that there is no lattice point in $\widetilde{P}_{\partial(\sigma_{d+1})} \setminus ((\frac{1}{2}Q + \mathbb{1}) \cup \partial \widetilde{P}_{\partial(\sigma_{d+1})})$ and hence $Q_{\partial(\sigma_{d+1})} \subseteq \frac{1}{2}Q + \mathbb{1}$. □

We define vectors $c^{(1)}, \dots, c^{(d+2)} \in \mathbb{R}^d$ by $c_k^{(\ell)} = \frac{d+2}{2}$ if $k = \ell - 2$ and $c_k^{(\ell)} = \max(0, (-1)^{k+\ell-1})$, otherwise. Combining Proposition 5.3.1 and Theorem 5.4.1 (c), we get the following description of the vertices of $Q_{\partial(\sigma_{d+1})}$ and its facets.

Corollary 5.4.2. *The vertices of $Q_{\partial(\sigma_{d+1})}$ are the vectors $c^{(1)},\dots,c^{(d+2)}$. Moreover, the vertices, which attain equality in Theorem 5.4.1 (i)–(iv), are given by the sets $\{c^{(\ell)} : 3 \le \ell \le d+2\}$, $\{c^{(\ell)} : \ell \in [d+2] \setminus \{1,i+2\}\}$, $\{c^{(\ell)} : \ell \in [d+2] \setminus \{2,j+2\}\}$ and $\{c^{(\ell)} : \ell \in [d+2] \setminus \{i+2,j+2\}\}$, respectively.*

We now recall several definitions and facts concerning regular unimodular triangulations (see [Haa+14, Subsection 2.3.2.] for more on these topics).

Given full-dimensional polytopes $P \subseteq \mathbb{R}^d$ and $P' \subseteq \mathbb{R}^{d'}$ of positive dimension, their *join* $P * P'$ is the $(d+d'+1)$-dimensional polytope defined by

$$\operatorname{conv}\left(P \times \{\mathbf{0}_{d'}\} \times \{0\} \quad \cup \quad \{\mathbf{0}_d\} \times P' \times \{1\}\right).$$

The next statement, which is well-known, will be crucial for the construction of a regular unimodular triangulation of $\widetilde{P}_{\partial(\sigma_{d+1})}$.

Theorem 5.4.3. *Let $P \subseteq \mathbb{R}^d$ and $P' \subseteq \mathbb{R}^{d'}$ be polytopes of dimension d and d', respectively. Let $S = \{S_i : i \in [n]\}$ and $S' = \{S'_j : j \in [m]\}$ be triangulations of P and P', respectively, where S_i and S'_j denote the full-dimensional cells. If both S and S' are regular and unimodular, then*

$$\mathcal{T} = \left\{S_i * S'_j : i \in [n], j \in [m]\right\}$$

is a regular unimodular triangulation of $P * P'$.

We will also make use of the following statement, see [Haa+14, Theorem 4.8].

Theorem 5.4.4. *If P has a (regular) unimodular triangulation $\mathcal{T}$, then so has any dilation cP, where c is a positive integer.*

A well-studied subdivision, which is related to the Veronese construction in algebra but also appears in topology [BW09; BR04; EG99; Gra89], is the so-called r^{th} *edgewise subdivision* of a simplicial complex. In the following, we review this definition for the special case that Δ is the $(n-1)$-dimensional simplex on vertex set $V = \{\mathbf{e}_1, \mathbf{e}_2, \dots, \mathbf{e}_n\} \subseteq \mathbb{R}^n$. For a positive integer r, let $\Omega_r = \{(i_1,\dots,i_n) \in \mathbb{N}^n : i_1 + i_2 + \cdots + i_n = r\}$ denote the set of lattice points $r\Delta \cap \mathbb{Z}^n$. For $x = (x_1,\dots,x_n) \in \mathbb{Z}^n$, we define

$$\varphi(x) \coloneqq (x_1, x_1+x_2, \dots, x_1+\cdots+x_n) \in \mathbb{R}^n.$$

The r^{th} *edgewise subdivision* of Δ is the simplicial complex $\operatorname{esd}_r(\Delta)$ on vertex set Ω_r, for which $F \subseteq \Omega_r$ is a face if for all $x, y \in F$

$$\varphi(x) - \varphi(y) \in \{0,1\}^n \qquad \text{or} \qquad \varphi(y) - \varphi(x) \in \{0,1\}^n.$$

By definition, the geometric realization of the r^{th} edgewise subdivision of Δ gives a lattice triangulation of $r\Delta$. It is known that this triangulation is regular [BR04, Proposition 6.4.], which is also unimodular since all maximal simplices have normalized volume 1. In the following, we will use $\operatorname{esd}_r(\Delta)$ to denote both, the triangulation as a simplicial complex and its geometric realization. Given any $(n-1)$-dimensional unimodular simplex $\Gamma \subseteq \mathbb{R}^n$, $\operatorname{esd}_r(\Delta)$, naturally induces a regular unimodular triangulation of $r\Gamma$ (by applying the corresponding unimodular transformation). Slightly abusing notation, we will refer to this triangulation as edgewise subdivision of Γ or even of $r\Gamma$, denoted $\operatorname{esd}_r(\Gamma)$. Moreover, the restriction of $\operatorname{esd}_r(\Gamma)$ to any face $F \in \Gamma$ equals $\operatorname{esd}_r(F)$ as a simplicial complex and as geometric realization.

Example 5.4.5. *Figure 5.2 depicts the 3^{rd} edgewise subdivision of the 2-dimensional simplex $\Delta_2 \coloneqq \operatorname{conv}((0,0),(1,0),(0,1))$ as triangulation of $3\Delta_2$. The vertex labels correspond to the vertex labels from the original definition and not the lattice points.*

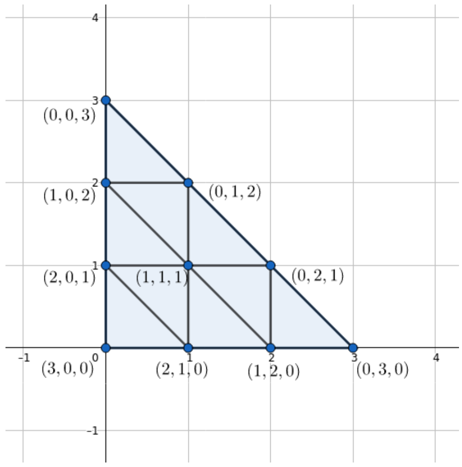

FIGURE 5.2: The triangulation of $3 \cdot \Delta_2$ given by $\operatorname{esd}_3(\Delta_2)$.

We now outline our strategy to show that $\widetilde{P}_{\partial(\sigma_{d+1})}$ has a regular unimodular triangulation. We first prove that $\widetilde{P}_{\partial(\sigma_{d+1})}$ and the facets of $Q_{\partial(\sigma_{d+1})}$, if d is odd and even, respectively, are unimodular equivalent to joins of dilated standard simplices. If d is odd and even, we can hence triangulate $\widetilde{P}_{\partial(\sigma_{d+1})}$ and facets of $Q_{\partial(\sigma_{d+1})}$ as join of edgewise subdivisions, respectively. If d is odd, the claim follows by Theorem 5.4.3. If d is even, we next show that these triangulations are consistent on intersections of facets. By coning with $\mathbb{1}$, we get a unimodular triangulation of $Q_{\partial(\sigma_{d+1})}$ (see Theorem 5.4.1 (d)) and hence of $\widetilde{P}_{\partial(\sigma_{d+1})}$ by Theorem 5.4.4. The regularity follows by using that the triangulation is regular on single facets and that each facet is triangulated in the same way.

The next statement yields the first step in the outlined strategy.

Proposition 5.4.6. *(a) Let $d \geq 2$ be even and $F \in \mathcal{F}\left(Q_{\partial(\sigma_{d+1})}\right)$. Then*

$$F \cong \left(\frac{d+2}{2}\Delta_{\frac{d-2}{2}} - \mathbb{1}_{\frac{d-2}{2}}\right) * \left(\frac{d+2}{2}\Delta_{\frac{d-2}{2}} - \mathbb{1}_{\frac{d-2}{2}}\right).$$

(b) Let $d \geq 1$ be an odd integer. Then

$$\widetilde{P}_{\partial(\sigma_{d+1})} \cong \left((d+2)\Delta_{\frac{d+1}{2}} - 2\cdot\mathbb{1}\right) * \left((d+2)\Delta_{\frac{d-1}{2}} - 2\cdot\mathbb{1}\right).$$

Proof. The proof of (a) is divided into four cases, according to the four classes of facets from Theorem 5.4.1 (a).

Let $F = \{x \in \mathbb{R}^d \; : \; \mathbb{1}^\top \cdot x \leq d+1\}$. By Corollary 5.4.2, the vertices of F are $c^{(3)}, \ldots, c^{(d+2)}$. We now consider the matrix A, whose ℓ^{th} column equals $c^{(2\ell+1)}$ if $1 \leq \ell \leq \frac{d}{2}$ and $c^{(2\ell+2-d)}$ if $\frac{d}{2}+1 \leq \ell \leq d$. If we reorder the rows of A, by taking first the rows with odd index and then the ones with even index, increasingly, we obtain a matrix S, which looks as follows:

$$S = \left(\begin{array}{c|c} \frac{d+2}{2}\cdot E_{\frac{d}{2}} & \mathbb{1}_{\frac{d}{2}\times\frac{d}{2}} \\ \hline \mathbb{1}_{\frac{d}{2}\times\frac{d}{2}} & \frac{d+2}{2}\cdot E_{\frac{d}{2}} \end{array}\right),$$

where $\mathbb{1}_{k\times k}$ denotes the $(k\times k)$-matrix with all entries equal to 1. Clearly, $F \cong \mathrm{conv}(S)$. Let $E'_k \in \mathbb{Z}^{(k-1)\times k}$ be the $(k\times k)$-identity matrix with its first row removed and let

$$U = \left(\begin{array}{ccc|ccc} & E'_{\frac{d}{2}} & & & \mathbf{0}_{\frac{d-2}{2}\times\frac{d}{2}} & \\ \hline & \mathbf{0}_{\frac{d-2}{2}\times\frac{d}{2}} & & & E'_{\frac{d}{2}} & \\ \hline 0 & \cdots & 0 & 1 & \cdots & 1 \\ 1 & \cdots & 1 & 1 & \cdots & 1 \end{array}\right) \in \mathbb{Z}^{d\times d}.$$

It is easily seen that U is unimodular and a direct computation shows that

$$U\cdot(S-\mathbb{1}_{d\times d}) = \left(\begin{array}{ccc|ccc} & \mathcal{M}\left(\frac{d+2}{2}\Delta_{\frac{d-2}{2}} - \mathbb{1}_{\frac{d-2}{2}\times\frac{d}{2}}\right) & & & \mathbf{0}_{\frac{d-2}{2}\times\frac{d}{2}} & \\ \hline & \mathbf{0}_{\frac{d-2}{2}\times\frac{d}{2}} & & & \mathcal{M}\left(\frac{d+2}{2}\Delta_{\frac{d-2}{2}} - \mathbb{1}_{\frac{d-2}{2}\times\frac{d}{2}}\right) & \\ \hline 0 & \cdots & 0 & 1 & \cdots & 1 \\ 1 & \cdots & 1 & 1 & \cdots & 1 \end{array}\right),$$

where $\mathbf{0}_{k\times k}$ denotes the $(k\times k)$-matrix with all entries equal to 0 and $\mathcal{M}\left(\frac{d+2}{2}\Delta_{\frac{d-2}{2}} - \mathbb{1}_{\frac{d-2}{2}\times\frac{d}{2}}\right)$ denotes the matrix whose columns are the vertices of $\frac{d+2}{2}\Delta_{\frac{d-2}{2}} - \mathbb{1}_{\frac{d-2}{2}\times\frac{d}{2}}$ in the obvious order. Since $F \cong \mathrm{conv}(U\cdot(S-\mathbb{1}_{d\times d}))$, the claim follows after projection on the first $d-1$ coordinates and by the definition of the join. We also note that the vertices of F corresponding to the vertices of the dilated simplices are $\{c^{(2\ell+1)} : 1\le \ell \le \frac{d}{2}\}$ and $\{c^{(2\ell)} : 2\le\ell\le\frac{d}{2}+1\}$.

Similarly, one can show that for the facets defined by

- $\mathbb{1}_{\text{odd}}^{\top}\cdot x - x_i \le \frac{d}{2}$, where $i\in[d]$ is even,
- $\mathbb{1}_{\text{even}}^{\top}\cdot x - x_j \le \frac{d}{2}$, where $j\in[d]$ is odd,
- $x_i + x_j \ge 1$ for $1\le i<j\le d$ such that $i+j$ is odd,

respectively, the vertices

- $\{c^{(2\ell+1)} : 1\le\ell\le\frac{d}{2}\}$ and $\{c^{(2\ell)} : 1\le\ell\le\frac{d}{2}+1, \ell\ne\frac{i+2}{2}\}$,
- $\{c^{(2\ell+1)} : 0\le\ell\le\frac{d}{2}, \ell\ne\frac{j+1}{2}\}$ and $\{c^{(2\ell)} : 2\le\ell\le\frac{d}{2}+1, \ell\ne\frac{i+2}{2}\}$,
- $\{c^{(2\ell+1)} : 0\le\ell\le\frac{d}{2}, \ell\ne\frac{j+1}{2}\}$ and $\{c^{(2\ell)} : 1\le\ell\le\frac{d}{2}+1, \ell\ne\frac{i+2}{2}\}$,

respectively, correspond to the vertices of the dilated simplices. The rather technical proofs can be found in the appendix. Similarly, (b) will be shown in the appendix. □

We recall and prove Theorem B.

Theorem B. *$P_{\partial(\sigma_{d+1})}$ has a regular unimodular triangulation for every integer $d\ge 0$.*

Proof. Since $\widetilde{P}_{\partial(\sigma_{d+1})}$ and $P_{\partial(\sigma_{d+1})}$ are unimodular equivalent, it suffices to show the statement for $\widetilde{P}_{\partial(\sigma_{d+1})}$. First assume that d is odd. By Proposition 5.4.6 (b), we know that

$$\widetilde{P}_{\partial(\sigma_{d+1})} \cong \left((d+2)\Delta_{\frac{d+1}{2}} - 2\cdot\mathbb{1}\right) * \left((d+2)\Delta_{\frac{d-1}{2}} - 2\cdot\mathbb{1}\right).$$

Since the $(d+2)^{\text{nd}}$ edgewise subdivision is a regular unimodular triangulation of the $(d+2)^{\text{nd}}$ dilation of any unimodular simplex (as well as of any translation), we conclude with Theorem 5.4.3 that $\widetilde{P}_{\partial(\sigma_{d+1})}$ has a regular unimodular triangulation.

Next assume that d is even. If $d=0$, $\widetilde{P}_{\partial(\sigma_{d+1})}$ is just a point and there is nothing to show.

Let $d \geq 2$. We construct a regular unimodular triangulation of the interior polytope $Q_{\partial(\sigma_{d+1})}$. By Proposition 5.4.6, every facet F of $Q_{\partial(\sigma_{d+1})}$ is unimodular equivalent to

$$\left(\frac{d+2}{2}\Delta_{\frac{d-2}{2}} - \mathbb{1}_{\frac{d-2}{2}}\right) * \left(\frac{d+2}{2}\Delta_{\frac{d-2}{2}} - \mathbb{1}_{\frac{d-2}{2}}\right). \tag{5.3}$$

By the same reasoning as for d odd, we can triangulate F as join of edgewise subdivisions of unimodular simplices. In this way, we obtain regular unimodular triangulations of each facet of $Q_{\partial(\sigma_{d+1})}$. We now show that the union of these triangulations, yields a triangulation of the boundary of $Q_{\partial(\sigma_{d+1})}$. For this aim, let F and G be facets of $Q_{\partial(\sigma_{d+1})}$ and let $\mathcal{T}(F)$ and $\mathcal{T}(G)$ be the considered triangulations. Let us further denote by F_i and G_i, where $i \in [2]$, the vertex sets corresponding to the vertex sets of the dilated (and translated) simplices in (5.3). It follows from the end of the proof of Proposition 5.4.6 that (after possible renumbering)

$$(F_1 \cup F_2) \cap (G_1 \cup G_2) = (F_1 \cap F_2) \cup (G_1 \cap G_2).$$

This directly yields that the restrictions of $\mathcal{T}(F)$ and $\mathcal{T}(G)$ to $F \cap G$ coincide: Indeed, they are given as the join of the edgewise subdivisions of the dilated (and translated) simplices on vertex sets $F_1 \cap F_2$ and $G_1 \cap G_2$. This shows that the union of the triangulations of the facets is indeed a triangulation of the boundary of $Q_{\partial(\sigma_{d+1})}$, which is, in particular, unimodular. Since, by Theorem 5.4.1 (b), $Q_{\partial(\sigma_{d+1})} - \mathbb{1}$ is reflexive, we can extend this triangulation to a unimodular triangulation of $Q_{\partial(\sigma_{d+1})}$ by coning over the unique interior lattice point $\mathbb{1}$. In the following, we call this triangulation $\mathcal{T}$.

It remains to show that $\mathcal{T}$ is a regular triangulation. The previous paragraph implies that the induced triangulations on facets $Q_{\partial(\sigma_{d+1})}$ are all regular and unimodular equivalent to each other. In particular, there exists a simultaneous lifting function ω yielding the triangulation of an arbitrary facet. Fix a facet F and let $\mathcal{T}(F)$ be the induced triangulation on F. Since F is a simplex, we can assume that $\omega(v) = 1$ for any vertex $v \in F$. Moreover, for any lattice point u in F, that is not a vertex, we have $\omega(u) < 1$, since otherwise u would not be a vertex of $\mathcal{T}(F)$. Hence, there exists a non-negative function g, whose values are bounded by 1, that vanishes on the vertices of F such that $\omega = 1 - g$. Moreover, for any $\epsilon > 0$, $\omega_\epsilon = 1 - \epsilon g$ is also a lifting function for F yielding $\mathcal{T}(F)$. Finally, ignoring $\mathbb{1}$ and lifting all other lattice points in $Q_{\partial(\sigma_{d+1})}$ according to the simultaneous lifting function ω_ϵ, gives a lifting function such that the projection of the lower envelope yields $\mathcal{T}$ on the boundary of $Q_{\partial(\sigma_{d+1})}$ and potentially additional faces in the interior. Lifting $\mathbb{1}$ at height 0, gives a lifting of all lattice points of $Q_{\partial(\sigma_{d+1})}$. If ϵ is sufficiently small, one can guarantee that the triangulation obtained as the lower envelope is the cone with $\mathbb{1}$ over the boundary of the previous triangulation (ignoring $\mathbb{1}$) since potential interior faces that we had seen before, do no longer lie in the lower envelope.

The claim follows by Theorem 5.4.1 (c) and Theorem 5.4.4. □

Analyzing the proof of Theorem B, we can compute the normalized volume of $P_{\partial(\sigma_{d+1})}$:

Corollary 5.4.7. *The normalized volume of $P_{\partial(\sigma_{d+1})}$ is $(d+2)^d$.*

Proof. We compute the normalized volume of $\widetilde{P}_{\partial(\sigma_{d+1})}$, which equals the one of $P_{\partial(\sigma_{d+1})}$, by counting the number of maximal simplices in the unimodular triangulation $\mathcal{T}$ constructed in the proof of Theorem B.

First assume that d is odd. We have seen that $\mathcal{T}$ is unimodular equivalent to

$$\operatorname{esd}_{d+2}\left(\Delta_{\frac{d+1}{2}}\right) * \operatorname{esd}_{d+2}\left(\Delta_{\frac{d-1}{2}}\right).$$

Since the r^{th} edgewise subdivision of an m-simplex, has r^m maximal simplices, it follows that the number of maximal simplices in the constructed unimodular triangulation of $\widetilde{P}_{\partial(\sigma_{d+1})}$ equals

$$(d+2)^{\frac{d+1}{2}} \cdot (d+2)^{\frac{d-1}{2}} = (d+2)^d.$$

Let d be even. We first compute the normalized volume of $Q_{\partial(\sigma_{d+1})}$. Combining Theorem 5.3.3 and Theorem 5.4.1, it follows that $Q_{\partial(\sigma_{d+1})}$ has exactly $\frac{(d+2)^2}{4}$ facets. By the proof of Theorem B, each of these has a unimodular triangulation that is unimodular equivalent to

$$\operatorname{esd}_{\frac{d+2}{2}}\left(\Delta_{\frac{d-2}{2}}\right) * \operatorname{esd}_{\frac{d+2}{2}}\left(\Delta_{\frac{d-2}{2}}\right).$$

As in the case that d is odd, we conclude that each facet is triangulated into $\left(\frac{d+2}{2}\right)^{\frac{d-2}{2}} \cdot \left(\frac{d+2}{2}\right)^{\frac{d-2}{2}} = \left(\frac{d+2}{2}\right)^{d-2}$ many maximal simplices and hence $Q_{\partial(\sigma_{d+1})}$ has normalized volume $\frac{(d+2)^d}{2^d}$. Since, by Theorem 5.4.1 (c), $\widetilde{P}_{\partial(\sigma_{d+1})} + \mathbb{1} = 2 \cdot Q_{\partial(\sigma_{d+1})}$, the claim follows. $\square$

5.4.2 Unimodality and real-rootedness

The goal of this subsection is to prove Theorem C.

If d is even, then by the proof of Theorem B, $Q_{\partial(\sigma_{d+1})}$ has a regular unimodular triangulation. Since it is also reflexive (after translation) by Theorem 5.4.1 (b), the next statement is immediate from [BR07, Theorem 1] (see also [Ath04, Theorem 1.3]):

Lemma 5.4.8. *Let d be an even positive integer. Then $h^*(Q_{\partial(\sigma_{d+1})})$ is symmetric and unimodal.*

To show unimodality of $h^*(\widetilde{P}_{\partial(\sigma_{d+1})})$, if d is even, we need to analyze the change of the h^*-vector under the second dilation of a polytope (cf., Theorem 5.4.1 (c)). Given a d-dimensional lattice polytope P, it follows, e.g., from [BW09, Theorem 1.1] (see also [BS10; Joc18]) that

$$h_i^*(2P) = \sum_{j=0}^{d} \binom{d+1}{2i-j} h_j^*(P). \tag{5.4}$$

We need the following technical but crucial lemma.

Lemma 5.4.9. *Let $i \in \mathbb{N}$ and $r_j := \binom{d+1}{2i+2-j} - \binom{d+1}{2i-j}$. Then for $k \in \mathbb{N}$, we have*

$$-r_{\lceil 2i+2-\frac{d+3}{2}\rceil - k} = r_{\lfloor 2i+2-\frac{d+3}{2}\rfloor + k}.$$

Proof. We set $a_j = \binom{d+1}{2i+2-j}$ and $b_j = \binom{d+1}{2i-j}$. The claim follows if both

$$a_{\lceil 2i+2-\frac{d+3}{2}\rceil - k} = b_{\lfloor 2i+2-\frac{d+3}{2}\rfloor + k} \quad \text{and} \quad b_{\lceil 2i+2-\frac{d+3}{2}\rceil - k} = a_{\lfloor 2i+2-\frac{d+3}{2}\rfloor + k}$$

hold. Due to the symmetry of the binomial coefficient it suffices to show that

(i) $(2i+2-\lceil 2i+2-\frac{d+3}{2}\rceil+k)+(2i-\lfloor 2i+2-\frac{d+3}{2}\rfloor-k)=d+1$

(ii) $(2i-\lceil 2i+2-\frac{d+3}{2}\rceil+k)+(2i+2-\lfloor 2i+2-\frac{d+3}{2}\rfloor-k)=d+1.$

It is obvious that (i) and (ii) are equivalent. The claim follows from direct computations. □

The next statement will be the key ingredient to show that $h^*(\widetilde{P}_{\partial(\sigma_{d+1})})$ is unimodal.

Proposition 5.4.10. *Let $b=(b_0,\dots,b_d)$ be a symmetric and unimodal sequence of non-negative reals. Let $c=(c_0,\dots,c_d)$ be defined by*

$$c_i=\sum_{j=0}^{d}\binom{d+1}{2i-j}b_j.$$

Then

$$c_0\le c_1\le\cdots\le c_{\lfloor\frac{d+1}{2}\rfloor}.$$

Proof. We define r_j as in Lemma 5.4.9. Note that $r_j\ge 0$ if and only if $j\ge 2i+2-\frac{d+3}{2}$. For $0\le i<\frac{d+1}{2}$, we have

$$\begin{aligned}
c_{i+1}-c_i&=\sum_{j=0}^{d}\left[\binom{d+1}{2i+2-j}-\binom{d+1}{2i-j}\right]b_j=\sum_{j=0}^{d}r_jb_j\\
&=\sum_{j=0}^{2(2i+2-\frac{d+3}{2})}r_jb_j+\sum_{j=2(2i+2-\frac{d+3}{2})+1}^{d}r_jb_j\\
&=\sum_{j=1}^{\lceil 2i+2-\frac{d+3}{2}\rceil}r_{\lfloor 2i+2-\frac{d+3}{2}\rfloor+j}\left(b_{\lfloor 2i+2-\frac{d+3}{2}\rfloor+j}-b_{\lceil 2i+2-\frac{d+3}{2}\rceil-j}\right)\\
&\quad+r_{2i+2-\frac{d+3}{2}}b_{2i+2-\frac{d+3}{2}}+\sum_{j=2(2i+2-\frac{d+3}{2})+1}^{d}r_jb_j,
\end{aligned}$$

where for the last equality, we use Lemma 5.4.9 and we set $r_{2i+2-\frac{d+3}{2}}b_{2i+2-\frac{d+3}{2}}=0$ if d is even. Since $b_j\ge 0$ and $r_j\ge 0$ for$j\ge 2i+2-\frac{d+3}{2}$, it follows that the single summand and the sum in the last line of the above computation are both non-negative. Concerning the first sum, the coefficients $r_{2i+2-\frac{d+3}{2}+j}$ are non-negative and therefore, in order to show non-negativity of $c_{i+1}-c_i$, it suffices to show that for $1\le j\le\lceil 2i+2-\frac{d+3}{2}\rceil$, we have

$$b_{\lfloor 2i+2-\frac{d+3}{2}\rfloor+j}\ge b_{\lceil 2i+2-\frac{d+3}{2}\rceil-j}.$$

This directly follows from the unimodality and symmetry of the sequence b if $2i+2-\frac{d+3}{2}+j\le\frac{d+1}{2}$. Assume $2i+2-\frac{d+3}{2}+j>\frac{d+1}{2}$. Since $i\le\frac{d}{2}$, we have

$$\frac{d+1}{2}<2i+2-\frac{d+3}{2}+j\le d+2-\frac{d+3}{2}+j=\frac{d+1}{2}+j\le\left\lfloor\frac{d+1}{2}\right\rfloor+j.$$

Using that b is symmetric and unimodal, it follows that

$$b_{\lfloor 2i+2-\frac{d+3}{2}\rfloor+j}\ge b_{\lfloor\frac{d+1}{2}\rfloor+j}=b_{d-\lfloor\frac{d}{2}\rfloor-j}\ge b_{\lceil 2i+2-\frac{d+3}{2}\rceil-j}.$$

This shows the claim. □

We now recall and prove Theorem C:

Theorem C. *(a) $h^*\left(P_{\partial(\sigma_{d+1})};t\right)$ has only real roots if $d \in \mathbb{N}$ is odd.*

(b) $h^*\left(P_{\partial(\sigma_{d+1})}\right)$ is unimodal with peak in the middle for every $d \in \mathbb{N}$.

Proof. Since $P_{\partial(\sigma_{d+1})}$ has a regular unimodular triangulation $\mathcal{T}$ by Theorem B, we have $h^*(P_{\partial(\sigma_{d+1})}) = h(\mathcal{T})$. If d is odd, such a triangulation is given by

$$\mathrm{esd}_{d+2}\left(\Delta_{\frac{d+1}{2}}\right) * \mathrm{esd}_{d+2}\left(\Delta_{\frac{d-1}{2}}\right)$$

and its h-polynomial equals $h\left(\mathrm{esd}_{d+2}\left(\Delta_{\frac{d+1}{2}}\right);t\right) \cdot h\left(\mathrm{esd}_{d+2}\left(\Delta_{\frac{d-1}{2}}\right);t\right)$. Since both factors are real-rooted by [Joc18, Corollary 4.4], so is $h^*\left(P_{\partial(\sigma_{d+1})};t\right)$.

Suppose that d is even. Combining Lemma 5.4.8, (5.4) and Proposition 5.4.10, we get that $h^*(P_{\partial(\sigma_{d+1})})$ is increasing up to the middle, i.e.,

$$h_0^*(P_{\partial(\sigma_{d+1})}) \leq h_1^*(P_{\partial(\sigma_{d+1})}) \leq \cdots \leq h_{\frac{d}{2}}^*(P_{\partial(\sigma_{d+1})}).$$

Since, by Theorem B, $P_{\partial(\sigma_{d+1})}$ has a regular unimodular triangulation it follows by [Ath04, Theorem 1.3] that $h^*(P_{\partial(\sigma_{d+1})})$ is decreasing beyond the middle, i.e.,

$$h_{\frac{d}{2}}^*(P_{\partial(\sigma_{d+1})}) \geq \cdots \geq h_d^*(P_{\partial(\sigma_{d+1})}).$$

The claim follows. □

We would like to remark that even though the interior polytope $Q_{\partial(\sigma_{d+1})}$ has a symmetric h^*-vector, this is not true for $P_{\partial(\sigma_{d+1})}$.

5.5 Open problems

We end this chapter with some obvious directions for future research.

We have initiated the study of Laplacian polytopes $P_\Delta^{(i)}$ by studying the special case that Δ is the boundary of a $(d+1)$-simplex and $i = d$. It is therefore natural to consider the following very general problem.

Problem 5.5.1. *Study geometric and combinatorial properties of $P_\Delta^{(i)}$ for (classes of) simplicial complexes and general $0 \leq i \leq \dim \Delta$. In particular: What is the normalized volume? When do these polytopes have a regular unimodular triangulation? What properties do the h^*-vector and the h^*-polynomial have?*

In view of Proposition 5.2.5, a good starting point might be to study $P_\Delta^{(d)}$ for simplicial d-balls, since in this case we already know that $P_\Delta^{(d)}$ is a simplex. As part of this problem, it might be useful to consider how Laplacian polytopes change under certain operations on the simplicial complex, e.g., deletion/contraction of vertices, taking links, connected sums, joins. We want to remark that for $i = 0$, we get Laplacian simplices as studied in [BM17] and [MT18].

We have shown that $P_{\partial(\sigma_{d+1})}$ has a regular unimodular triangulation by explicitly constructing one. However, for more general classes of simplicial complexes, a better approach might be to compute a Gröbner basis of the toric ideal. This gives rise to the following problem whose solution would also contribute to Problem 5.5.1:

Problem 5.5.2. *Describe a Gröbner basis of the toric ideal of $P_\Delta^{(i)}$ in terms of the combinatorics of Δ. When does there exist a squarefree Gröbner basis (giving rise to a regular unimodular triangulation)?*

We want to emphasize that the Laplacian polytope depends on the ordering of the vertices of Δ (see Example 5.2.2). It is therefore natural to ask the following question:

Question 5.5.3. *Which orderings yield (up to unimodular or combinatorial equivalence) the same Laplacian polytope? How many equivalence classes are there?*

Apart from these more general problems, there are several open questions that are directly related to our results. In Corollary 5.4.7, we have computed the normalized volume of $P_{\partial(\sigma_{d+1})}$ explicitly and thereby have obtained a precise formula for the sum of the h^*-vector entries. Using the explicit regular unimodular triangulation from Theorem B and inclusion-exclusion, we can also express the h^*-polynomial as alternating sum, where all summands are products of h^*-polynomials of edgewise subdivisions of dilated simplices of varying dimension. Note that for d odd, we only have one summand. However, this does not yield a direct combinatorial interpretation of the entries of the h^*-vector. We therefore propose the following problem:

Problem 5.5.4. *Find a combinatorial interpretation of the entries of the h^*-vector of $P_{\partial(\sigma_{d+1})}$ (see Table 5.1 for the h^*-vectors if $1 \le d \le 8$).*

d	$h^*\left(P_{\partial\sigma_{d+1}}\right)$
1	$(1,2,0)$
2	$(1,10,5)$
3	$(1,22,78,24,0)$
4	$(1,131,726,419,19)$
5	$(1,149,4049,8558,3750,300,0)$
6	$(1,1478,38179,126372,85623,10422,69)$
7	$(1,926,157566,1135846,2188310,1150800,145600,3920,0)$
8	$(1,17617,1581403,6864069,43252570,31729319,6314903,239867,251)$

TABLE 5.1: The h^*-vectors of $P_{\partial\sigma_{d+1}}$ for $d = 1,\ldots,8$.

Finally, in view of Theorem C (a), we have the following conjecture:

Conjecture 5.5.5. *Let d be even. Then $h^*\left(P_{\partial(\sigma_{d+1})};x\right)$ is real-rooted.*

We have verified this conjecture computationally up to $d = 10$. For this problem, we suspect that an approach via interlacing sequences might be helpful, but we have not been able to carry it out so far.

5.6 Appendix

We provide the missing parts of the proof of Proposition 5.4.6. We recall some notation. We denote by $E'_k \in \mathbb{Z}^{(k-1)\times k}$ the $(k\times k)$-identity matrix with its first row removed and by $\mathbb{1}_{m\times n}$ and $\mathbf{0}_{m\times n}$ the $(m\times n)$-matrices whose entries are all equal to 1 and 0, respectively. Moreover, we denote by $\mathcal{M}\left(\frac{d+2}{2}\Delta_{\frac{d-2}{2}} - \mathbb{1}_{\frac{d-2}{2}\times\frac{d}{2}}\right)$ the matrix whose columns are the vertices of $\frac{d+2}{2}\Delta_{\frac{d-2}{2}} - \mathbb{1}_{\frac{d-2}{2}\times\frac{d}{2}}$ in the obvious order.

Proof of Proposition 5.4.6 (a). Let $d \geq 2$ and for a fixed even integer $i \in [d]$, consider the facet $F = \{x \in \mathbb{R}^d \,:\, \mathbb{1}_{\mathrm{odd}}^{\top} \cdot x - x_i \leq \frac{d}{2}\}$ of $Q_{\partial(\sigma_{d+1})}$. By Corollary 5.4.2, the vertices of F are $\{c^{(\ell)} \,:\, \ell \in [d+2] \setminus \{1, i+2\}\}$. We now consider the matrix $B \in \mathbb{Z}^{d\times d}$ whose ℓ^{th} column equals $c^{(2\ell+1)}$ if $1 \leq \ell \leq \frac{d}{2}$ and $c^{(2\ell-d)}$ if $\frac{d}{2}+1 \leq \ell \leq \frac{i+d}{2}$ and $c^{(2\ell+2-d)}$ if $\frac{i+d}{2}+1 \leq \ell \leq d$. If we reorder the rows of B, by taking first the rows with odd index, increasingly, followed by the row with index i and then the remaining rows with even index, increasingly, we obtain a matrix S, which looks as follows:

$$S = \left(\begin{array}{ccc|ccc} \multicolumn{3}{c|}{E_{\frac{d}{2}} \cdot \frac{d+2}{2}} & \multicolumn{3}{c}{\mathbb{1}_{\frac{d}{2}\times\frac{d}{2}}} \\ \hline 1 & \cdots & 1 & 0 & \cdots & 0 \\ \hline \multicolumn{3}{c|}{\mathbb{1}_{\frac{d-2}{2}\times\frac{d}{2}}} & \multicolumn{3}{c}{E'_{\frac{d}{2}} \cdot \frac{d+2}{2}} \end{array}\right).$$

Clearly, $F \cong \operatorname{conv}(T)$. Let

$$U = \left(\begin{array}{ccc|cccc} \multicolumn{3}{c|}{E'_{\frac{d}{2}}} & \multicolumn{4}{c}{\mathbf{0}_{\frac{d-2}{2}\times\frac{d}{2}}} \\ \hline \multicolumn{3}{c|}{\mathbf{0}_{\frac{d-2}{2}\times\frac{d}{2}}} & \multicolumn{4}{c}{E'_{\frac{d}{2}}} \\ \hline 0 & \cdots & 0 & -1 & 0 & \cdots & 0 \\ \hline 1 & \cdots & 1 & -1 & 0 & \cdots & 0 \end{array}\right) \in \mathbb{Z}^{d\times d}.$$

It is easy to see that U is unimodular and a direct computation shows that

$$U \cdot (S - \mathbb{1}_{d\times d}) = \left(\begin{array}{ccc|ccc} \multicolumn{3}{c|}{\mathcal{M}\left(\frac{d+2}{2}\Delta_{\frac{d-2}{2}} - \mathbb{1}_{\frac{d-2}{2}\times\frac{d}{2}}\right)} & \multicolumn{3}{c}{\mathbf{0}_{\frac{d-2}{2}\times\frac{d}{2}}} \\ \hline \multicolumn{3}{c|}{\mathbf{0}_{\frac{d-2}{2}\times\frac{d}{2}}} & \multicolumn{3}{c}{\mathcal{M}\left(\frac{d+2}{2}\Delta_{\frac{d-2}{2}} - \mathbb{1}_{\frac{d-2}{2}\times\frac{d}{2}}\right)} \\ \hline 0 & \cdots & 0 & 1 & \cdots & 1 \\ 1 & \cdots & 1 & 1 & \cdots & 1 \end{array}\right).$$

Since $F \cong \operatorname{conv}(U \cdot (S - \mathbb{1}_{d\times d}))$, the claim follows after projection on the first $d-1$ coordinates and by the definition of the join. We also note that the vertices of F corresponding to the vertices of the dilated simplices are $\{c^{(2\ell+1)} \,:\, 1 \leq \ell \leq \frac{d}{2}\}$ and $\{c^{(2\ell)} \,:\, 2 \leq \ell \leq \frac{d}{2}+1,\ \ell \neq \frac{i+2}{2}\}$.

For a fixed odd integer $j \in [d]$, consider the facet $G = \{x \in \mathbb{R}^d \,:\, \mathbb{1}_{\mathrm{even}}^{\top} \cdot x - x_j \leq \frac{d}{2}\}$ of $Q_{\partial(\sigma_{d+1})}$. By Corollary 5.4.2, the vertices of F are $\{c^{(\ell)} \,:\, \ell \in [d+2] \setminus \{2, j+2\}\}$. We now consider the matrix $C \in \mathbb{Z}^{d\times d}$ whose ℓ^{th} column equals $c^{(2\ell-1)}$ if $1 \leq \ell \leq \frac{j+1}{2}$ and $c^{(2\ell+1)}$ if $\frac{j+3}{2} \leq \ell \leq \frac{d}{2}$ and $c^{(2\ell+2-d)}$ if $\frac{d}{2}+1 \leq \ell \leq d$. If we reorder the rows of C by taking first the rows with odd index $k \in [d] \setminus \{j\}$, increasingly, followed by row j and then the rows with even index, increasingly, we obtain a matrix S, which looks as follows:

$$S = \left(\begin{array}{ccc|ccc} \multicolumn{3}{c|}{E'_{\frac{d}{2}} \cdot \frac{d+2}{2}} & \multicolumn{3}{c}{\mathbb{1}_{\frac{d-2}{2}\times\frac{d}{2}}} \\ \hline 0 & \cdots & 0 & 1 & \cdots & 1 \\ \hline \multicolumn{3}{c|}{\mathbb{1}_{\frac{d}{2}\times\frac{d}{2}}} & \multicolumn{3}{c}{E_{\frac{d}{2}} \cdot \frac{d+2}{2}} \end{array}\right).$$

Clearly, $G \cong \operatorname{conv}(S)$. Let

$$U = \left(\begin{array}{c|c} E_{\frac{d}{2}-1} & \mathbf{0}_{\frac{d-2}{2}\times\frac{d+2}{2}} \\ \hline \mathbf{0}_{\frac{d-2}{2}\times\frac{d}{2}} & E'_{\frac{d}{2}} \\ \hline 0 \quad \cdots \quad 0 & 1 \quad \cdots \quad 1 \\ \hline 0 \cdots \quad 0 \quad -1 & 1 \quad \cdots \quad 1 \end{array}\right) \in \mathbb{Z}^{d\times d}.$$

It is easy to see that U is unimodular and a direct computation shows that

$$U\cdot(S-\mathbb{1}_{d\times d}) = \left(\begin{array}{c|c} \mathcal{M}\left(\frac{d+2}{2}\Delta_{\frac{d-2}{2}} - \mathbb{1}_{\frac{d-2}{2}\times\frac{d}{2}}\right) & \mathbf{0}_{\frac{d-2}{2}\times\frac{d}{2}} \\ \hline \mathbf{0}_{\frac{d-2}{2}\times\frac{d}{2}} & \mathcal{M}\left(\frac{d+2}{2}\Delta_{\frac{d-2}{2}} - \mathbb{1}_{\frac{d-2}{2}\times\frac{d}{2}}\right) \\ \hline 0 \quad \cdots \quad 0 & 1 \quad \cdots \quad 1 \\ 1 \quad \cdots \quad 1 & 1 \quad \cdots \quad 1 \end{array}\right).$$

Since $G \cong \operatorname{conv}(U\cdot(S-\mathbb{1}_{d\times d}))$, the claim follows after projection on the first $d-1$ coordinates and by the definition of the join. We also note that the vertices of G corresponding to the vertices of the dilated simplices are $\{c^{(2\ell+1)} : 0 \le \ell \le \frac{d}{2}, \ell \ne \frac{j+1}{2}\}$ and $\{c^{(2\ell)} : 2 \le \ell \le \frac{d}{2}+1, \ell \ne \frac{i+2}{2}\}$.

For fixed integers $1 \le i < j \le d$ of different parity consider the facet $H = \{x \in \mathbb{R}^d : x_i + x_j \ge 1\}$ of $Q_{\partial(\sigma_{d+1})}$. Without loss of generality assume that i is odd j is even. By Corollary 5.4.2, the vertices of F are $\{c^{(\ell)} : \ell \in [d+2] \smallsetminus \{i+2, j+2\}\}$. We now consider the matrix $D \in \mathbb{Z}^{d\times d}$ whose ℓ^{th} column equals $c^{(2\ell-1)}$ if $1 \le \ell \le \frac{i+1}{2}$, $c^{(2\ell+1)}$ if $\frac{i+3}{2} \le \ell \le \frac{d}{2}$, $c^{(2\ell-d)}$ if $\frac{d}{2}+1 \le \ell \le \frac{j+d}{2}$ and $c^{(2\ell+2-d)}$ if $\frac{j+d}{2}+1 \le \ell \le d$. If we reorder the rows of D by taking first the rows with odd index $k \in [d] \smallsetminus \{i\}$, increasingly, followed by row i, followed by the rows with even index $\ell \in [d] \smallsetminus \{j\}$, increasingly, followed by row j as the last row, we obtain a matrix S, which looks as follows:

$$S = \left(\begin{array}{c|c} \frac{d+2}{2}\cdot E'_{\frac{d}{2}} & \mathbb{1}'_{\frac{d}{2}} \\ \hline 0 \quad \cdots \quad 0 & 1 \quad \cdots \quad 1 \\ \hline \mathbb{1}'_{\frac{d}{2}} & \frac{d+2}{2}\cdot E'_{\frac{d}{2}} \\ \hline 1 \quad \cdots \quad 1 & 0 \quad \cdots \quad 0 \end{array}\right).$$

Clearly, $H \cong \operatorname{conv}(S)$. Let

$$U = \left(\begin{array}{c|c|c} E_{\frac{d}{2}-1} & \multicolumn{2}{c}{\mathbf{0}^{(\frac{d}{2}-1)\times(\frac{d}{2}+1)}} \\ \hline \mathbf{0}'_{\frac{d}{2}} & E_{\frac{d}{2}-1} & \mathbf{0}^{(\frac{d}{2}-1)\times 1} \\ \hline \multicolumn{3}{c}{-e_d^{\top}} \\ \hline \multicolumn{3}{c}{-(e_{\frac{d}{2}}+e_d)^{\top}} \end{array}\right) \in \mathbb{Z}^{d\times d}.$$

It is easy to see that U is unimodular and a direct computation shows that

$$U \cdot (S - \mathbb{1}_{d\times d}) = \left(\begin{array}{ccc|ccc} \multicolumn{3}{c|}{\mathcal{M}\left(\frac{d+2}{2}\Delta_{\frac{d-2}{2}} - \mathbb{1}_{\frac{d-2}{2}\times\frac{d}{2}}\right)} & \multicolumn{3}{c}{\mathbf{0}_{\frac{d-2}{2}\times\frac{d}{2}}} \\ \hline \multicolumn{3}{c|}{\mathbf{0}_{\frac{d-2}{2}\times\frac{d}{2}}} & \multicolumn{3}{c}{\mathcal{M}\left(\frac{d+2}{2}\Delta_{\frac{d-2}{2}} - \mathbb{1}_{\frac{d-2}{2}\times\frac{d}{2}}\right)} \\ \hline 0 & \cdots & 0 & 1 & \cdots & 1 \\ 1 & \cdots & 1 & 1 & \cdots & 1 \end{array}\right).$$

Since $H \cong \operatorname{conv}(U \cdot (S - \mathbb{1}_{d\times d}))$, the claim follows after projection on the first $d-1$ coordinates and by the definition of the join. We also note that the vertices of H corresponding to the vertices of the dilated simplices are $\{c^{(2\ell+1)} : 0 \le \ell \le \frac{d}{2}, \ell \ne \frac{i+1}{2}\}$ and $\{c^{(2\ell)} : 1 \le \ell \le \frac{d}{2}+1, \ell \ne \frac{j+2}{2}\}$. □

Proof of Proposition 5.4.6 (ii). Let $d \ge 1$ be an odd integer. We define vectors $u^{(1)}, \dots, u^{d+2} \in \mathbb{R}^{d+1}$ by $u^{(\ell)}_k = d+1$ if $k = \ell-1$ and $u^{(\ell)}_k = (-1)^{k+\ell-1}$, otherwise. By Lemma 5.2.10, $u^{(1)}, \dots, u^{(d+2)}$ are the vertices of $\widetilde{P}_{\partial(\sigma_{d+1})}$. We now consider the matrix $E \in \mathbb{Z}^{(d+1)\times(d+2)}$ whose ℓ^{th} column equals $u^{(2\ell-1)}$ if $1 \le \ell \le \frac{d+3}{2}$ and $u^{(2\ell-(d+3))}$ if $\frac{d+3}{2}+1 \le \ell \le d+2$. If we reorder the rows of E, by taking first the rows with even index and then the ones with odd index, increasingly, we obtain a matrix $Q = (q_{k,\ell}) \in \mathbb{Z}^{(d+1)\times(d+2)}$ with

- $q_{k,k+1} = d+1$ for $k \in [d+1]$,
- $q_{k,\ell} = 1$ if $k \le \frac{d+1}{2}$ and $\ell > \frac{d+3}{2}$, or $k > \frac{d+1}{2}$ and $\ell \le \frac{d+3}{2}$
- $q_{k,\ell} = -1$, otherwise.

Clearly, $\widetilde{P}_{\partial(\sigma_{d+1})} \cong \operatorname{conv}(Q)$. Let

$$U = \left(\begin{array}{ccc|ccc} \multicolumn{3}{c|}{E_{\frac{d+1}{2}}} & \multicolumn{3}{c}{\mathbf{0}_{\frac{d+1}{2}\times\frac{d+1}{2}}} \\ \hline & & & 0 & & \\ \multicolumn{3}{c|}{\mathbf{0}_{\frac{d-1}{2}\times\frac{d+1}{2}}} & \vdots & E_{\frac{d-1}{2}} & \\ & & & 0 & & \\ \hline 0 & \cdots & 0 & 1 & \cdots & 1 \end{array}\right) \in \mathbb{Z}^{(d+1)\times(d+1)}.$$

It is easy to see that U is unimodular and a direct computation shows that

$$\begin{aligned} &U \cdot (Q - \mathbb{1}_{(d+1)\times(d+2)}) \\ &= \left(\begin{array}{ccc|ccc} \multicolumn{3}{c|}{\mathcal{M}\left((d+2)\Delta_{\frac{d+1}{2}} - 2\cdot\mathbb{1}\right)} & \multicolumn{3}{c}{\mathbf{0}} \\ \hline \multicolumn{3}{c|}{\mathbf{0}} & \multicolumn{3}{c}{\mathcal{M}\left((d+2)\Delta_{\frac{d-1}{2}} - 2\cdot\mathbb{1}\right)} \\ \hline 0 & \cdots & 0 & 1 & \cdots & 1 \end{array}\right). \end{aligned}$$

Since $\widetilde{P}_{\partial(\sigma_{d+1})} \cong \operatorname{conv}(U \cdot (Q - \mathbb{1}_{(d+1)\times(d+2)}))$, the claim follows by definition of the join. □

Bibliography

[ATMP21] B. Acosta-Tripailao, P. S. Moya, and D. Pastén. "Applying the Horizontal Visibility Graph Method to Study Irreversibility of Electromagnetic Turbulence in Non-Thermal Plasmas". In: *Entropy* 23.4 (2021), p. 470.

[Adi+22] K. Adiprasito, S. A. Papadakis, V. Petrotou, and J. Steinmeyer. *Beyond positivity in Ehrhart Theory*. 2022. arXiv: 2210.10734.

[Aig06] M. Aigner. *Diskrete Mathematik*. Vol. 6. 2006.

[Ais14] N. Aisbett. "Frankl-Füredi-Kalai inequalities on the γ-vectors of flag nestohedra". In: *Discrete Comput. Geom.* 51.2 (2014), pp. 323–336. ISSN: 0179-5376.

[AV20] N. Aisbett and V. Volodin. "Geometric realization of γ-vectors of subdivided cross polytopes". In: *Electron. J. Combin.* 27.2 (2020), Paper No. 2.43, 12.

[AS16] N. Alon and J. H. Spencer. *The probabilistic method*. 4th ed. Wiley Series in Discrete Mathematics and Optimization. John Wiley & Sons, Inc., Hoboken, NJ, 2016, pp. xiv+375. ISBN: 978-1-119-06195-3.

[Ame+20] S. Ameer, M. Gibson-Lopez, E. Krohn, S. Soderman, and Q. Wang. "Terrain Visibility Graphs: Persistence is Not Enough". In: *36th International Symposium on Computational Geometry (SoCG 2020)*. Vol. 164. Leibniz International Proceedings in Informatics (LIPIcs). Dagstuhl, Germany: Schloss Dagstuhl–Leibniz-Zentrum für Informatik, 2020, 6:1–6:13. ISBN: 978-3-95977-143-6.

[Ara+16] A. Aragoneses, L. Carpi, D. V. Churkin, C. Masoller, N. Tarasov, M. C. Torrent, and S. K. Turitsyn. "Unveiling temporal correlations characteristic of a phase transition in the output intensity of a fiber laser". In: *Physical review letters* 116.3 (2016), p. 033902.

[AJP13] B. Assarf, M. Joswig, and A. Paffenholz. "On a classification of smooth Fano polytopes". In: *Discrete Mathematics and Theoretical Computer Science* (2013).

[Ath12] C. A. Athanasiadis. "Flag subdivisions and γ-vectors". In: *Pacific J. Math.* 259.2 (2012), pp. 257–278. ISSN: 0030-8730.

[Ath04] C.A. Athanasiadis. "h^*-vectors, Eulerian polynomials and stable polytopes of graphs". In: *Electron. J. Combin.* 11(2) (2004/06), Research Paper 6, 13 pp. (electronic).

[Bal+09] F. Ballesteros, L. Lacasa, B. Luque, and J. Luque. "Horizontal visibility graphs: Exact results for random time series". In: *Physical Review E* 80.4 (2009), p. 046103.

[Bal+08] F. Ballesteros, L. Lacasa, B. Luque, J. Luque, and J.C. Nuno. "From time series to complex networks: The visibility graph". In: *Proceedings of the National Academy of Sciences* 105.13 (2008), pp. 4972–4975.

[Bal+18] G. Balletti, T. Hibi, M. Meyer, and A. Tsuchiya. "Laplacian Simplices Associated to Digraphs". In: *Arkiv för matematik* 56 (2018).

[BM86] F. Barahona and A. Mahjoub. "On the cut polytope". In: *Mathematical Programming* 36 (1986), pp. 157–173.

[Bec+04] M. Beck, J. Loera, M. Develin, J. Pfeifle, and R. Stanley. "Coefficients and Roots of Ehrhart Polynomials". In: *Contemp. Math.* 374 (2004).

[BR15] M. Beck and S. Robins. *Computing the Continuous Discretely Integer-Point Enumeration in Polyhedra.* Vol. 2nd ed. 2015. ISBN: 978-0-387-29139-0.

[BS10] M. Beck and A. Stapledon. "On the log-concavity of Hilbert series of Veronese subrings and Ehrhart series". In: *Math. Z.* 264.1 (2010), pp. 195–207. ISSN: 0025-5874.

[Bol01] B. Bollobás. *Random graphs.* Second. Vol. 73. Cambridge Studies in Advanced Mathematics. Cambridge University Press, Cambridge, 2001, pp. xviii+498. ISBN: 0-521-80920-7; 0-521-79722-5.

[Brä15] P. Brändén. "Unimodality, Log-concavity, Real-rootedness and Beyond". In: *Handbook of Enumerative Combinatorics.* Discrete Math. Appl. (Boca Raton). CRC Press, Boca Raton, FL, 2015, pp. 437–483.

[BJ21] P. Brändén and K. Jochemko. "The Eulerian transformation". In: *Transactions of the American Mathematical Society* 375 (2021), pp. 1917–1931.

[BM17] B. Braun and M. Meyer. "Laplacian Simplices". In: *Advances in Applied Mathematics* 114 (2017).

[BW09] F. Brenti and V. Welker. "The Veronese construction for formal power series and graded algebras". In: *Advances in Applied Mathematics* 42.4 (2009), pp. 545–556. ISSN: 0196-8858.

[BR04] M. Brun and T. Römer. "Subdivisions of Toric Complexes". In: *Journal of Algebraic Combinatorics* 21 (2004).

[BG09] W. Bruns and J. Gubeladze. *Polytopes, rings, and K-theory.* Springer Monographs in Mathematics. Springer, Dordrecht, 2009, pp. xiv+461. ISBN: 978-0-387-76355-2.

[BH98] W. Bruns and H. J. Herzog. *Cohen-Macaulay Rings.* 2nd ed. Cambridge Studies in Advanced Mathematics. Cambridge University Press, 1998.

[BR07] W. Bruns and T. Römer. "h-vectors of Gorenstein polytopes". In: *J. Combin. Theory Ser. A* 114.1 (2007), pp. 65–76. ISSN: 0097-3165.

[Cao+20] Z. Cao, C. Lin, G. Liu, and F. Xiao. "A Fuzzy Interval Time-Series Energy and Financial Forecasting Model Using Network-Based Multiple Time-Frequency Spaces and the Induced-Ordered Weighted Averaging Aggregation Operation". In: *IEEE Transactions on Fuzzy Systems* 28.11 (2020), pp. 2677–2690.

[Çel+21] T. Ö. Çelik, A. Jamneshan, G. Montúfar, B. Sturmfels, and L. Venturello. "Wasserstein distance to independence models". In: *J. Symbolic Comput.* 104 (2021), pp. 855–873. ISSN: 0747-7171.

[CD95] R. Charney and M. Davis. "The Euler characteristic of a nonpositively curved, piecewise Euclidean manifold". In: *Pacific J. Math.* 171.1 (1995), pp. 117–137. ISSN: 0030-8730.

[Che+22] C. Chen et al. "Constructing Time-Varying Directed EEG Network by Multivariate Nonparametric Dynamical Granger Causality". In: *IEEE Transactions on Neural Systems and Rehabilitation Engineering* 30 (2022), pp. 1412–1421.

[Che+15] S. Chen, Y. Deng, Q. Liu, X. Lan, and H. Mo. "Fast transformation from time series to visibility graphs". In: *Chaos: An Interdisciplinary Journal of Nonlinear Science* 25.8 (2015), p. 083105.

[Che19] T. Chen. "Directed acyclic decomposition of Kuramoto equations". In: *Chaos* 29.9 (2019), pp. 093101, 12. ISSN: 1054-1500.

[CDK23] T. Chen, R. Davis, and E. Korchevskaia. "Facets and facet subgraphs of symmetric edge polytopes". In: *Discrete Appl. Math.* 328 (2023), pp. 139–153. ISSN: 0166-218X.

[CDM18] T. Chen, R. Davis, and D. Mehta. "Counting equilibria of the Kuramoto model using birationally invariant intersection index". In: *SIAM J. Appl. Algebra Geom.* 2.4 (2018), pp. 489–507.

[CN20] M. Chudnovsky and E. Nevo. "Induced equators in flag spheres". In: *J. Combin. Theory Ser. A* 176 (2020), pp. 105283, 14. ISSN: 0097-3165.

[CN22] M. Chudnovsky and E. Nevo. "Stable sets in flag spheres". In: *Sém. Lothar. Combin.* 86B (2022), Art. 10, 11.

[DDM22] A. D'Alì, E. Delucchi, and M. Michałek. "Many Faces of Symmetric Edge Polytopes". In: *Electron. J. Combin.* 29.3 (2022), Paper No. 3.24–.

[D'A+23] A. D'Alì, M. Juhnke-Kubitzke, D. Köhne, and L. Venturello. "On the gamma-vector of symmetric edge polytopes". In: *SIAM J. Discrete Math.* 37.2 (2023), pp. 487–515.

[Das+22] D. Dastan, M. J. Kartha, B.A. Reshi, and P. S. Walke. "Morphological study of thin films: Simulation and experimental insights using horizontal visibility graph". In: *Ceramics International* 48.4 (2022), pp. 5066–5074. ISSN: 0272-8842.

[DO01] M. W. Davis and B. Okun. "Vanishing theorems and conjectures for the ℓ^2-homology of right-angled Coxeter groups". In: *Geom. Topol.* 5 (2001), pp. 7–74. ISSN: 1465-3060.

[DH20] E. Delucchi and L. Hoessly. "Fundamental polytopes of metric trees via parallel connections of matroids". In: *European J. Combin.* 87 (2020), pp. 103098, 18. ISSN: 0195-6698.

[Des+09] G. Deshpande, S. LaConte, G. A. James, S. Peltier, and X. Hu. "Multivariate Granger causality analysis of fMRI data". In: *Human Brain Mapping* 30.4 (2009), pp. 1361–1373.

[Die17] R. Diestel. *Graph theory.* Fifth. Vol. 173. Graduate Texts in Mathematics. Springer, Berlin, 2017, pp. xviii+428. ISBN: 978-3-662-53621-6.

[DDK13] J. F. Donges, R. V. Donner, and J. Kurths. "Testing time series irreversibility using complex network methods". In: *EPL (Europhysics Letters)* 102.1 (2013), p. 10004.

[Don+10] R. V. Donner, Y. Zou, J. F. Donges, N. Marwan, and J. Kurths. "Ambiguities in recurrence-based complex network representations of time series". In: *Physical Review E* 81.1 (2010), p. 015101.

[EG99] H. Edelsbrunner and D. R. Grayson. "Edgewise subdivision of a simplex". In: *Proceedings of the Fifteenth Annual Symposium on Computational Geometry (Miami Beach, FL, 1999).* ACM, New York, 1999, pp. 24–30.

[Ehr62] E. Ehrhart. "Sur les polyèdres rationnels homothétiques à n dimensions". In: *C. R. Acad. Sci. Paris* 254 (1962), pp. 616–618. ISSN: 0001-4036.

[FN99] P. Flajolet and M. Noy. "Analytic combinatorics of non-crossing configurations". In: *Discrete Mathematics, 1999.* 204 (1999), pp. 203–229.

[FK16] A. Frieze and M. Karoński. *Introduction to random graphs.* Cambridge University Press, Cambridge, 2016, pp. xvii+464. ISBN: 978-1-107-11850-8.

[Gal05] Ś. R. Gal. "Real root conjecture fails for five- and higher-dimensional spheres". In: *Discrete Comput. Geom.* 34.2 (2005), pp. 269–284. ISSN: 0179-5376.

[GWY20] Y. Gao, H. Wang, and D. Yu. "Fault diagnosis of rolling bearings using weighted horizontal visibility graph and graph Fourier transform". In: *Measurement* 149 (2020), p. 107036.

[Gar+93] J. S. Garofolo et al. "TIMIT Acoustic-Phonetic Continuous Speech Corpus LDC93S1". In: *Web Download. Philadelphia: Linguistic Data Consortium* (1993).

[Gol02] T.E. Goldberg. "Combinatorial Laplacians of Simplicial Complexes". In: *A Senior Project submitted to The Division of Natural Science and Mathematics of Bard College* (2002).

[GP17] J. Gordon and F. Petrov. "Combinatorics of the Lipschitz polytope". In: *Arnold Math. J.* 3.2 (2017), pp. 205–218. ISSN: 2199-6792.

[Gra89] D. R. Grayson. "Exterior power operations on higher K-theory". In: *K-Theory* 3.3 (1989), pp. 247–260. ISSN: 0920-3036.

[Grü03] B. Grünbaum. *Convex Polytopes.* Springer, 2003.

[GMS11] G. Gutin, T. Mansour, and S. Severini. "A characterization of horizontal visibility graphs and combinatorics on words". In: *Physica A: Statistical Mechanics and its Applications* 390.12 (2011), pp. 2421–2428.

[Haa+14] C. Haase, A. Paffenholz, L. Piechnik, and F. Santos. "Existence of unimodular triangulations - positive results". In: *Memoirs of the American Mathematical Society* 270 (2014).

[HMM18] J. Healy, L. McInnes, and J. Melville. *UMAP: Uniform Manifold Approximation and Projection for Dimension Reduction.* 2018.

[HHO18] J. Herzog, T. Hibi, and H. Ohsugi. "Edge Polytopes and Edge Rings". In: 2018, pp. 117–140. ISBN: 978-3-319-95347-2.

[Hib90] T. Hibi. "Some results on Ehrhart polynomials of convex polytopes". In: *Discrete Math.* 83 (1990), pp. 119–121.

[Hib92] T. Hibi. "Dual polytopes of rational convex polytopes". In: *Combinatorica* 12.2 (1992), pp. 237–240. ISSN: 0209-9683.

[Hib94] T. Hibi. "A lower bound theorem for Ehrhart polynomials of convex polytopes". In: *Adv. Math.* 105 (1994), pp. 162–165.

[Hib95] T. Hibi. "Star-shaped complexes and Ehrhart polynomials". In: *Proc. Amer. Math. Soc.* 123 (1995), pp. 723–726.

[Hib+10] T. Hibi, A. Higashitani, T. Matsui, Y. Nagazawa, and H. Ohsugi. "Roots of Ehrhart polynomials arising from graphs". In: *Journal of Algebraic Combinatorics - J ALGEBR COMB* 34 (2010).

[Hib+19] T. Hibi, A. Higashitani, A. Tsuchiya, and K. Yoshida. "Ehrhart Polynomials with Negative Coefficients". In: *Graphs and Combinatorics* 35 (2019).

[HO06] T. Hibi and H. Ohsugi. "Special simplices and Gorenstein toric rings". In: *J. Combin. Theory Ser. A* 113.4 (2006), pp. 718–725. ISSN: 0097-3165.

[HO14] T. Hibi and H. Ohsugi. "Centrally symmetric configurations of integer matrices". In: *Nagoya Math. J.* 216 (2014), pp. 153–170. ISSN: 0027-7630.

[Hig15] A. Higashitani. "Smooth Fano polytopes arising from finite directed graphs". In: *Kyoto J. Math.* 55.3 (2015), pp. 579–592. ISSN: 2156-2261.

[HJM19] A. Higashitani, K. Jochemko, and M. Michałek. "Arithmetic aspects of symmetric edge polytopes". In: *Mathematika* 65.3 (2019), pp. 763–784. ISSN: 0025-5793.

[HKM17] A. Higashitani, M. Kummer, and M. Michałek. "Interlacing Ehrhart polynomials of reflexive polytopes". In: *Selecta Math. (N.S.)* 23.4 (2017), pp. 2977–2998. ISSN: 1022-1824.

[Hu+22] J. Hu, H. Li, P. Wu, and Y. Zhang. "An analysis of the global fuel-trading market based on the visibility graph approach". In: *Chaos, Solitons & Fractals* 154 (2022), p. 111613. ISSN: 0960-0779.

[HX22a] Y. Hu and F. Xiao. "A novel method for forecasting time series based on directed visibility graph and improved random walk". In: *Physica A: Statistical Mechanics and its Applications* 594 (2022), p. 127029. ISSN: 0378-4371.

[HX22b] Y. Hu and F. Xiao. "An efficient forecasting method for time series based on visibility graph and multi-subgraph similarity". In: *Chaos, Solitons & Fractals* 160 (2022), p. 112243. ISSN: 0960-0779.

[Joc18] K. Jochemko. "On the real-rootedness of the Veronese construction for rational formal power series". In: *International Mathematics Research Notices* 2018 (2018), pp. 4780–4798.

[JKK23] M. Juhnke-Kubitzke and D. Köhne. *Laplacian polytopes of simplicial complexes*. 2023. arXiv: 2301.11602.

[JKKS21] M. Juhnke-Kubitzke, D. Köhne, and J. Schmidt. *Counting Horizontal Visibility Graphs*. 2021. arXiv: 2111.02723.

[KT22] T. Kálmán and L. Tóthmérész. *Ehrhart theory of symmetric edge polytopes via ribbon structures*. 2022. arXiv: 2201.10501.

[KS23] D. Köhne and J. Schmidt. "A simple scalable linear time algorithm for horizontal visibility graphs". In: *Physica A: Statistical Mechanics and its Applications* (2023), p. 128601. ISSN: 0378-4371.

[Kos09] T. Koshy. *Catalan Numbers with Applications*. Oxford University Press, 2009. ISBN: 9780199868766.

[KS98] M. Kreuzer and H. Skarke. "Classification of Reflexive Polyhedra in Three Dimensions". In: *Advances in Theoretical and Mathematical Physics* 2 (1998).

[KS00] M. Kreuzer and H. Skarke. “Complete classification of reflexive polyhedra in four dimensions”. In: *Adv. Theor. Math. Phys.* 4 (2000).

[LN17] J.-P. Labbé and E. Nevo. “Bounds for entries of γ-vectors of flag homology spheres”. In: *SIAM J. Discrete Math.* 31.3 (2017), pp. 2064–2078. ISSN: 0895-4801.

[LL17] L. Lacasa and B. Luque. “Canonical horizontal visibility graphs are uniquely determined by their degree sequence”. In: *The European Physical Journal Special Topics* 226.3 (2017), pp. 383–389.

[Lac+12] L. Lacasa, B. Luque, A. Nunez, J. M. R. Parrondo, and É. Roldán. “Time series irreversibility: a visibility graph approach”. In: *The European Physical Journal B* 85.6 (2012), pp. 1–11.

[LZ91] C. L. Lagarias and G. Ziegler. “Bounds for lattice polytopes con- taining a fixed number of interior points in a sublattice”. In: *Canadian J. Math.* 43 (1991), pp. 1022–1035.

[LLM10] E. Lehman, T. Leighton, and A. R. Meyer. *Mathematics for computer science*. Tech. rep. Technical report, 2006. Lecture notes, 2010.

[Li+14] Y. Li, S. Wang, P. Wen, and G. Zhu. “Analysis of alcoholic EEG signals based on horizontal visibility graph entropy”. In: *Brain informatics* 1.1-4 (2014), pp. 19–25.

[LWZ12] Y. Li, P. Wen, and G. Zhu. “An Efficient Visibility Graph Similarity Algorithm and Its Application on Sleep Stages Classification”. In: *Brain Informatics*. Berlin, Heidelberg: Springer Berlin Heidelberg, 2012, pp. 185–195. ISBN: 978-3-642-35139-6.

[LWZ14] Y. Li, P. Wen, and G. Zhu. “Epileptic seizure detection in EEGs signals using a fast weighted horizontal visibility algorithm”. In: *Computer Methods and Programs in Biomedicine* 115.2 (2014), pp. 64–75. ISSN: 0169-2607.

[Lia+11] W. Liao, J. Ding, D. Marinazzo, Q. Xu, Z. Wang, C. Yuan, Z. Zhang, G. Lu, and H. Chen. “Small-world directed networks in the human brain: multivariate Granger causality analysis of resting-state fMRI”. In: *Neuroimage* 54.4 (2011), pp. 2683–2694.

[LP86] L. Lovász and M. D. Plummer. “Matching Theory”. In: *Annals of Discrete Mathematics* 29 (1986).

[LN16] F. H. Lutz and E. Nevo. “Stellar theory for flag complexes”. In: *Math. Scand.* 118.1 (2016), pp. 70–82. ISSN: 0025-5521.

[MPT15] P. Manshour, J. Peinke, and M. R. R. Tabar. “Fully developed turbulence in the view of horizontal visibility graphs”. In: *Journal of Statistical Mechanics: Theory and Experiment* 2015.8 (2015), P08031.

[Mar+09] N. Marwan, J. F. Donges, Y. Zou, R. V. Donner, and J. Kurths. “Complex network approach for recurrence analysis of time series”. In: *Physics Letters A* 373.46 (2009), pp. 4246–4254.

[Mat+11] T. Matsui, A. Higashitani, Y. Nagazawa, H. Ohsugi, and T. Hibi. “Roots of Ehrhart polynomials arising from graphs”. In: *J. Algebraic Combin.* 34.4 (2011), pp. 721–749. ISSN: 0925-9899.

[Mcd71] I. G. Mcdonald. “Polynomials associated with finite cell complexes”. In: *J. London Math. Soc. (2)* 4 (1971), pp. 181–192.

[Mes03] R. Meshulam. “Domination numbers and homology”. In: *J. Combin. Theory Ser. A* 102.2 (2003), pp. 321–330. ISSN: 0097-3165.

[MT18] M. Meyer and Pllaha T. *Laplacian Simplices II: A Coding Theoretic Approach*. 2018. arXiv: 1809.02960.

[MHJ22] R. Mulas, D. Horak, and J. Jost. “Graphs, Simplicial Complexes and Hypergraphs: Spectral Theory and Topology”. In: *Higher-Order Systems*. Cham: Springer International Publishing, 2022, pp. 1–58. ISBN: 978-3-030-91374-8.

[Nev07] E. Nevo. “Higher minors and Van Kampen’s obstruction”. In: *Math. Scand.* 101.2 (2007), pp. 161–176. ISSN: 0025-5521.

[NP11] E. Nevo and T. K. Petersen. “On γ-vectors satisfying the Kruskal-Katona inequalities”. In: *Discrete Comput. Geom.* 45.3 (2011), pp. 503–521. ISSN: 0179-5376.

[NPT11] E. Nevo, T. K. Petersen, and B. E. Tenner. “The γ-vector of a barycentric subdivision”. In: *J. Combin. Theory Ser. A* 118.4 (2011), pp. 1364–1380. ISSN: 0097-3165.

[Nic+20] V. Nicosia, M. Sandler, D. Stowell, F. Thalmann, and D. F. Yela. “Online visibility graphs: Encoding visibility in a binary search tree”. In: *Phys. Rev. Research 2, 023069* (2020).

[Øbr08] M. Øbro. “Classification of terminal simplicial reflexive d-polytopes with 3d–1 vertices”. In: *Manuscripta Math.* 125 (2008), pp. 69–79.

[OT20] H. Ohsugi and A. Tsuchiya. “Reflexive polytopes arising from bipartite graphs with γ-positivity associated to interior polynomials”. In: *Selecta Mathematica* 26 (2020).

[OT21a] H. Ohsugi and A. Tsuchiya. “Symmetric edge polytopes and matching generating polynomials”. In: *Comb. Theory* 1 (2021), Paper No. 9, 19.

[OT21b] H. Ohsugi and A. Tsuchiya. “The h^*-polynomials of locally anti-blocking lattice polytopes and their γ-positivity”. In: *Discrete Comput. Geom.* 66.2 (2021), pp. 701–722. ISSN: 0179-5376.

[OT22] H. Ohsugi and A. Tsuchiya. “PQ-type adjacency polytopes of join graphs”. In: *Discrete Comput. Geom.* (2022).

[O’P19] J. O’Pella. “Horizontal visibility graphs are uniquely determined by their directed degree sequence”. In: *Physica A: Statistical Mechanics and its Applications* 536 (2019), p. 120923.

[Pet15] T. K. Petersen. *Eulerian Numbers*. Birkhäuser Advanced Texts Basler Lehrbücher. Birkhäuser New York, NY, 2015. ISBN: 978-1-4939-3090-6.

[Ree57] J. E. Reeve. “On the Volume of Lattice Polyhedra”. In: *Proceedings of The London Mathematical Society* 1 (1957), pp. 378–395.

[RS18] L. Rong and P. Shang. “Topological entropy and geometric entropy and their application to the horizontal visibility graph for financial time series”. In: *Nonlinear Dynamics* 92.1 (2018), pp. 41–58.

[Sch22a] J. Schmidt. *Runtime Data of Horizontal Visibility Algorithms for synthetic and empirical Time Series*. 2022. osnaData: https://doi.org/10.26249/FK2/MXFPLV.

[Sch22b] J. Schmidt. "Tire Pressure Monitoring using Weighted Horizontal Visibility Graphs". In: *2022 International Conference on Control, Automation and Diagnosis (ICCAD)*. 2022, pp. 1–6.

[Sch86] Alexander Schrijver. *Theory of linear and integer programming*. Wiley-Interscience Series in Discrete Mathematics. A Wiley-Interscience Publication. John Wiley & Sons, Ltd., Chichester, 1986, pp. xii+471. ISBN: 0-471-90854-1.

[Sch03] Alexander Schrijver. *Combinatorial optimization. Polyhedra and efficiency. (3 volumes)*. Vol. 24. Algorithms and Combinatorics. Disjoint paths, hypergraphs, Chapters 70–83. Springer-Verlag, Berlin, 2003. ISBN: 3-540-44389-4.

[Sch70] E. Schröder. "Vier combinatorische Probleme". In: *Zeitschrift für Mathematik und Physik. Band 15* (1870), pp. 361–376.

[Seg58] A. de Segner. "Enumeratio modorum, quibus figurae planae rectilineae per diagonales dividuntur in triangula." In: *Novi commentarii academiae scientiarum Petropolitanae* (1758/59), pp. 203–209.

[SS00] L. W. Shapiro and R. A. Sulanke. "Bijections for the Schröder numbers". In: *Math. Mag.* 73.5 (2000), pp. 369–376. ISSN: 0025-570X.

[Sta74] R. P. Stanley. "Combinatorial reciprocity theorems". In: *Advances in Math.* 14 (1974), pp. 194–253.

[Sta80] R. P. Stanley. "Decompositions of rational convex polytopes". In: *Ann. Discrete Math.* 6 (1980), pp. 333–342.

[Sta91] R. P. Stanley. "On the Hilbert function of a graded Cohen-Macaulay domain". In: *J. Pure Appl. Algebra* 73 (1991), pp. 307–314.

[Sta96] R. P. Stanley. *Combinatorics and commutative algebra*. Second. Vol. 41. Progress in Mathematics. Birkhäuser Boston, Inc., Boston, MA, 1996, pp. x+164. ISBN: 0-8176-3836-9.

[Sta15] R. P. Stanley. *Catalan numbers*. Cambridge University Press, New York, 2015, pp. viii+215. ISBN: 978-1-107-42774-7; 978-1-107-07509-2.

[Sta09] A. Stapledon. "Inequalities and Ehrhart δ-vectors". In: *Transactions of the American Mathematical Society* 361 (2009).

[Ste21] C. Stephen. "A Scalable Linear-Time Algorithm for Horizontal Visibility Graph Construction Over Long Sequences". In: *2021 IEEE International Conference on Big Data (Big Data)*. IEEE. 2021, pp. 40–50.

[Stu96] B. Sturmfels. *Gröbner bases and convex polytopes*. Vol. 8. University Lecture Series. American Mathematical Society, Providence, RI, 1996, pp. xii+162. ISBN: 0-8218-0487-1.

[The] The On-Line Encyclopedia of Integer Sequences. Published electronically at OEIS: https://oeis.org/A007815.

[Ver15] A. M. Vershik. "Classification of finite metric spaces and combinatorics of convex polytopes". In: *Arnold Math. J.* 1.1 (2015), pp. 75–81. ISSN: 2199-6792.

[Vol10] Vadim D. Volodin. "Cubical realizations of flag nestohedra and a proof of Gal's conjecture for them". In: *Russian Math. Surveys* 65 (2010), pp. 188–190.

[Xia+12] R. Xiang, J. Zhang, X. Xu, and M. Small. "Multiscale characterization of recurrence-based phase space networks constructed from time series". In: *Chaos: an interdisciplinary journal of nonlinear science* 22.1 (2012), p. 013107.

[YY08] Y. Yang and H. Yang. "Complex network-based time series analysis". In: *Physica A: Statistical Mechanics and its Applications* 387.5 (2008), pp. 1381–1386. ISSN: 0378-4371.

[Yel+20] D. F. Yela, F. Thalmann, V. Nicosia, D. Stowell, and M. Sandler. "Online visibility graphs: Encoding visibility in a binary search tree". In: *Physical Review Research* 2.2 (2020), p. 023069.

[Zie95] G. Ziegler. "Lectures on Polytopes". In: *Graduate Texts in Mathematics* (1995).